

General Disclaimer

One or more of the Following Statements may affect this Document

- This document has been reproduced from the best copy furnished by the organizational source. It is being released in the interest of making available as much information as possible.
- This document may contain data, which exceeds the sheet parameters. It was furnished in this condition by the organizational source and is the best copy available.
- This document may contain tone-on-tone or color graphs, charts and/or pictures, which have been reproduced in black and white.
- This document is paginated as submitted by the original source.
- Portions of this document are not fully legible due to the historical nature of some of the material. However, it is the best reproduction available from the original submission.

E85-10066

NASA

Technical Memorandum 86180

ALTIMETRY, ORBITS AND TIDES

(E85-10066 NASA-TM-86180) ALTIMETRY, ORBITS
AND TIDES (NASA) 183 p HC AC9/MF A01

N85-17404

CSCL 05B

G3/43 Unclass
 00066

by Oscar L. Colombo ✓

November 1984

National Aeronautics and
Space Administration

Goddard Space Flight Center
Greenbelt, Maryland 20771



Technical Memorandum 86180

ALTIMETRY, ORBITS AND TIDES

by Oscar L. Colombo

November 1984

National Aeronautics and
Space Administration

Goddard Space Flight Center
Greenbelt, Maryland 20771

ABSTRACT

A theory of radial orbit errors is derived from first principles; the basic ideas are presented in a reasonably self-contained way. There is also a section about tides, their effects on orbits, and their possible mapping with satellite altimetry. The theory seems to explain well the outcomes of computer simulations made independently by this author and by others. Orbits with precisely repeating ground tracks are considered in detail. SEASAT was kept in an orbit like that during its last month of operation, and future satellites with altimeters are likely to be in orbits of this type (TOPEX, ERS-1, POSEIDON). In this special case, $\Delta r^{(g)}$, the part of the radial error caused by the gravitational field model, has a component that depends only on position along the repeating ground track; the remainder of $\Delta r^{(g)}$ is caused by deep orbital resonance (mostly with the zonals) and consists mainly of a slowly increasing oscillation of one cycle per revolution (non-gravitational force models may produce similar "resonant" errors). Moreover, the periodical errors due to the zonals are functions of latitude only, and unobservable in crossover differences. Repeat orbits, where the perigee librates very slowly, are not the most suitable, therefore, for using altimetry to compute the mean sea surface by the "bias+tilt" and similar methods, or for gaining new information about the zonal part of the field. These orbits are best for studying temporal changes of the sea surface, because the error can be filtered out easily using colinear pass differences. Conversely, non-repeating orbits, where the perigee precesses, are worse for studying changes but are better for mapping the mean sea surface and modelling the field, provided the altimeter observations span a substantial part of one apsidal cycle.

PRECEDING PAGE BLANK NOT FILMED

ACKNOWLEDGEMENTS

I am grateful to a number of colleagues for helping me gather the necessary material, for their explanations of theoretical and practical points, for their readiness to listen to my ideas and to discuss them at length, and for setting up computer runs for the simulations. I would like to thank, on one or more of these counts, J.G. Marsh, C.A. Wagner, R.G. Williamson, B.V. Sanchez, D.B. Rao, D.C. Christodoulidis, D.E. Smith, S.M. Klosko, B.D. Beckley, D.T. Sandwell, V. Zlotnicki, R.H. Estes, T.V. Martin, J. McCarthy, N. Weiss, A.F. Schanzle, and last, but most certainly not least, F.J. Lerch.

Nancy Gebicke and Margaret Payne, who typed the final draft, have shown, as the reader may realize, great patience as well as competence. The illustrations were drawn by Mark Dunn.

This work has been supported under NASA Contract NAS5-28067.

TABLE OF CONTENTS

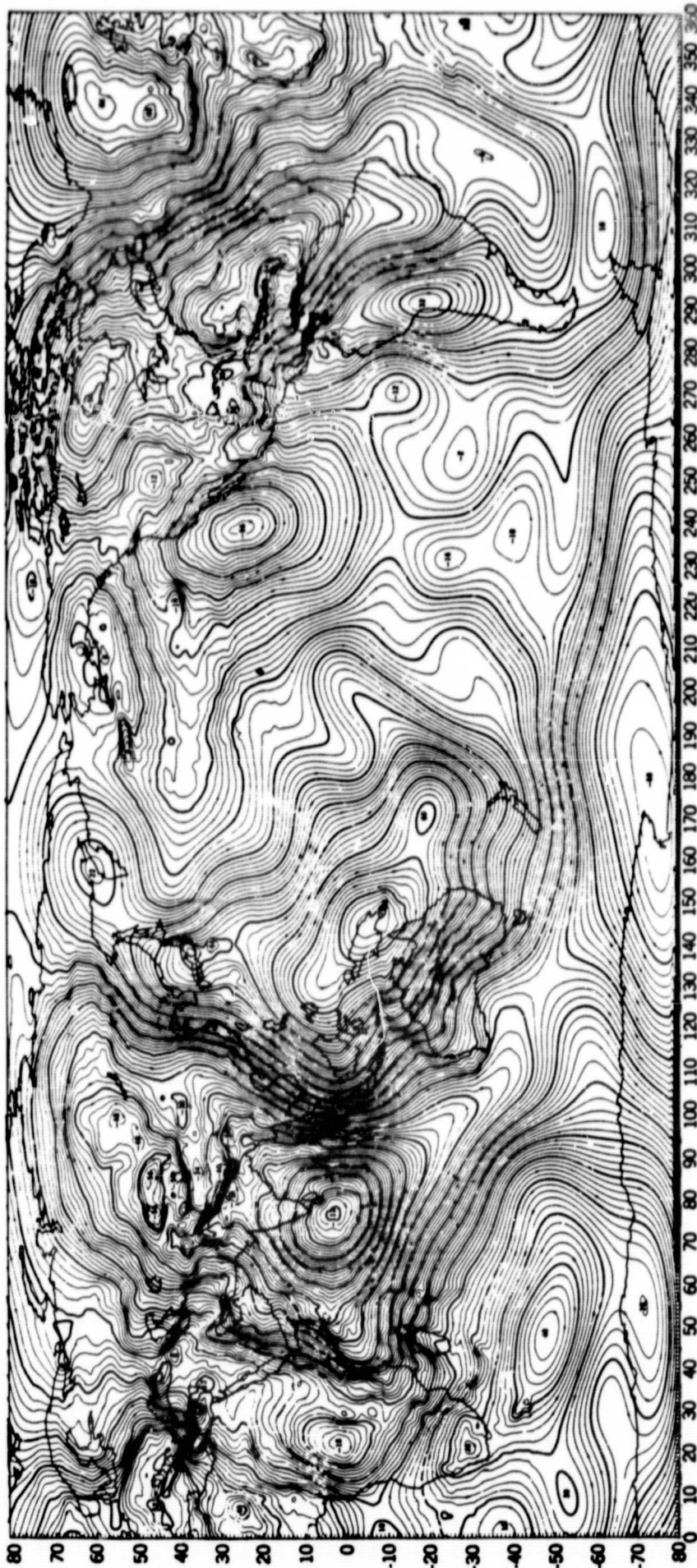
	<u>Page</u>
ABSTRACT	iii
ACKNOWLEDGEMENTS	iv
1.0 INTRODUCTION	1
1.1 Motivation	2
2.0 ALTIMETRY	6
2.1 Residual sea heights	6
3.0 ORBITS	13
3.1 Orbital motion and Keplerian elements	13
3.2 The mean ellipse	22
3.3 The reference orbit	26
3.4 The radial orbit error	29
3.5 Temporal characteristics of the error	31
(a) Practically constant part	31
(b) Nearly secular part	31
(c) Periodical part	32
(d) Other temporal variations	32
3.6 The equations of motion and their linearization	34
3.7 The homogeneous linearized equations	37
3.8 Orbit error due to the estimated initial state	39
3.9 The free response of the linearized equations and resonance	41
3.10 The spherical harmonic expansion of the geopotential in Keplerian elements	43

TABLE OF CONTENTS (Cont.)

	<u>Page</u>
3.11 The equations of motion in Keplerian elements	49
3.12 The forced linearized equations	52
3.13 Orbit error due to incorrect potential coefficients $C_{nm\alpha}$	56
(a) $(n-2p+q) (\dot{M}+\dot{\omega}) -q\dot{\omega}+m\dot{\theta} \neq 0$	56
(b) $(n-2p+q) (\dot{M}+\dot{\omega}) -q\dot{\omega}+m\dot{\theta} = 0$ (Resonance)	61
3.14 Orbit error due to incorrect GM	65
3.15 Expression of the radial error excluding its tidal part	66
 4.0 ORBITS WITH REPEATING GROUND TRACKS	 69
4.1 The "frozen", repeat orbit	69
4.2 Periodicity and resonance	74
4.3 The stability of a "frozen" orbit	77
4.4 The repeating ground track	80
(a) Geometry	80
(b) Finding the crossovers	82
4.5 Orbit error in a "frozen", repeat orbit; its geographical characteristics	86
4.6 Observability of zonal, initial state, and other errors in differences of altimetric heights	90
4.7 Numerical simulations of the error in a "frozen", repeat orbit	93
 5.0 TIDES	 100
5.1 The tidal forces	100
5.2 The tidal response	114

TABLE OF CONTENTS (Cont.)

	<u>Page</u>
5.3 Linearity and time-invariance	115
5.4 The admittance function	116
5.5 Love numbers	121
5.6 Representing the ocean tides	126
5.7 The tidal part of the orbit error	133
5.8 The case of the "frozen", repeat orbit	136
5.9 The aliasing of ocean tides with the mean sea surface and with each other	138
5.10 The complete expression of the radial orbit error	140
6.0 IMPLICATIONS FOR THE ANALYSIS OF ALTIMETRY	142
6.1 General	142
6.2 Crossover points and overlapping arcs	143
6.3 Direct mapping of ocean tides	146
7.0 CONCLUSIONS	152
REFERENCES	156



1974: The Marsh-Vincent Global Detailed Gravimetric Geoid

- CONTOUR INTERVAL = 2 m

(From "Geophysical Surveys", Vol. 1, pp. 481-511, 1974).

1984: "Ocean Geoid" based on SEASAT Altimeter Data

- CONTOUR INTERVAL = 1 m

(Mean Sea Surface according to J. Marsh, A.C. Brenner, B.D. Beckley and T.V. Martin, November 1984; reproduced by kind permission of J. Marsh).



1.0 INTRODUCTION

The face of the ocean has been examined with artificial satellites in the last decade and found to be covered with remarkable features hardly suspected before, when more than two thirds of the globe were still largely unsurveyed. Among the millions of measurements made with diverse instruments, those taken with the radar altimeters of GEOS 3 and SEASAT have proven of particular value for studying our planet, because of their high and homogeneous quality, dense coverage, and range of application. So it is not surprising that new space missions involving the use of altimeters are being planned for the next decade: those of TOPEX (NASA), ERS-1 (ESA) and POSEIDON (CNES), among others.

The importance of altimetry is suggested by the volume and variety of the scientific literature related to it. One could mention, for example, three special issues of the Journal of Geophysical Research (Vol. 84, B8, 1979 on GEOS 3; and Vols. 87, C5, 1982 and 88, C3, 1983 on SEASAT), one of Marine Geodesy (Vol. 8, 1984), or one of the Journal of the Astronautical Sciences (Vol. 28, October-December 1980 on orbit determination for SEASAT), as well as the proceedings of a number of international symposia. Two comprehensive reviews of the work published in the USA alone from 1975 to 1982 have been made by Stanley (1979) and by Marsh (1983).

1.1 Motivation

Since the earliest days of GEOS 3 it has been clear that the orbit error constitutes a serious problem. Things have improved, but the problem persists. While the error has its uses, too, as a source of information on what is not known about the gravitational field (Shum, 1982, and Wagner, 1984), it remains mostly a nuisance that can be mitigated with more or less empirical remedies, but that still limits the usefulness of the data in many applications. For this reason, efforts to get better models of the forces acting on the spacecraft, of which the gravitational ones are the most significant, are currently under way on both sides of the Atlantic.

An approach to the orbit problem based on celestial mechanics can give further insight into the way the empirical methods work and, perhaps, into how to improve them. As the relevant literature on satellite geodesy includes many important papers, reports and books either out of print or hard to get, I have written here a rather detailed introduction to the basic concepts. This may be of some value to those who wish to understand the nature of the orbit error better and are not very familiar with the subject.

The theory, as given here, is slanted towards orbits determined by the methods now in common use for geodetic satellites (Martin et al., 1976; Putney, 1976; Schutz et al., 1980). The orbits of GEOS 3 and SEASAT

have been computed by those methods, which are also the main ones considered, at this stage, for future missions. One possible alternative is to find the position of the spacecraft from simultaneous observations of several GPS-NAVSTAR navigation satellites. If the ephemerides of these satellites were sufficiently well known, this would eliminate the need to integrate long arcs numerically with imperfect force models, thus avoiding the orbit errors due to those models. The idea has been studied by Bender and Larden (1982) and by Ondrasik and Wu (1982). It may be used, on an experimental basis, during part of the TOPEX mission.

The analytical orbit perturbation theory explained here is only meant to give a qualitative understanding of the error. Its formulation includes several simplifying assumptions, so it is quantitatively less accurate than the numerical integration of the exact differential equations involved, which is also much more adequate for handling non-gravitational forces (drag, radiation pressure, etc.), and so it has become the standard procedure in satellite geodesy today (its main limitation complementing that of the analytical approach: it trades insight for numbers). Nevertheless, efforts to refine and extend the analytical method still continue, as shown in a review by Gaposchkin (1978). The treatment of the radial error along a precisely repeating ground track is a new version, using Keplerian elements, of part of a complete theory developed by me for this special type of orbit while visiting at the Department of Geodesy of the Technical University at Delft, in the Netherlands, over the period 1982-83 (Colombo, 1984). More

recently, a similar theory for the periodical part of that error has been worked out independently by C.A. Wagner (ib., 1984).

While oriented towards oceanography (the main field of application of altimetry until now) the present discussion of the orbit error is also relevant to the uses of data taken on land, ice, etc.

The topic of tides is intimately linked to that of altimetry. Tides modify the gravitational field, affecting the orbits of spacecraft and contributing to the errors in their determination. They also show up as part of the signal in the altimeter measurements. In principle, it is possible to map them directly over the whole of the oceans using altimetry. Attempts have been made several times, mostly with scant success. This must be blamed, to some extent, on the inadequate temporal and spatial sampling and limited accuracy of the GEOS 3 data, and on the short life of SEASAT. But, perhaps, better results could be obtained, even with such measurements, if one were to take full advantage of what can be predicted from first principles about the nature of the orbit errors. As mentioned in the section on "Tides", some of the best results so far have come from data collected during the last useful month of SEASAT. At that time, the satellite had a precisely repeating ground track which, in theory, should make the radial error particularly easy to filter, because of the strong symmetry of the orbit.

The literature on tides is very extensive. Cartwright estimated in 1977 that, over the previous 200-odd years, the number of publications had grown almost exponentially with time (to illustrate this, he tabulated the increment in this number at fifty years' intervals). Hendershott and Munk (1970), Cartwright (1977) and Schwiderski (1980) have made comprehensive reviews. The basic ideas needed to consider the tides in the context of satellite altimetry are scattered far and wide in works on astronomy, geodesy, oceanography and geophysics. I have tried to bring these ideas together in a way that shows, as clearly as possible, the links between the theory of tides and that of orbits.

Tides have always fascinated those with imagination: regular movements in an otherwise unpredictable element, following the rhythms of the sky. Now they are beginning to be mapped from that same sky, with modern instruments whose proper use requires understanding the timeless rules by which the sea, the Sun, the Moon, the satellites and the Earth join together in a complex dance. In the end, through the combination of techniques old and new, a task formulated nearly three centuries ago shall be fulfilled. At the very dawn of modern celestial mechanics and tidal theory, Newton wrote in his "Principia":

"Thus have I explained the causes of the motions of the Moon and the sea. Now it is fit to subjoin something concerning the amount of those motions."

2.0 ALTIMETRY

2.1 Residual Sea Heights

The height h_w of the sea surface above a reference ellipsoid, or ellipsoidal height of the surface, can be expressed as the sum

$$h_w = N + w_o + \zeta_G + w_t \quad , \quad (1)$$

where N is the geoid height, w_o is the constant part of the difference between h_w and N , or stationary sea surface topography, ζ_G represents the total geocentric tide (a regular movement of the sea surface towards and away from the center of mass of the Earth, or geocenter), while w_t corresponds to all temporal variations in surface height other than tides.

The value of N can be calculated using a gravitational field model. This model, for some ocean studies and for the computation of satellite orbits, has usually the form of a sum of spherical harmonics. In this work I shall assume that the field model is of this type. The high frequency part of the geoid at sea is known quite well nowadays thanks to the two altimetric missions already carried out, GEOS-3 and SEASAT. Spherical harmonic models up to degree and order 180 (and even higher) have been obtained from combinations of altimetry with land gravimetry, and they appear to be quite reliable over the oceans, particularly in details smaller than 1000 km (see, for example, Lerch et al., 1981, and

Rapp, 1982). As shown by calibration against independent data and each other, existing models seem to be weakest in the frequency range between degrees 10 and 40. Information on the low degrees comes mostly from satellite tracking data. Recent intercomparisons of satellite-derived models have been made by Reigber (1983), Lambeck and Coleman (1983), and Lerch et al. (1984). The broadest features (below degree 8) may be quite reliable already (Wagner, 1983).

The contemporary ocean tidal charts are believed to be reasonably good (Schwiderski, *ib.* 1980), but direct evidence for this is limited to data from tidal stations scattered widely along the coasts and in islands, most of which have been used to make the charts in the first place. Solid earth tides are thought to be known much better than ocean tides at present. No model for the prediction of w_t exists today, though some of the phenomena involved are understood to some extent, such as mesoscale eddies, the piling up of water along the coast caused by wind, etc. There is reason to believe that much of w_t can be treated, geographically, mostly as a random variable (see Wunsch, 1980, for further details) whose standard deviation, while changing from place to place according to how energetic are the currents and winds that agitate the sea surface, can be estimated directly from the study of overlapping altimetry passes as in (Cheney et al., 1983), for example. Maps of the mean sea surface topography, based on general circulation models, are also available, but their accuracy is unclear. As examples one can mention those by Lisitzin (1974), Levitus and Dort (1977), etc. Attempts to map w_0 using altimetry

have been severely hampered by the orbit and geoid errors, directly linked to the long wave uncertainties in existing gravitational field models. This problem was recognized very long ago, as shown in a paper written by Von Arx (1966) almost a decade before the launch of GEOS 3. Wunsch and Gaposchkin (1980) have proposed the simultaneous determination of w_0 and N by analyzing a combination of gravitational, altimetric and oceanographic data with a suitable form of generalized linear regression estimator (see Rao, 1965, Ch. 2, (g) and also Moritz (1980)). Extensive discussions of the sea surface topography problem, and reviews of much of the work done using GEOS 3 data, have been written by Rizos (1980) and Coleman (1981).

If N_c is the geoid height computed from the field model, and ΔN the corresponding error in N_c , then

$$N = N_c - \Delta N . \quad (2a)$$

Similarly, if $\Delta \zeta_G$ is the error in ζ_{Gc} , the geocentric tide calculated from charts of the ocean and the Earth tide with the corresponding Love numbers (expression (77) in the section "Tides"),

$$\zeta_G = \zeta_{Gc} - \Delta \zeta_G . \quad (2b)$$

If h_s is the ellipsoidal height of the altimeter satellite, and Λ the shortest distance between the center of mass of the spacecraft and the sea surface, then, as a very good approximation,

$$h_w = h_s - \Lambda . \quad (3)$$

After several corrections have been made to the raw data ("pre-processing", see Hancock et al., 1980, and Tapley et al., 1982), including those resulting from "in-flight" calibration of the altimeter (Kolenkiewicz and Martin, 1982; Marsh and Williamson, 1982), the radar altimeter ranges Λ_m can be regarded as successive values of Λ plus a measurement error $\Delta\Lambda$, where $\Delta\Lambda$ is mostly random noise. For GEOS-3, the first satellite dedicated to altimetric observations, $\Delta\Lambda$ stood at about 75 cm; the error came down to near 10 cm for SEASAT, launched three years later (in 1978); for future missions, a third generation of altimeters is likely to bring $\Delta\Lambda$ into the centimeters' range (see MacArthur, 1980).

The height of the satellite h_s can be calculated from its computed orbit, or ephemeris, which is obtained by adjusting the initial position, velocity and a few other parameters in an iterative Gauss-Newton (or similar) procedure to minimize the sum of the squares of the differences between the values of the tracking data available and the corresponding values calculated from the estimated ephemeris (see Martin et al., *ib.*, 1976). This fitted orbit usually spans a few days (up to one week), and

then a new orbit fit is made for the following several days, and so on. While not unique, this is today a common procedure for getting accurate ephemerides of altimeter satellites, so in this study I consider only orbits computed in this way. At present, the error Δh_s in h_s is believed to be of the order of 1.5 meters (r.m.s.) (see Marsh and Williamson, 1980; Lerch et al., 1982).⁽¹⁾

The reasons why the ephemeris are not exact are multiple: errors in tracking data and in tracking station coordinates; the abundance and distribution, temporal as well as geographical, of these data; imperfect refraction corrections in the tracking; errors in the models for calculating the forces that shape the orbit, etc. Of the force errors, the most prominent, at present, are errors in the gravitational field model, followed at some distance by errors in the models of surface forces such as air drag and solar radiation pressure. The last two are particularly serious in satellites like SEASAT, because of the large solar panels needed to feed their power-hungry equipment, as well as the presence of a number of large antennas and other objects of complex shape, all of which is made worse by the changing attitude of the spacecraft, as this varies the effective cross-section opposed to the surface forces. Often today orbits are estimated assuming that a satellite is a

⁽¹⁾Horizontal orbital errors can be disregarded. They are, at present, of the order of less than 100 m, and because of the smoothness of the sea-surface (averaged over the cross-section of the radar altimeter beam, or footprint, usually 1 km or more in diameter) their effects on the accuracy of the calculated height is negligible. Numerical integration errors in precise ephemeris are insignificant.

homogeneous sphere, a "cannonball", and then trying to compensate for the obvious deficiencies of this model by adjusting, together with the initial position and velocity, the coefficients that scale the drag and the solar pressure; this is usually done at intervals shorter than the total length of the arc, such as once per day (Marsh and Williamson, *ib.*, 1980). A study of the consequences of using various simplistic, but practical, ways of handling the surface forces can be found in (Colquitt et al., 1980).

If Λ_m is the (pre-processed) altimeter measurement, h_{sc} the computed satellite ellipsoidal height, and Δh_s the error in the latter, then the calculated value h_{wc} of h_w obtained from h_c and Λ_m is, according to (3),

$$\begin{aligned}
 h_{wc} &= h_{sc} - \Lambda_m \\
 &= (h_s + \Delta h_s) - (\Lambda + \Delta\Lambda) \\
 &= h_w + \Delta r - \Delta\Lambda .
 \end{aligned}
 \tag{4}$$

where the error Δr in the computed radial geocentric distance to the satellite has been put in place of the ellipsoidal Δh_s , both being almost identical, to simplify the mathematical treatment. Replacing N and ζ_G according to (2a) and (2b) in (1) and the resulting expression for h_w in (4) leads to

$$h_{wc} = ((N_c - \Delta N) + w_o + \zeta_{Gc} - \Delta\zeta_G + w_c) + \Delta r - \Delta\Lambda .
 \tag{5}$$

Let

$$\Delta h_w = h_{wc} - (N_c + \zeta_{Gc}) \quad (6)$$

be the residual sea height. Subtracting N_c and ζ_{Gc} from both sides in (5) one gets, after rearranging terms,

$$\Delta h_w = \Delta r - \Delta N - \Delta \zeta_G + w_o + w_t - \Delta \Lambda, \quad (7)$$

where $\Delta \zeta_G = \zeta_{Gc} - (\zeta_o + \delta + \delta')$, δ' being the yielding of the solid Earth to the ocean tide ζ_o , and δ the solid Earth tide.

On present evidence, and according to the way in which they have been defined above, ΔN , Δr , $\Delta \zeta_G$ and w_o seem to have mostly long-wavelength spatial features (larger than 1000 km). The r.m.s. for each term in (7) is thought to be: 2 m or less (today) for both Δr and ΔN ; nearly 1 m for w_o and for the geocentric tide; less than 0.1 m for w_t (except over a small percentage of the sea surface); and 0.1 m (or less) for $\Delta \Lambda$, provided there is a microwave radiometer onboard, as in SEASAT, that can measure the amount of water vapor along the altimeter beam, to estimate accurately the delay due to "wet" tropospheric refraction.

3.0 ORBITS

3.1 Orbital Motion and Keplerian Elements

As the orbits considered here are approximately elliptical, it is convenient to formulate their theory in coordinates that make the description of elliptical motion particularly simple. Among several possible choices, the most common is that of the six quantities known as the osculating Keplerian elements, which can be translated into the three Cartesian coordinates (x, y, z) for position and the three $(\dot{x}, \dot{y}, \dot{z})$ for velocity, and vice versa, in an unambiguous way (see Table 1(a-b) and Fig. 1). Keplerian elements are used in the classical analytical theory of satellite geodesy. This theory has its origins in the old method for the study of planetary perturbations known as "Variation of Constants" (see Brouwer and Clemence, 1961), adapted by geodesists, in the early days of the "Space Age" (late 'fifties and early 'sixties), to the special task of mapping the complex gravitational field of the Earth.

Before defining the "elliptical" coordinates, consider a Cartesian system with the origin at the center of mass of the Earth, or geocenter, the \vec{x} and \vec{y} axes on the plane occupied by the equator at the start of the orbit, or equator of epoch, the \vec{z} axis aligned with the Earth's spin axis at that epoch, and the \vec{x} axis lying along the intersection of the equator with the plane of the ecliptic, and pointing towards the vernal equinox. The orientation is fixed with respect to the distant stars; in general,

because the whole Earth, including its center of mass, is accelerated by external gravitational forces (the pull of the Sun, the Moon and the other planets), the system is quasi-inertial. The analytical theory is developed as if it were truly inertial, by making use of the idea of tidal potential as explained in the section "Tides".

The osculating ellipse is the two-body orbit that the satellite will begin to follow, from the point of view of an observer fixed to the system just defined, if, while driven only by their mutual gravitational attraction, both the Earth and the spacecraft were to shrink suddenly at time t , becoming point-like particles situated at their original centers of mass, but each retaining its velocity and momentum. The mass-center of the satellite would still have the same position vector \underline{r} with respect to the geocenter (the modulus $|\underline{r}|$ being the geocentric distance r) and the same velocity vector $\dot{\underline{r}}$, which means that the osculating ellipse is tangent to the true orbit at time t (hence its name). Because of the nature of Newtonian physics (which is the one used here) given \underline{r} and $\dot{\underline{r}}$ at t , the trajectory after t is entirely determined, so the osculating ellipse is defined by these two vectors. Furthermore, it lies entirely in the same plane as them, the instantaneous orbital plane, and has one

focus at the geocenter.⁽¹⁾ The ascending node is where the satellite would cross the equator going north if it were to continue along the osculating ellipse, and the descending node is the point where it would cross that plane going south. The line of nodes, determined by these two points, is the trace of the instantaneous orbital plane on the equator. The closest point to the geocenter is the perigee, the furthest is the apogee; they lie at opposite ends of the major axis of the ellipse, or line of apsides. The osculating Keplerian elements a, e, I, Ω, ω and M are: the semi-major axis a , the eccentricity e ($0 < e < 1$), the inclination I (angle between the equator and the orbit plane), the argument of the node Ω (angle between the \vec{x} axis and the line of nodes as shown in Figure 1), the argument of perigee ω (angle between the line of nodes and the major axis), and the mean anomaly M . The latter is related to the eccentric anomaly E (shown in Figure 1) through Kepler's equation

$$M = E - e \sin E, \quad (8)$$

(1) The reason why the osculating ellipse of the satellite has a focus at the geocenter is not the much smaller mass of the satellite, compared to that of the Earth. Even if both bodies had the same mass, or the system were attached to the center of mass of the satellite, rather than to the Earth's, the focus would still be at the origin of coordinates. This is because the osculating ellipse describes the instantaneous relative motion of one center of mass with respect to the other, whatever the masses involved, as long as the relative velocity is below the escape value (see, for example, Brouwer and Clemence (ib., Ch. I, 1961)). An example is the "orbit" of the Sun in classical tidal theory (see paragraph "The tidal forces").

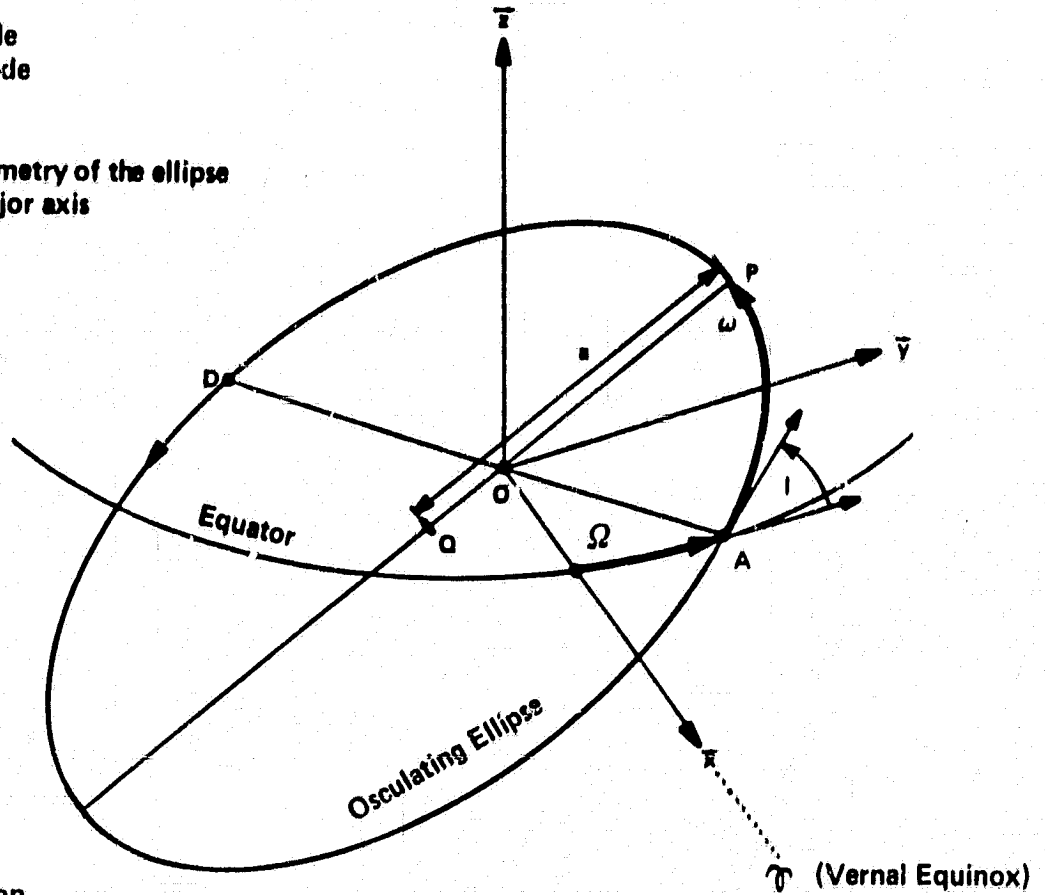
a transcendental equation in E which must be solved iteratively, given M . The mean anomaly would be the angular distance from perigee of a satellite moving at a constant angular velocity equal to n , the mean motion,

$$n = (\mu a^{-3})^{1/2} \tag{9}$$

$$= \frac{d}{dt} M(t) ,$$

where $\frac{d}{dt} M(t)$ is the rate of change of M in the osculating ellipse, μ is the product of G (the universal constant of gravitation) times the sum ($M_e + M_s$) of the masses of the Earth and the satellite. As $M_e \gg M_s$, this reduces to $\mu = G M_e$. If the Earth and the spacecraft were truly particles, (9) would be Kepler's Third Law, and the orbital period would be $T_o = 2\pi n^{-1}$. The ground track of a satellite is the line described on the Earth's surface by the point directly below the spacecraft, or subsattellite point. Table 1c gives the relationship between the elements and ϕ and λ at the subsattellite point. Because of the rotation of the Earth and the motion of the satellite, the ground track is a (nearly) spherical helix wound up between the parallels of latitude $\pm I$. The pitch of this helix depends on the ratio between the terrestrial and the orbital angular frequencies. By tuning the orbit carefully, the helix can be made to close upon itself after a given number of days, forming a repeating ground track which is also rotationally symmetrical with respect to the Earth's axis. This is done sometimes in Earth-surveying missions, including altimeter ones.

- A : ascending node
- D : descending node
- P : perigee
- O : geocenter
- Q : center of symmetry of the ellipse
- $\overline{QP} = a$, the semimajor axis



- S : satellite position
- S' : projection of S on circle of radius $a = \overline{QP}$
- E : eccentric anomaly
- f : true anomaly

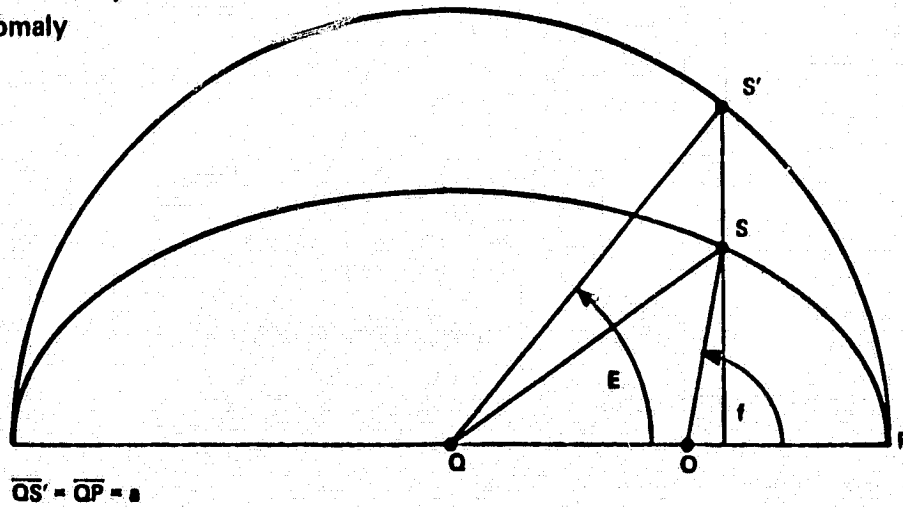


FIGURE 1. Geometry of the Osculating Ellipse

TABLE 1(a)

CONVERSION FROM INERTIAL TO ELLIPTIC COORDINATES

Given $\underline{r} = x\underline{i}^* + y\underline{j}^* + z\underline{k}^*$
 $\underline{\dot{r}} = \dot{x}\underline{i}^* + \dot{y}\underline{j}^* + \dot{z}\underline{k}^*$

where \underline{i}^* , \underline{j}^* , \underline{k}^* are unit vectors in the directions x , y , z .

1. Compute a . Let

$$r = |\underline{r}| = (x^2 + y^2 + z^2)^{1/2}$$

and

$$v = |\underline{\dot{r}}| = (\dot{x}^2 + \dot{y}^2 + \dot{z}^2)^{1/2}$$

Then

$$a = \frac{r \mu}{2\mu - v^2 r}$$

2. Compute e

$$e \cos E = 1 - \frac{r}{a}$$

$$e \sin E = \frac{\underline{r} \cdot \underline{\dot{r}}}{\sqrt{\mu a}}$$

$$e = \sqrt{e^2 \cos^2 E + e^2 \sin^2 E}$$

3. Compute M

$$E = \text{tg}^{-1} \left(\frac{e \sin E}{e \cos E} \right)$$

(E is in the quadrant where $e \sin E$ and $e \cos E$ have their signs as in the previous step.)

$$M = E - e \sin E \quad (M > \pi \text{ if } E > \pi)$$

4. Compute Ω

$$\Omega = \text{tg}^{-1} \left(\frac{y\dot{z} - z\dot{y}}{xz - zx} \right)$$

(Same comment as for E , regarding the signs of numerator and denominator inside the brackets.)

5. Compute I

$$I = \text{tg}^{-1} \left(\frac{1}{\cos \Omega} \frac{-z\dot{x} + x\dot{z}}{xy - yx} \right) \quad (I \text{ is always less than } \pi.)$$

6. Compute ω

$$\omega = \text{tg}^{-1} \left[\frac{z}{(\sin I)(x \cos \Omega + y \sin \Omega)} \right]$$

$$- 2 \text{tg}^{-1} \left(\sqrt{\frac{1+e}{1-e}} \tan \frac{E}{2} \right)$$

(See comments for E and for Ω .)

TABLE 1(b)

CONVERSION FROM ELLIPTIC TO INERTIAL COORDINATES

1. Compute the constants

$$P_x = \cos \Omega \cos \omega - \sin \omega \cos I \sin \Omega$$

$$Q_x = -\cos \Omega \sin \omega - \cos \omega \cos I \sin \Omega$$

$$P_y = \sin \Omega \cos \omega + \sin \omega \cos I \cos \Omega$$

$$Q_y = -\sin \Omega \sin \omega + \cos \omega \cos I \cos \Omega$$

$$P_z = \sin I \sin \omega$$

$$Q_z = \sin I \cos \omega$$

2. Compute E

Solve Kepler's equation

$$E = M - e \sin E$$

iteratively, starting with $E^{(0)} = M$.

3. Compute $xyz\dot{x}\dot{y}\dot{z}$

$$\underline{r} = \underline{p} a (\cos E - e) + \underline{q} a \sqrt{1-e^2} \sin E$$

$$\underline{\dot{r}} = \frac{\sqrt{\mu} \sqrt{a}}{r} [\underline{q} \sqrt{1-e^2} \cos E - \underline{p} \sin E]$$

where

$$\underline{p} = P_x \underline{i}^* + P_y \underline{j}^* + P_z \underline{k}^* \quad \text{and} \quad \underline{q} = Q_x \underline{i}^* + Q_y \underline{j}^* + Q_z \underline{k}^*$$

TABLE 1(c)

CONVERSION FROM ELLIPTIC TO SPHERICAL COORDINATES

1. Compute
- r

$$r = a(1 - e \cos E) \quad \text{where}$$

$$E = M + \left(e - \frac{e^3}{8}\right) \sin M + \frac{1}{2} e^2 \sin 2M + O(e^3)$$

(or solve Kepler's equation iteratively, as suggested in Table 1b).

2. Compute the
- true anomaly
- f
- (shown in Figure 1)

$$f = M + \left(2e - \frac{1}{4} e^3\right) \sin M + \frac{5}{4} e^2 \sin 2M + O(e^3)$$

which is the equation of the center (for rough calculations, $f=M$ is acceptable if e is small).

3. Compute
- ϕ

$$\phi = \sin^{-1} [\sin I \sin(\omega + f)]$$

where $\sin^{-1}(0) = 0$ and ϕ is in the same quadrant as $\omega+f$ if $-\frac{\pi}{2} < \omega+f < \frac{\pi}{2}$, otherwise it is in the same quadrant as $\pi - (\omega+f)$.

4. Compute
- λ

$$\lambda = \sin^{-1} [\cos I \sin(\omega+f)/\cos\phi] + \Omega - \theta,$$

where θ is the sidereal angle of Greenwich, and $\lambda - \Omega + \theta$ is in the same quadrant as $(\omega+f) \operatorname{sign} \left[\frac{\pi}{2} - I\right]$ if $I \neq \frac{\pi}{2}$; when $I = \frac{\pi}{2}$, $\lambda - \Omega + \theta = 0$ if $\omega+f < \pi$, and $\lambda - \Omega + \theta = \pi$ if $\omega+f > \pi$ (of course, λ is not defined at the poles).

These expressions for ϕ and λ are the equations of the ground track.

Knowledge of a , e , I , Ω and ω determines the size, shape and orientation of the osculating ellipse relative to the \vec{x} , \vec{y} , \vec{z} axes, while M defines the position of the satellite in that ellipse and (together with a , e and μ) also its velocity. Consequently, these six elements are equivalent to $x, y, z, \dot{x}, \dot{y}, \dot{z}$, and can be used instead of them. The advantage of doing so is that they do not vary nearly as much along the orbit, with the exception of M , as the Cartesian coordinates and their derivatives do. There are other groups of six orbital variables used as coordinates (see Giacaglia, 1977, for example), but the Keplerian elements are sufficient for the purpose of this study.

Satellites are sizeable, complex objects, so a full theory of their movements requires many more than six state variables. They spin, tumble (if not properly stabilized) and even change shape. Their detailed dynamics can be quite difficult to describe and doing so is the purpose of attitude control theory (see, for example, Kaplan (1976)). Any spacecraft considered here is designed to be sufficiently rigid so, once its attitude has been determined with the help of on-board sensors, the location of its center of mass relative to the altimeter is also well known. In such a "rigid" satellite, the position and velocity of the center of mass vary in time much like those of a material point with the same mass and driven by the same forces. For this reason, satellites are discussed here as if they were particles, and expressions such as "state", "position" and "velocity" actually refer to their centers of mass.

3.2 The Mean Ellipse

Averaging the osculating elements up to time t over many revolutions of the orbiting body gives the mean elements \bar{a} , \bar{e} , \bar{I} , $\bar{\Omega}$, $\bar{\omega}$ and \bar{M} at this time. These running averages describe the slow trends in the evolution of the orbit. They define a gradually changing mean ellipse. Usually, the main variations in this ellipse are: a steady, slow turning of its plane about the Earth's axis (precession of the line of nodes), a rotation of the major axis in the mean orbit plane about the geocenter (precession of the argument of perigee), and a slight departure from Kepler's Third Law (expression (9)) in the orbital frequency.⁽¹⁾ These changes occur because the Earth is not a homogeneous sphere, but a rather flattened ellipsoid.

For an Earth-orbiting satellite, and except for equatorial orbits ($I = 0$) where the line of nodes is not defined, the precession of the nodes is given by the approximate law

$$\dot{\Omega} \approx \frac{3}{2} \bar{n} C_{200} \left(\frac{R}{\bar{a}}\right)^2 (1-\bar{e}^2)^{-2} \cos \bar{I}, \quad (10)$$

where $\bar{n} = (\mu/\bar{a}^3)^{1/2}$, R is the mean equatorial Earth radius, and C_{200} is the second zonal potential coefficient (this notation shall be explained

(1) A further explanation of the behaviour of the mean ellipse is given later, in the paragraphs "The equations of motion in Keplerian elements", "The 'frozen', repeat orbit", et seq.

later, see formula (26)).⁽¹⁾ Expression (10) shows that $\dot{\Omega}$ is ruled mostly by the gravitational pull on the satellite of the equatorial bulge represented by C_{200} . This pull adds a force normal to the orbital plane (except when the orbit is polar), causing this plane to precess much as a gyroscope does, and for the same reasons: to maintain the angular momentum vector constant in inertial space. Therefore, $\dot{\Omega} \neq 0$ unless $I = \frac{\pi}{2}$. For some values of \bar{a} , \bar{e} and \bar{I} , $\dot{\Omega} \sim 1^\circ/\text{day}$ and the orbital plane completes a full revolution in one sidereal year. Such an orbit is known as heliosynchronous because it follows the Sun, keeping the angle between its plane and the direction Earth-Sun approximately fixed. A heliosynchronous orbit is chosen, sometimes, so that some onboard devices may maintain a proper orientation relative to the Sun. Possible examples could be the orbits of ERS-1 (Dow and Klinkrad, 1982) and POSEIDON (see POSEIDON report, 1983).

The story for $\dot{\omega}$ is somewhat more complicated. If \bar{e} is large enough, $\dot{\omega}$ is also governed by C_{200} according to the expression

$$\dot{\omega} \approx \frac{3}{4} \bar{n} C_{200} \left(\frac{R}{\bar{a}}\right)^2 (1-\bar{e}^2)^{-2} [1-5 \cos^2 \bar{I}], \quad (11)$$

so at $\bar{I} = \arccos \sqrt{\frac{1}{5}} \approx 63.4^\circ$, (or $\approx 116.6^\circ$), known as the critical inclinations, $\dot{\omega} \approx 0$, changing sign as \bar{I} goes through this value. However, for very low eccentricities (as those of the orbits of altimeter

(1) $R \sim 6378.2$ km; $\mu \sim 398600.3$ km³/sec²; $C_{200} \sim -1082.63 \times 10^{-6}$; the 3rd zonal $C_{300} \sim 2.5 \times 10^{-6}$, and $C_{n00} < C_{300}$ for all $n > 3$.

satellites) and depending on \bar{a} , \bar{I} and \bar{e} , the perigee may not precess at all but librate (oscillate slowly) about a mean value of $\pi/2$, or even stay for a very long time at $\pi/2$ with no significant change, as in the so-called "frozen orbits" (see Cook, 1966, and Hough, 1981), which are important for altimetry because they can have very precisely repeating ground tracks (Cutting et al., 1980; Dow and Klinkrad, ib. 1982). In the precessing case, the period $2\pi/\dot{\omega}$ of a complete revolution of the perigee is known as the apsidal period.

The oblateness of the Earth also affects \dot{M} , making it slightly different from the Keplerian mean motion \bar{n} :

$$\dot{M} \approx \bar{n} \left\{ 1 - \frac{3}{4} C_{200} \left(\frac{R}{a} \right)^2 (1 - \bar{e}^2)^{-3/2} [3 \cos^2 \bar{I} - 1] \right\}. \quad (9')$$

Values of $\dot{\Omega}$ and $\dot{\omega}$ of $\pm 3^\circ$ per day, and of \dot{M} of 13-14 revolutions per day, are typical for the satellites discussed here. For a near circular orbit ($\bar{e} \sim 10^{-3}$), the orbital frequency (of successive passages through the ascending node) fluctuates slightly in each apsidal period about $\dot{M} + \dot{\omega}$. Itself quite close to \dot{M} (as $\dot{\omega} \ll \dot{M}$), the angular frequency $\dot{M} + \dot{\omega}$ appears in many important analytical expressions of orbit theory that will be seen later on.

The combined influence of C_{300} and other zonals makes orbits with $\bar{e} = 0$ unstable, forcing them to become gradually more eccentric (until $\bar{e} \sim 10^{-3}$ for altitudes of about 1000 km, see expression (49)).

Otherwise, changes in \bar{a} , \bar{e} , and \bar{I} are negligible, specially over the week or so that is the normal duration of the orbit arcs considered here. Variations in \bar{I} , always very small, are somewhat more pronounced in the heliosynchronous case; they are caused mostly by the Sun's gravitational attraction.

NOTE: While the time derivatives of \bar{M} , $\bar{\omega}$, etc. are $\dot{\bar{M}}$, $\dot{\bar{\omega}}$, etc., those of the osculating elements are $\dot{M}(t)$, $\dot{\omega}(t)$, etc.

An orbit is shaped not only by gravitation, but also by surface forces such as air-drag and electromagnetic radiation pressure, which tend to change considerably the total mean energy \bar{E} (kinetic + potential). With the sign convention adopted in physics, for spacecraft moving below the scape velocity (at which \bar{a} turns infinite) this energy is

$$\bar{E} = -\mu/2\bar{a} \quad . \quad (12)$$

Clearly, the decrease of \bar{E} implies the decrease of \bar{a} (notice that \bar{E} is negative), which, in turn, means the increase of the mean velocity \bar{v} (for nearly circular orbits) because

$$\bar{v} \sim (\mu/\bar{a})^{1/2} \quad . \quad (13)$$

Therefore, dissipative forces like air drag tend to bring a spacecraft down while accelerating it. This is true as long as the braking force is gentle and the orbit remains close to circular, but is no longer the case when a satellite re-enters the denser layers of the atmosphere. The effect of drag on orbital motion has been explained in detail by

King-Hele (1964). As for electromagnetic radiation pressure (principally caused by the light of the Sun, either received by the spacecraft directly, or else reflected, or re-radiated as heat, from the Earth), its effect can be either a loss or a gain of energy, depending on the direction of the incoming rays, which may either push forward or brake the satellite. A paper by Rubincam (1982) gives a thorough description of non-gravitational forces, besides drag and radiation pressure, and also lists many references on this subject.

3.3 The Reference Orbit

Altimeter satellites are placed in orbits of small eccentricity to keep the distance to the surface below always close to the optimum range of their instruments. They are also put high enough to make air drag small, but sufficiently low to have short orbital periods and, sometimes, finely spaced ground tracks. The inclinations are chosen so most of the ocean surface is scanned. These and other often conflicting requirements result in compromise orbits that are, typically, about 1000 km high ($\bar{a} \sim 7300$ km), nearly circular ($e \sim 10^{-3}$), and with inclinations larger than 60° . The orbital periods are all close to 1.7 hours, or some 14 revolutions per day. Departure from circularity is of the order of ± 10 km. The ephemerides are calculated, usually, in arcs of up to one week in duration; their position and velocity errors nowadays are, according to available evidence, of the order of a few meters and a few millimeters per second, respectively. These errors are

sufficiently small to be studied using a first order orbit perturbation theory. The one introduced in this section is atuned to the particular characteristics of the orbits of altimeter satellites. It differs from the more conventional formulation (Kaula, 1966) in the choice of the reference orbit based on which the equations of motion and other relationships are linearized.

In the standard treatment, the reference orbit is a precessing ellipse of constant e , a , and I with M , Ω and ω varying according to expressions (9'), (10) and (11). This orbit is governed by the Earth's "central force term" μ/r and the attraction of the equatorial bulge alone. In what follows, instead, the reference orbit consists of a precessing ellipse defined by the arc averages \bar{a} , \bar{e} , \bar{I} , $\dot{\bar{\Omega}}$, $\dot{\bar{\omega}}$ and $\dot{\bar{M}}$ of the corresponding computed osculating elements and their rates, together with starting values $\bar{\Omega}_0$, $\bar{\omega}_0$ and \bar{M}_0 at time t_0 , the beginning of the arc, that give the best fits to Ω , ω and M , in the sense that $\bar{\omega}_0 + \dot{\bar{\omega}}(t-t_0) \sim \omega(t)$, etc. The rate $\dot{\bar{\Omega}}$, in particular, is always quite close to the value given by expression (10). In general, unless the orbit is stabilized by on-board rocket engines, the mean elements and their rates will be different from one arc to the next, but this change should be very small.

To see if the choice of the weekly reference orbit is reasonable, one can look at the actual orbit of SEASAT according to the ephemeris published by the Jet Propulsion Laboratory (Bauer, 1978). During its last

month in operation (mid-September to mid-October of 1978), the satellite was kept in a "frozen", repeat orbit (i.e., with a repeating ground track and $\dot{\omega} \sim 0$). Over that period, \bar{a} decreased some 20 m per week, or 3 parts per million of its average value of 7169 km, while \bar{e} and \bar{T} changed, in any of the four weeks, by less than 1% of their monthly averages of 10^{-3} and 108° , respectively. Likewise, $\dot{\omega}$ fluctuated slightly each week about a mean of less than 1° per month; also the orbital frequency (approximately $\dot{M} + \dot{\omega} \sim \dot{M}$), as indicated by the log of equatorial crossings, departed by less than 1 part in six thousand from its overall monthly average of about one cycle every 101 minutes, while $\dot{\Omega}$ was close to 15° per week, and nearly constant. Therefore, the type of reference orbit adopted here can be a reasonable approximation to the true mean ellipse, over a weekly arc, at least for satellites like SEASAT.

The radial orbital error is, at present, of the order of a few meters for altimeter satellites. The mean ellipse, on the other hand, can be several kilometers away from the true position of the spacecraft, mostly because of short period perturbations due to the large second and third zonals (caused by the oblateness and "pear-shape" of the Earth). Is it valid to describe, at least qualitatively, the radial error using a first order perturbation theory based on such a reference orbit?

To separate the useful signal from the radial orbit error Δr it is more important to know well the frequencies and phases of the spectral lines of this error than the precise values of the amplitudes. From this

point of view, the choice of reference orbit made here is probably adequate. In fact (as shown later), the corresponding perturbation theory seems to explain quite well the results of some computer simulations, at least qualitatively.

3.4 The Radial Orbit Error

The error that matters here is that in the geocentric distance r , i.e., Δr in expression (7). In osculating Keplerian elements, this distance is

$$r = a(1 - e \cos E) ,$$

where, expanding E as a function of M , as in Smart (Ch. V, par. 71, 1931 (6th ed., 1977)), one gets, to the order of e^3 (or $O(e^3)$),

$$\cos E = \left(1 - \frac{1}{8} e^2\right) \cos M - \frac{1}{2} e \cos 2M + \frac{3}{8} e^2 \cos 3M$$

so

$$r = a(1 - e \cos M) + O(e^2) . \quad (14)$$

Because of the small eccentricity of an altimeter satellite ($\sim 10^{-3}$), the second term in (14) can be neglected, and

$$r = a(1 - e \cos M) . \quad (15)$$

This equation applies also to the mean ellipse, so the maximum radial departure of the mean orbit from a circle is $\bar{a}\bar{e}$, or some 10 km for $e \sim 10^{-3}$ and $\bar{a} \sim 10^4$ km. Differentiating (15) gives the first order approximation to the radial error

$$\Delta r = \Delta a - (\Delta \bar{a} \bar{e} + \Delta e \bar{a}) \cos \bar{M} + \Delta M \bar{a} \bar{e} \sin \bar{M} , \quad (16)$$

where

$$\bar{M} = \dot{\bar{M}}(t - t_0^k) + \bar{M}(t_0^k) \quad (17)$$

and t_0^k is the time (or epoch) when the k weekly arc starts; the overbars indicate that the partial derivatives are taken on the reference orbit corresponding to this arc.

3.5 Temporal Characteristics of the Error

The frequency spectra of Δa , Δe and ΔM can be separated into four parts. The first three are sets of well defined lines with frequencies ranging: (a) from zero to a small fraction of a cycle per year; (b) from a small fraction of a cycle per year to a cycle every few months; (c) from a cycle every few months to about 50 cycles per day. Superimposed on these lines there is (d) a continuous background, due mostly to the inaccuracies in the modelling of the surface forces.

(a) Practically Constant Part: Over one week or less, any oscillation in the lowest range of frequencies is indistinguishable from a constant, and it will be regarded here as such. If Δa , Δe and ΔM in (16) are constants, the resulting Δr consists of an offset between the computed and the true orbit, equal to Δa , and of an oscillation at frequency \dot{M} , which is close to $(\dot{M} + \dot{\omega})$, or about one cycle per revolution. The amplitude of this oscillation is $[(\Delta a \bar{e} + \Delta e \bar{a})^2 + (\Delta M \bar{a} e)^2]^{1/2}$.

(b) Nearly Secular Part: Oscillations with periods in the second band may show appreciable variations during one week, but their rate of change will vary so slowly that they will resemble secular changes. If t_0^k is the time at the beginning of the k weekly arc, these changes can be approximated very well by expressions of the form $c^k(t-t_0^k) + d^k(t-t_0^k)^2$ (where c^k and d^k are constant and $c^k \ll d^k$) for all the Keplerian elements. Both c^k and d^k will vary slightly from one arc to the next.

The plots of the corresponding Δa , Δe , ΔM , etc., versus time will depart from straight lines just enough to show that they are not truly secular. These slow variations must be reflected in Δr , according to (16), as a slow change plus an increasing oscillation of frequency \dot{M} with a slightly bent (quadratic) envelope. As $\dot{\omega}$ is usually very small, \dot{M} will be very close to one cycle per revolution.

(c) Periodical Part: Mostly caused by errors in the geopotential field model, it consists of sinewaves whose frequencies depend on the rates $\dot{\Omega}$, $\dot{\omega}$ and \dot{M} of the reference orbit, as well as on the spin rate of the Earth, $\dot{\theta}$. Because these frequencies are higher than those of the errors mentioned previously, the oscillations in this band will be called, in what follows, "shorter period" errors. Other periodic errors are produced by uncertainties in the tidal models; these are smaller and have different frequencies, in general, than those due to the field model.

(d) Other Temporal Variations: While they may also include secular variations and oscillations, errors caused by inadequately modelled surface forces, etc., do not have sharply defined lines in their frequency spectra. During one week, however, probably much of their total effect on Δr not included in (a), (b), or (c) can be represented by a low degree polynomial (a cubic or a quartic) of the general form:

$$\Delta r^{(ng)} = \sum_{j=0}^J r_{jk}^{(ng)} (t-t_0^k)^j, \quad (18)$$

where J is a small integer, (ng) denotes "non-gravitational," and the $r_{jk}^{(ng)}$ are constants which may vary from arc to arc (" k " is the sequential number of the arc).

Errors in the calculated precession and nutation of the Earth modify some of the lines in the spectrum of Δr related to the diurnal tides. The periods of any significant effects are long enough for them to be lumped together with the constant, secular and polynomial parts (a), (b) and (d), and, in any case, their amplitudes are very small. Therefore, they will not be considered here further. For details, see Reigber (1981) (he considers the total effects of precession-nutation on the actual orbit).

Having outlined the features of the radial error, it is time to consider the mechanisms that shape them.

3.6 The Equations of Motion and Their Linearization

Let V be the part of the gravitational potential of the Earth (or geopotential) which is invariant in an Earth-fixed system of coordinates (the time-varying part due to the tides will be discussed in "Tides"); the gradient ∇V is the corresponding gravitational acceleration. If \underline{f} is a vector representing both tidal and non-gravitational accelerations, then the Newtonian equations for the motion of the center of mass of a satellite in an inertial frame can be written in vector form as

$$\ddot{\underline{r}} = \nabla V(\underline{r}, t) + \underline{f} ; \quad (19)$$

V is given here as a function of both position and time, because the field is rotating along with the Earth. One interesting consequence of this time dependence is that the total energy (kinetic+potential) of the satellite in an inertial system of coordinates is not conserved, in general. Only a central force field, or a zonal field, both of them invariant with respect to a rotation about the \hat{z} axis, are conservative; not so the more irregular field of our planet, except in Earth-fixed

coordinates.⁽¹⁾ For a discussion of this problem, see Hotine (Ch., 28, 1969). In general, f is also a function of \underline{r} , t , and $\dot{\underline{r}}$.

The accelerations in (19) are nonlinear functions of \underline{r} (think, for example, of the simple case of the field of a particle, where $|\nabla V| = \mu r^{-2}$). For the treatment that follows, (19) has to be expressed in terms of the Keplerian elements and of θ , the sidereal angle of Greenwich that accounts for the Earth's rotation. Lagrange obtained his transformation of the equations of motion by a very ingenious and rather laborious process described in Brouwer and Clemence (ib., 1961) and also in Kaula (ib., 1966). The end-product is a system of six first order differential equations, Lagrange's Planetary Equations, one for each osculating element " s_i " ($i = 1, 2 \dots 6$); as used in geodesy, they are of the general form

$$\dot{s}_i = L_{s_i} (a, e, I, \Omega, \omega, \theta, M, \beta, \underline{s}_0^k), \quad (20)$$

(1) The potential part of the total energy depends, like V , on the position of the satellite relative to each of the particles that form the Earth. Such relative positions and the resulting V are coordinate invariant. The kinetic energy, on the other hand, is proportional to the square of the velocity, which depends on how the spacecraft moves with respect to the reference frame, so it is not coordinate invariant. In any reference frame, however, the sum of the potential and kinetic energies of the spacecraft and the Earth are constant. To keep the books straight, the Earth must change its own velocity in the chosen frame, to compensate for the variations in the kinetic energy of the satellite; our planet being, by far, the more massive of the two bodies, such changes are imperceptible. The only system where an orbit must have always a constant total energy is, therefore, an Earth-fixed system which moves and rotates with the planet, so the velocity of the planet is always zero.

where L_{s_i} is a nonlinear function, $\underline{\beta}$ is a vector of parameters that appear in the expressions of V and \underline{f} , and \underline{s}_0^k is the vector of the initial conditions at $t = t_0^k$ (the start of the k arc):
 $\underline{s}_0^k = (a_0^k, e_0^k, I_0^k, \omega_0^k, M_0^k, \Omega_0^k - \theta_0^k)$. These equations are shown in detail later (expressions (36)).

To first order, the error $\Delta \dot{s}_i$ in \dot{s}_i due to small errors $\Delta \beta_j$ and Δs_{i0}^k in the components β_j of $\underline{\beta}$ and s_{i0}^k of \underline{s}_0^k , respectively, can be approximated by the differential of \dot{s}_i which, according to (20), is

$$\Delta \dot{s}_i = \sum_j D_{\beta_j} (L_{s_i}) \Delta \beta_j + \sum_{u=1}^6 D_{s_{u0}} (L_{s_i}) \Delta s_{u0}^k, \quad (21a)$$

where the derivatives are taken at $s_i = \bar{s}_i$ and

$$\begin{aligned} D_{\beta_j} (L_{s_i}) &= \frac{\partial L_{s_i}}{\partial \beta_j} + \sum_{u=1}^6 \frac{\partial L_{s_i}}{\partial s_u} \frac{\partial s_u}{\partial \beta_j} \\ &= \frac{\partial \dot{s}_i}{\partial \beta_j}, \end{aligned} \quad (21b)$$

while $D_{u_0}(L_{s_i})$ has a similar expression. Equation (21a) is the general form of the linearized equations of motion, and (21b), that of the variational (or sensitivity) equations. The variationals, which make up the "skeleton" of the linearized equations, are solved often by themselves to find the values of the unknown $\partial s_u / \partial \beta_j$. These values, in turn, are used to calculate the elements of the matrix of "partials" needed for orbital adjustments, force model improvements, sensitivity studies, etc. The sum in (21b) represents the dynamic terms, and $\partial L_{s_i} / \partial \beta_i$ the forcing terms of the variationals.

3.7 The Homogeneous Linearized Equations

The differential equations given by (21) are thoroughly coupled to each other through their "interaction terms" $\frac{\partial L_{s_i}}{\partial s_u}$, which multiply the unknown $\Delta s_{\beta_j} = \frac{\partial s_u}{\partial \beta_j} \Delta \beta_j$. They are also time-dependent, in general, like the $\frac{\partial L_{s_i}}{\partial s_u}$ themselves. These characteristics make the exact solution possible only by numerical integration with electronic computers. To obtain the analytical expressions needed for the present study it is necessary to resort to some simplifications. This limits the numerical accuracy of the solutions, but leaves virtually intact their qualitative properties, which are the ones of real interest here. The usual approach is to ignore the disturbing forces represented by \underline{f} in (19) (including all dissipative forces like drag) and also the departure of the terrestrial field from that of a perfect sphere (or of a point-like mass), thus

disregarding Earth-rotation as well. This dissipation-free, spherical approximation, can be accurate enough to describe the main characteristics of the errors in precise ephemeris calculated with force models that take already into account most of f and of the "non-spherical" part of V , so the main long period effects (particularly regarding \dot{M} and $\dot{\omega}$) are included in the mean ellipse of the computed arc, which is also the reference orbit here. The simplifications are more admissible when the inclination I is high and the eccentricity e is small, as in the case of altimeter satellite orbits, because most of the main terms ignored are proportional to e or to $\cos I$ (see Kaula, *ib.*, 1966, Ch. 4, par. 4.3).

In a spherical, or central, force field, when $f = 0$, the orbit of a satellite would be a simple ellipse obeying Kepler's Laws (two-body orbit). The elements a , e , I , ω and Ω would be constant for all time, and only M would change according to the Third Law: $\dot{M} = n = (\mu/a^3)^{1/2}$, where "n" is the mean motion. Consider a "true" elliptical orbit and a "computed version" of it obtained with the exact value of μ , (i.e., the field is known), and assume that they differ slightly in the initial values of their elements. Then $\Delta\dot{M}(t) = \dot{M}_{(\text{computed})} - \dot{M}_{(\text{true})} \approx \frac{\partial \dot{M}}{\partial a} \Delta a(t) = -\frac{3}{2} \frac{n}{a} \Delta a(t)$. Since none of the other s_i depend on t , $\Delta \dot{s}_i = 0$ for all of them. As now the osculating ellipse must be the same as the mean ellipse, $a = \bar{a}$ and $n = \bar{n} = (\mu/\bar{a}^3)^{1/2}$. Therefore, the effects of the initial state errors on the computed $a(t)$, $e(t)$ and $M(t)$ must satisfy

$$\Delta \dot{a}(t) = 0 \quad (21'a)$$

$$\Delta \dot{e}(t) = 0 \quad (21'b)$$

$$\Delta \dot{M}(t) = -\frac{3}{2} \frac{\bar{n}}{\bar{a}} \Delta a(t) , \quad (21'c)$$

These are three of the six homogeneous, or unforced, linearized equations of motion (i.e., all $\partial L_{s_i} / \partial \beta_j = 0$ in (21b)) for the spherical, dissipationless case. For I , ω and Ω the corresponding unforced equations are all of the form $\Delta \dot{s}_i = 0$, like (21'a-b), but they are not relevant to the study of Δr (see expression (16)). As the linearization is made along the computed orbit, both \bar{a} and \bar{n} correspond to this orbit.

3.8 Orbit Error Due to the Estimated Initial State

Each arc of the computed orbit is fitted to the tracking data by a least squares adjustment of the initial conditions⁽¹⁾ (the s_{i0}^k , where "k" is the number of the arc) and of a few other parameters, such as drag and

(1) "As all our observations, on account of the imperfection of the instruments and of the senses, are only approximations to the truth, an orbit based only on the six absolutely necessary data may still be liable to considerable errors. In order to diminish these as much as possible, and thus reach the greatest precision attainable, no other method will be given except to accumulate the greatest number of the most perfect observations, and to adjust the elements, not so as to satisfy this or that set of observations with absolute exactness, but so as to agree with all in the best possible manner."

Carl Friedrich Gauss, "Theoria Motus" (1857).

radiation pressure coefficients. The data, the coordinates of the tracking stations and the various force models used to integrate the orbit are not perfect, resulting in adjusted values that are wrong to some extent. To understand the radial errors that an incorrect initial state produces in the computed orbit, one can solve the approximate linearized homogeneous equations of motion (21') for Δa , Δe , and ΔM with the errors Δs_{i0}^k as initial conditions:

$$\Delta a(t) = \Delta a_o^k \quad (22a)$$

$$\Delta e(t) = \Delta e_o^k \quad (22b)$$

$$\Delta M(t) = -\frac{3}{2} \frac{\bar{n}}{a} \Delta a_o^k (t-t_o^k) + \Delta M_o^k, \quad (22c)$$

where t_o^k is the starting time of the arc. Kaula gives more complete expressions (ib., Ch.4, equations 4-25) by including small "interaction terms" $\frac{\partial L_{s1}}{\partial s_{uo}}$ approximately proportional to C_{200} that have been neglected in (21'a-b) because they would be zero for a spherically symmetrical Earth. As shown in (22), the adjusted initial conditions, by being slightly wrong, can cancel some of the constant errors in a and e , and some of the constant and secular errors in M . Replacing Δa , Δe and ΔM from (22) in (16), the contribution $\Delta r^{(1c)}$ of the initial conditions to the total radial error is

$$\begin{aligned}
\Delta r^{(ic)}(t) &= \Delta a_0^k + [-(\Delta a_0^k \bar{e} + \Delta e_0^k \bar{a}) \cos(\bar{M}_0^k - \dot{M} t_0^k) - (\frac{3}{2} \frac{\bar{n}}{a} \Delta a_0^k t_0^k + \Delta M_0^k) \bar{a} e \\
&\quad \sin(\bar{M}_0^k - \dot{M} t_0^k)] \cos \dot{M} t + [(\Delta \bar{a}_0^k \bar{e} + \Delta e_0^k \bar{a}) \sin(\bar{M}_0^k - \dot{M} t_0^k) - (\frac{3}{2} \frac{\bar{n}}{a} \Delta a_0^k t_0^k + \Delta M_0^k) \bar{a} e \\
&\quad \cos(\bar{M}_0^k - \dot{M} t_0^k)] \sin \dot{M} t - [\bar{a} e \frac{3}{2} \frac{\bar{n}}{a} \Delta a_0^k t_0^k \sin(\bar{M}_0^k - \dot{M} t_0^k)] t \cos \dot{M} t \\
&\quad - [\bar{a} e \frac{3}{2} \frac{\bar{n}}{a} \Delta a_0^k t_0^k \cos(\bar{M}_0^k - \dot{M} t_0^k)] t \sin \dot{M} t \\
&= \Delta a_0^k + A_k^{(ic)} \cos \dot{M} t + B_k^{(ic)} \sin \dot{M} t + C_k^{(ic)} t \cos \dot{M} t + D_k^{(ic)} t \sin \dot{M} t,
\end{aligned}
\tag{23}$$

where $A_k^{(ic)}, B_k^{(ic)}, C_k^{(ic)}$ and $D_k^{(ic)}$ are the values of the square brackets. In general, \dot{M} will change slightly from arc to arc, due to orbital decay.

3.9 The Free Response of the Linearized Equations and Resonance

Expression (23) gives the radial component of the unforced, homogeneous, or natural response of the linearized equations of motion. As the linearization has been done ignoring the term f that, in (19), accounts for all dissipative forces, (23) describes the behaviour of an undamped dynamic system, whose unforced response includes a non-decaying

oscillation of angular frequency \dot{M} , the natural frequency. In reality, there is damping due to drag, etc., but for orbits higher than 200 km this damping is very light. For altimeter satellites, where $\bar{e} \sim 0$, the system is virtually a stable harmonic oscillator.⁽¹⁾ The along track and across track free responses consist of similar oscillations, plus a slow secular drift along track, so the complete error due to initial state uncertainties makes the computed position "circle" the true one in an elliptical path once in every revolution of the spacecraft, while also moving slowly away from it along the orbit. When driven by a disturbing force that has a periodical component at a natural frequency, the forced response of an undamped system must contain growing oscillations of the same frequency. This is known as resonance. In the present case, this happens when the ephemeris crosses the same disturbance at repeated intervals equal to the period of \dot{M} , or about once per revolution. As shown later, certain errors in V and in f can produce this effect, which may grow into a large perturbation over a sufficiently long time.

The resonant character of the linearized equations is not plain from their formulation in Keplerian elements, but is quite clear when they are given in terms of the perturbations of the radial, along track and across track components of the position vector, and of their first time-

(1) The "unstable" last two terms of (23) appear only in a first order approximation to Δr . The actual effect is an oscillation of frequency \dot{M} modulated by a periodic envelope whose fundamental frequency is $\Delta\dot{M}$, the error in \dot{M} . As $\Delta\dot{M} \ll \dot{M}$, over a sufficiently short interval of time (in which the perturbations remain small) the envelope seems to be expanding very slowly, at a steady rate.

derivatives. Written in this way, the equations are sometimes known as Hill's equations (see Kaplan (1976), and also Colombo (ib., 1984, Ch. 1)).

The best known and most striking effect of resonance in the whole solar system is the series of gaps that divide the rings of Saturn. Inside each gap, any orbiting particles would have a period congruent with that of a major moon, but the gravitation of this moon disturbs greatly the motion of such particles, sweeping them out and keeping the gap open.

3.10 The Spherical Harmonic Expansion of the Geopotential in Keplerian Elements

Outside any ideal geocentric sphere S that contains virtually all the matter of the Earth, including that in the atmosphere, V (the time-invariant part of the potential in Earth-fixed coordinates) can be treated as a harmonic function satisfying Laplace's equation

$$\nabla^2 V = 0, \quad (24)$$

which expresses the conservation of the flux of lines of force in empty space.

Let the spherical coordinates (r, ϕ, λ) correspond to the geocentric distance, latitude and longitude in an Earth-fixed equatorial system, $\lambda=0$ being the longitude of the Greenwich Meridian. A spherical harmonic of degree n and order m has the form

$$Y_{nm\alpha}(\phi, \lambda) = P_{nm}(\sin \phi) \cos(m\lambda - \frac{\pi}{2} \alpha), \quad (25)$$

where P_{nm} is the associated Legendre function of the first kind with the same degree and order. The $Y_{nm\alpha}(\phi, \lambda)$ are orthogonal in the sense that the integral of $Y_{nm\alpha}(\phi, \lambda) Y_{n'm'\alpha'}(\phi, \lambda)$ over the unit sphere is zero if $n \neq n'$, or $m \neq m'$ or $\alpha \neq \alpha'$. The product $(\frac{R}{r})^{n+1} Y_{nm\alpha}(\phi, \lambda)$, known as a solid spherical harmonic, is a solution of Laplace's equation, and any other solution, V for example, can be expanded in a series of solid spherical harmonics

$$V = \frac{\mu}{R} \sum_{n=0}^{\infty} \sum_{m=0}^n \sum_{\alpha=0}^1 C_{nm\alpha} \left(\frac{R}{r}\right)^{n+1} Y_{nm\alpha}(\phi, \lambda) \quad (26)$$

outside any Earth-enclosing sphere S (see Hobson, Ch. III and IV, 1931, and Heiskanen and Moritz, Ch. I and II, 1967). R is usually the mean equatorial radius of the Earth; $C_{nm\alpha}$ is the (dimensionless) spherical harmonic potential coefficient of degree n and order m . By definition, $C_{000} = 1$ and all $C_{n01} = 0$, while all the $C_{lm\alpha} = 0$ in a geocentric system

(r, ϕ, λ) .⁽¹⁾ The geoidal height N has a similar expansion, with both r and μ/R replaced by R (this spherical approximation is quite adequate for the relatively low degree terms that dominate the geoid). The expansion of the geoid inside the sphere S (i.e., on the reference ellipsoid) is valid, but the reason for this is subtle (see Moritz, 1980). The error ΔV in V is

$$\Delta V = \frac{\mu}{R} \sum_{n=2}^{\infty} \sum_{m=0}^n \sum_{\alpha=0}^1 \Delta C_{nm\alpha} \left(\frac{R}{r}\right)^{n+1} Y_{nm\alpha}(\phi, \lambda) , \quad (27)$$

where the $\Delta C_{nm\alpha}$ are the errors in the coefficients of the field model, and they are zero for $0 < n < 1$.

To study the motion of satellites, these formulae have to be converted to osculating Keplerian elements; the details of the transformation are given in (Kaula, ib., 1966, Ch. 3). The variable

$$\theta' = \Omega - \theta , \quad (28)$$

(1) If the Cartesian \vec{z} axis were always aligned with the Earth's main axis of inertia, the $C_{21\alpha} = 0$. In the actual instantaneous field they are not zero but very small and time-varying, depending strongly on the definition of the "Earth-fixed" equatorial system (see Reigber, ib., 1981). Their mean values (which enter in the expansion of the time-invariant V) are also very small.

where θ is the Greenwich sidereal angle, must be used instead of Ω to take into account the rotation of the Earth. Introducing momentarily the true anomaly f (Figure 1), expression (25) can be written as⁽¹⁾

$$\begin{aligned}
 Y_{nm\alpha}(\phi, \lambda) &= \sum_{p=0}^n F_{nmp}(I) \cos [(n-2p)(\omega+f) - m\theta'] \\
 &\approx \sum_{p=0}^n F_{nmp}(I) c_{nm\alpha pq=0}(\omega, M, \theta')
 \end{aligned}
 \tag{29}$$

for small e , where

$$c_{nm\alpha pq}(\omega, M, \theta') = \cos \{ (n-2p+q)(\omega+M) - q\omega + m\theta' \} - \frac{\pi}{2} \left[\alpha + \frac{1}{2}(1-(-1)^{n-m}) \right]
 \tag{30}$$

Expression (29) will be used later on to formulate the ocean tides in Keplerian coordinates. Solid spherical harmonics can be written as functions of the osculating elements of a satellite at a point (r, ϕ, λ) as follows (Kaula, 1961):

$$\left(\frac{R}{r}\right)^{n+1} Y_{nm\alpha}(\phi, \lambda) = \left(\frac{R}{a}\right)^{n+1} \sum_{p=0}^n F_{nmp}(I) \sum_{q=-\infty}^{\infty} G_{npq}(e) c_{nm\alpha pq}(\omega, M, \theta')
 \tag{31}$$

(1) The approximation above would become exact if $e=0$. From the "equation of the center" and the expressions for ϕ and λ at the ground track (all given in Table 1c, see also Smart, *ib.*, 1931, ch. V), the maximum along track departure between a slightly elliptical orbit and a circular one of the same period is $\delta u \sim 2ae$ (consider the simple case where $I=0$, in Table 1c). For $e \sim 10^{-3}$ and $a \sim 10^3$ km, $\delta u \sim 20$ km, so (29) must hold well up to degree $n \sim 200$, i.e., up to spatial wavelengths of some 200 km.

The $F_{nmp}(I)$ and $G_{npq}(e)$ are commonly known as inclination and eccentricity functions, for obvious reasons; the $G_{npq}(e)$ are also called "Hansen's coefficients". There are expressions for computing the $F_{nmp}^{(I)}$ and the $G_{npq}^{(e)}$, some of which can be found in (Kaula ib., 1966, or in Giacaglia, 1977); they are not needed here.

For near circular orbits (small e), two important properties of the $G_{npq}^{(e)}$ are: that they are approximately proportional to $e^{-|q|}$, so they decrease very fast with increasing $|q|$, and that

$$\lim_{e \rightarrow 0} G_{npq}(e) = \begin{cases} 1 & \text{if } q = 0 \\ 0 & \text{otherwise} \end{cases} .$$

The expansion of V or ΔV , in Keplerian elements, takes the form

$$\begin{matrix} V \\ \text{or} \\ \Delta V \end{matrix} = \frac{\mu}{R} \sum_{n=0}^{\infty} \sum_{m=0}^n \sum_{\alpha=0}^1 \left(\frac{R}{a}\right)^{n+1} \begin{matrix} C_{nm\alpha} \\ \text{or} \\ \Delta C_{nm\alpha} \end{matrix} \sum_{p=0}^n F_{nmp}^{(I)} \sum_{q=-\infty}^{\infty} G_{npq}(e) c_{nm\alpha pq}(\omega, M, \theta) .$$

(32)

Because of the altitude attenuation factor $(R/a)^{(n+1)}$, the higher the degree of a spherical harmonic coefficient, or of its error, the lesser its effect on the potential and on the gravitational acceleration acting on the satellite. As a consequence, for computing near circular orbits, the series for V can be truncated roughly at degree $n \approx 2\pi R/(a-R)$, or $n \sim 40$ when $a - R \approx 10^3$ km. Also, except for a few coefficients,

mainly of low order ($n < 10$) or of "shallow resonant" order ($n=13-15, 26-30, 39-45$), the orbit errors due to the $\Delta C_{nm\alpha}$ tend to vary in proportion to the attenuation factor $(R/a)^{n+1}$ and the size of the $\Delta C_{nm\alpha}$. The latter ones, in today's models, appear to increase with n and m until they reach nearly 100% of the $C_{nm\alpha}$ at $n=m \sim 30$. Above this degree and order, the combined effect of all the estimated coefficients reproduce the data (tracking, altimetric ocean heights, gravimetry, etc.) reasonably well, but their individual values cannot be trusted. The size of the actual coefficients follows the approximate law

$$|C_{nm\alpha}| \approx \sigma_n^{1/2} \left\{ \frac{(n-m)!(2-\delta_{m0})}{(n+m)!} \right\}^{1/2}$$

where δ_{m0} is the delta Kronecker and

$$\sigma_n^{1/2} \approx \frac{10^{-5}}{n^2} (2n+1)^{1/2} \quad (33)$$

according to "Kaula's rule of thumb" (Kaula, *ib.*, 1966, Ch. 5, and Kaula, 1967); σ_n is the degree variance

$$\sigma_n = \sum_{m=0}^n \sum_{\alpha=0}^1 \frac{(n+m)! (C_{nm\alpha})^2}{(n-m)!(2n+1)(2-\delta_{m0})}, \quad (34)$$

and equals the mean square value (or "power") of the sum of all harmonics of V of degree n over the whole of the Earth's surface (see Kaula, 1967b). The quantity $\{\sigma_n/(2n+1)\}^{1/2}$ is approximately the average size of

the fully normalized coefficient $\bar{C}_{nm\alpha}$ (whose square is the general term of the sum in (34)). These coefficients correspond to the fully normalized harmonics, scaled versions of the $Y_{nm\alpha}$, the integrals of whose squares on the unit sphere are all unity. The σ_n define the spherical harmonic power spectrum of V . "Kaula's rule", based on studies of terrestrial gravity measurements and of early field models obtained from satellite tracking data, has been shown to be a reasonably close guess of the actual power spectrum of the geopotential for n as high as 200, although its values for the σ_n are, on the whole, rather high between degrees 8 and 60, and rather low above 60. This conclusion is the result of a number of global analyses of altimetry and gravimetry. Wagner and Colombo (1979), and Rapp (1979) have given more accurate formulations for the σ_n , but "Kaula's rule" still has the convenience of its greater simplicity.

3.11 The Equation of Motion in Keplerian Elements

In Keplerian elements, the equations of motion of the satellite are known as Lagrange's planetary equations. If E is the total energy (kinetic + potential) at any given time, and $F=-E$, then it can be shown that:

$$F = \frac{\mu}{2a} + V - \frac{\mu}{r} , \quad (35)$$

where F , r and a are instantaneous values. The Lagrangian equations are

$$\dot{a}(t) = \frac{2}{na} \frac{\partial F}{\partial M} \quad (36a)$$

$$\dot{e}(t) = \frac{(1-e^2)}{na^2 e} \frac{\partial F}{\partial M} - \frac{(1-e^2)^{1/2}}{na^2 e} \frac{\partial F}{\partial \omega} \quad (36b)$$

$$\dot{M}(t) = - \frac{1-e^2}{na^2 e} \frac{\partial F}{\partial e} - \frac{2}{na} \frac{\partial F}{\partial a} \quad (36c)$$

$$\dot{\omega}(t) = - \frac{\cos I}{na^2 (1-e^2)^{1/2} \sin I} \frac{\partial F}{\partial I} + \frac{(1-e)^{1/2}}{na^2 e} \frac{\partial F}{\partial e} \quad (36d)$$

$$\dot{I}(t) = \frac{\cos I}{na^2 (1-e^2)^{1/2} \sin I} \frac{\partial F}{\partial \omega} - \frac{1}{na^2 (1-e^2)^{1/2} \sin I} \frac{\partial F}{\partial \Omega} \quad (36e)$$

$$\dot{\Omega}(t) = \frac{1}{na^2 (1-e)^{1/2} \sin I} \frac{\partial F}{\partial I} \quad (36f)$$

where $n = (\mu/a^3)^{1/2}$.

The largest effects produced by the gravitational field come from the central force (C_{000}) and the oblateness (C_{200}). The first gives orbits their general elliptical shape, and the second causes most of the secular variations in their mean ellipses. Careful inspection of (32) shows that C_{200} is associated with a term in the expansion in Keplerian elements of V that does not contain the fast changing M . This term is $V' = \mu \frac{C_{200}}{a} \left(\frac{R}{a}\right)^2 F_{201}(I) G_{210}(e)$. According to Kaula (ib., 1966):

$$F_{201}(I) = \frac{3}{4} \sin^2 I - \frac{1}{2}$$

and

$$G_{210}(e) = (1-e^2)^{-3/2} .$$

Replacing V with $\frac{\mu}{r} C_{000} + V'$ in (35) and the resulting F in (36), the equations of motion become, taking the formulae for $F_{201}(I)$ and $G_{210}(e)$ into account,

$$\ddot{a}(t) = 0$$

$$\ddot{e}(t) = 0$$

$$\ddot{I}(t) = 0$$

$$\dot{\Omega}(t) = \frac{3}{2} n C_{200} \left(\frac{R}{a}\right)^2 \frac{\cos I}{(1-e^2)^2}$$

$$\dot{\omega}(t) = \frac{3}{4} n C_{200} \left(\frac{R}{a}\right)^2 [1 - 5 \cos^2 I]$$

$$\dot{M}(t) = n - \frac{3}{4} n C_{200} \left(\frac{R}{a}\right)^2 \frac{[3 \cos^2 I - 1]}{(1-e^2)^{3/2}} .$$

The first three expressions show that the oblateness cannot cause secular changes in a , e or I . Replacing instantaneous values with mean values (which are very close to the former, in general) the last three expressions become (10), (11) and (9'), respectively.

3.12 The Forced Linearized Equations

Clearly, Lagrange's equations are not linear in their unknowns, the Keplerian elements. Linearizing according to (21), but assuming that the only errors are those in the $C_{nm\alpha}$ of the field model, so all $\Delta s_{i0}^k = 0$, produces equations of the form:

$$\Delta \dot{s}_i^{(g)} = \sum_{n=2}^{\infty} \sum_{m=0}^n \sum_{\alpha=0}^1 \frac{\partial L_{s_i}}{\partial C_{nm\alpha}} \Delta C_{nm\alpha} + \sum_{j=1}^6 \frac{\partial L_{s_i}}{\partial s_j} \Delta s_j^{(g)}, \quad (37)$$

where the superscript (g) indicates the gravitational origin of the perturbation or error (i.e., the $\Delta C_{nm\alpha}$).

Notice that the sum with respect to "j" in (37) is the dynamic part of the linearized equations (21), while the $(\partial L_{s_i} / \partial C_{nm\alpha}) \Delta C_{nm\alpha}$ are forcing terms. The linearized equations are mutually coupled by "interaction terms" of the form $\frac{\partial L_{s_i}}{\partial s_j} \Delta s_j^{(g)}$ where the derivative can be a

function of time. This time-dependence makes an analytical or closed expression for the solution impossible in general. Fortunately, as pointed out when deriving the approximate homogeneous form of the equations, the terrestrial field is close to that of a spherically symmetrical body (a point mass, for example) where $F = \mu/2a$ is constant and all interaction terms in (37) are zero except $\frac{\partial L_M}{\partial a} \Delta a^{(g)} = -(3n/2a) \Delta a^{(g)}$ in the equation for ΔM . These vanishing terms are, in the actual field, of the order of C_{200} , or about 10^{-3} times smaller than the rest of (37), and it is quite reasonable to ignore them for the purposes of this study.

To arrive at the equations for Δa , Δe , and ΔM , which are the ones needed to find that of Δr , replace $V = \mu/r$ in (35) with its expansion in Keplerian elements according to (30) and (31) and then carry out the partial differentiations indicated by (36) and (37) at the reference orbit, where $\vec{M} = \vec{M}_0 + \dot{M}(t-t_0)$, $\vec{\omega} = \vec{\omega}_0 + \dot{\omega}(t-t_0)$ and $\vec{\theta}' = \vec{\theta}'_0 - \dot{\theta}'(t-t_0)$, ignoring all $\frac{\partial L_{S_j}}{\partial s_j} \Delta s_j^{(g)}$ except $\frac{\partial L_M}{\partial a} \Delta a^{(g)}$.

The result is:

$$\dot{a}^{(g)}(t) = 2\mu/(\bar{n} \bar{a}^2) \sum_{nm\alpha pq} \Delta C_{nm\alpha} \left(\frac{R}{\bar{a}}\right)^n F_{nmp}(\bar{I}) G_{npq}(\bar{e}) (n-2p+q) \cos[(n-2p+q)(\dot{\omega} + \dot{M}) - q\dot{\omega} + m\dot{\theta}']t + \phi_{nm\alpha pq} + \frac{\pi}{2}]$$

(38a)

$$\Delta \dot{e}(t)^{(g)} = \mu / (\bar{n} \bar{a}^3) \sum_{nmpq\alpha} \Delta C_{nm\alpha} \left(\frac{R}{\bar{a}}\right)^n F_{nmp}(\bar{I}) G_{npq}(\bar{e}) [(1-\bar{e})^{2/2} (n-2p+q) - (n-2p)] (1-\bar{e})^{2/2} \cos [((n-2p+q)(\dot{\omega} + \dot{M}) - q\dot{\omega} + m\dot{\theta}')t + \phi_{nmpq\alpha} + \frac{\pi}{2}] \quad (38b)$$

$$\Delta \dot{M}(t)^{(g)} = \mu / (\bar{n} \bar{a}^3) \sum_{nmpq\alpha} \Delta C_{nm\alpha} \left(\frac{R}{\bar{a}}\right)^n \left[-\left(\frac{1-\bar{e}^2}{e}\right) \left(\frac{\partial G_{npq}(\bar{e})}{\partial e}\right) + 2(n+1)G_{npq}(\bar{e}) \right] F_{nmp}(\bar{I}) \cos [((n-2p+q)(\dot{\omega} + \dot{M}) - q\dot{\omega} + m\dot{\theta}')t + \phi_{nmpq\alpha}] - \frac{3}{2} \frac{\bar{n}}{\bar{a}} \Delta a(t)^{(g)}, \quad (38c)$$

where

$$\phi_{nmpq\alpha} = (n-2p+q)(\bar{\omega}_0 + \bar{M}_0) - q\bar{\omega}_0 + m\bar{\theta}'_0 - \frac{1}{2} \pi \left[\alpha + \frac{1}{2} (1 - (-1)^{n-m}) \right] \quad (39)$$

and

$$\bar{\theta}' = \dot{\Omega} - \dot{\theta} \quad (40a)$$

$$\bar{n} = (\mu / \bar{a}^3)^{1/2} \quad (40b)$$

$$\bar{M}_0 = \bar{M}(t_0^k) - \dot{\omega} t_0^k \quad (40c)$$

and similarly for $\bar{\omega}_0$ and $\bar{\theta}'_0$; t_0^k is the starting time of the k arc. A different choice of starting time can be made in the case of "frozen", repeat orbits (as explained in the comments following equation (52)), to show more clearly the main properties of both Δr and the tidal signal in

altimeter measurements taken along such orbits, which have precisely repeating ground tracks.

Expressions (38a-c) are the forced or unhomogeneous linearized equations. Notice that if all the $\Delta C_{nm\alpha}$ are zero, the (38) become identical to the unforced or homogeneous equations (21'a-c). While the former are based on a precessing reference ellipse, as shown by \dot{M} , $\dot{\omega}$ and $\dot{\theta}'$ in the arguments of the cosines of their forcing terms, the (21') are not. However, both sets of equations agree perfectly with each other because both involve the same "spherical approximation" that neglects among their dynamic terms those proportional to C_{200} linking $\Delta a^{(g)}$, $\Delta e^{(g)}$, $\Delta M^{(g)}$ to $\Delta \omega^{(g)}$, $\Delta \Omega^{(g)}$ and, thus, to any secular variations in ω and Ω whatsoever. The term $-\frac{3}{2}(\bar{n}/\bar{a})\Delta a(t)^{(g)}$ is often ignored in the formulation of these equations, because the factor (\bar{n}/\bar{a}) is very small, so only very large perturbations in the semimajor axis would have an effect on $\Delta M^{(g)}$, and leaving it out makes the integration of the equations immediate. Here this term has been retained mostly for the sake of consistency.

To solve (38a-c) the first two equations are solved by direct integration respect to time in the interval $t_0^k < t < t_0^{k+1}$:

$$\Delta a^{(g)}(t) = \int_{t_0^k}^t \dot{\Delta a}^{(g)}(t') dt'$$

$$\Delta e^{(g)}(t) = \int_{t_0^k}^t \dot{\Delta e}^{(g)}(t') dt' .$$

Next, $\Delta a^{(g)}(t)$ is replaced in (38c) and this is, then, integrated to obtain $\Delta M^{(g)}(t)$.

Clearly, all solutions $\Delta s_i^{(g)}(t)$ obtained in this way satisfy the condition

$$\Delta s_i^{(g)}(t_0^k) = 0. \quad (41)$$

This is physically meaningful, because, due to inertia, the finite change in the driving force due to the $\Delta C_{nm\alpha}$ cannot affect the ephemeris instantly.

3.13 Orbit Error Due to Incorrect Potential Coefficients $C_{nm\alpha}$

When integrating the various terms in (38), there are two situations that must be considered separately.

(a) $(n-2p+q) (\dot{\omega}+M) - q\dot{\omega}+m\dot{\theta} \neq 0$

This is the normal case: the corresponding part $\tilde{\Delta s}_i$ of the solution, for $\tilde{\Delta \bar{a}}$ and $\tilde{\Delta \bar{e}}$ is of the form

$$\Delta \tilde{s}_1 = \sum_{nmpq(\text{nonres})} \Delta C_{nma} \tilde{s}_{inmpq} \cos[(n-2p+q)(\dot{\omega} + \dot{M}) - q\dot{\omega} + m\dot{\theta}'] t + \phi_{nmapqo} + \Delta \tilde{s}_{io}^k \quad (42)$$

with

$$\tilde{s}_{inmpq} = s_{inmpq} [(n-2p+q)(\dot{\omega} + \dot{M}) - q\dot{\omega} + m\dot{\theta}']^{-1}, \quad (43)$$

where the s_{inmpq} are the functions of \bar{a} , \bar{e} and \bar{I} in (38) and the $\Delta \tilde{s}_{io}^k$ satisfy the inertia condition (41). The symbol " $\sum_{nmapq(\text{nonres})}$ " denotes the sum of all terms where the frequency is not zero. As for $\Delta \tilde{M}^{(g)}$, after replacing $\Delta \tilde{a}^{(g)}$ in (38c) according to (42) and (43) and integrating, one gets

$$\Delta \tilde{M}^{(g)} = \Delta \tilde{M}' - \frac{3}{2} \frac{\bar{n}}{\bar{a}} \Delta \tilde{a}_o^k (t - t_o^k), \\ - \Delta \tilde{M}' + \overset{<}{M} t + \Delta \tilde{M}_o^k$$

where $\Delta \tilde{M}'$ is of the form (42), except that it now includes an extra term proportional to $[(2n-p+q)(\dot{\omega} + \dot{M}) - q\dot{\omega} + m\dot{\theta}']^{-2}$ in the coefficient \tilde{M}_{nmpq} (corresponding to \tilde{s}_{inmpq} in (43)), because of the double integration of $\Delta \tilde{a}^{(g)}$, while $\Delta \tilde{M}_o^k$ is such that the inertia condition $\Delta \tilde{M}^{(g)}(t_o^k) = 0$ is fulfilled. The term $\overset{<}{M} t$ can be included in the secular component of M (explained in part (b) of this paragraph), so only the periodical part

$$\Delta \tilde{M}^{(g)}(t) = \sum_{nm\dot{a}pq(\text{nonres})} \Delta C_{nm\dot{a}} \tilde{M}_{nmpq} \cos[(n-2p+q)(\dot{\omega} + \dot{M}) - q\dot{\omega} + m\dot{\theta}']t + \phi_{nm\dot{a}pq} - \frac{\pi}{2}] + \Delta \tilde{M}_0^k, \quad (42')$$

shall be considered here. The coefficients \tilde{s}_{inmpq} in (42) and (42') are proportional to the inverse of the frequency. Accordingly, the closer this frequency is to zero, the larger \tilde{s}_{inmpq} and, thus, the contribution $\Delta C_{nm\dot{a}} \tilde{s}_{inmpq}$ of $\Delta C_{nm\dot{a}}$ to the $\Delta \tilde{s}_1$. At about 1000 km height an orbiting spacecraft completes between 13 and 14 revolutions in one "nodal day", which is the time $T_D = |2\pi/\dot{\theta}'|$ it takes the Earth to do a full turn with respect to the precessing orbital plane. If this number were exactly 13 or 14 then, calling it N_R and assuming that $\dot{\omega} = 0$, there would be always some combination of n , p and q such that $(n-2p+q)\dot{M} + m\dot{\theta}' = 0$ for all potential coefficients of order

$$m = k N_R, \quad \text{where } k = 0, 1, 2, 3, \dots$$

When the frequency is zero, \tilde{s}_{inmpq} becomes infinite and the solution of the linearized equations given by (42) and (42') does not apply any longer. This case, to be discussed in the next paragraph, is known as a perfect resonance. In practice, $\dot{\omega}$ is quite small for altimeter satellites, but not zero. If the number N_R for one "nodal day" is still

very close to an integer, the effect must be very similar to that just described, at least over a period of time of a week or so, which is much smaller than the period of ω . The perturbations, though very large, become periodical, in agreement with (42) and (42'), even if their periods are very long. This is a case of deep resonance, and the resulting perturbations, if given enough time to grow, may have peak amplitudes of the order of a kilometer or more; in that case, a linear theory is no longer adequate and one has to use a nonlinear approach. This is not the case for the errors of weekly altimeter satellite arcs, which never reach more than a few meters in size. In reality, N_R differs considerably from an integer, though those $\Delta\bar{C}_{nm\alpha}$ errors whose orders come closest to satisfying the resonance condition given above, or resonant orders, still can produce long period effects much larger than those of the other orders. This is known as shallow resonance, and altimeter satellites have orbits with such resonances at orders close to whole multiples of 13 or 14. In particular, when $k = 1, 2, 3$ one has the so-called primary, secondary and tertiary shallow resonances, respectively. Orbits where $\omega = 0$ and there is an integer number of turns N_R over a whole number of "nodal days" N_D , are known as "frozen", repeat orbits. The same argument used when $N_D = 1$ applies now: these orbits must experience perfect resonances with those $\Delta\bar{C}_{nm\alpha}$ that satisfy the condition $m = k N_R$, which includes the zonals for $k = 0$. This type of orbit turns out to be quite important in satellite altimetry, and more shall be said about it presently.

Next in importance to perfect, deep or shallow resonances are the effects of those terms in (42) and (42') where $(n-2p+q) = 0$, as the frequency then is reduced to $-q\dot{\omega} + m\dot{\theta}$. For the orbits under consideration, this sum is quite small compared to the "once per revolution" frequency, approximately equal to $(\dot{M} + \dot{\omega}) \sim \dot{M}$, so it must be much smaller than any other where $(n-2p+q) \neq 0$, provided that q and m are small integers. At altitudes of 1000 km, $|q| < 2$ for all terms of any real account, and the perturbations are substantial only if $m < 10$. Given the prevalence of $m\dot{\theta}$ over $q\dot{\omega}$, these frequencies and the corresponding terms are usually known as "m-dailies". Because of the size of their effects, which show quite clearly in data from satellite tracking, deep resonances, shallow resonances and "m-dailies" are quite useful for estimating the $\Delta C_{nm\alpha}$ from this type of data, as they comprise most of the signal. For the same reason they are quite important in understanding the nature of orbital errors, which is the subject of this work.

The total amplitude of the oscillation associated with any particular frequency in (42) and (42') is

$$\sum_{npq} \Delta C_{nm\alpha} \tilde{s}_{inmpq}, \text{ where } (n-2p), q \text{ and } m \text{ must be all constant,}$$

so only $\Delta C_{nm\alpha}$ of the same order m and degree n of the same parity (even, odd) can contribute. This amplitude, being a weighted sum of $\Delta C_{nm\alpha}$, is known as a "lumped coefficient". The weights in the sum are functions of inclination and of eccentricity through the $F_{nmp}(\bar{I})$ and $G_{npq}(\bar{e})$

functions in expression (38); which $\Delta C_{nm\alpha}$ dominates the sum will depend on both I and \bar{e} . Thus, modelling the gravitational field with tracking data requires satellites with a wide variety of inclinations and eccentricities, to disentangle better the various $\Delta C_{nm\alpha}$; also for a given order m , coefficient errors of even degree n produce perturbations most of whose frequencies differ only in $\pm q\dot{\omega}$ from those of odd degree (the main ones having $|q| \leq 2$), so it is desirable that the interval between the first and the last observation of a satellite be at least a substantial part of its apsidal period $2\pi/\dot{\omega}$.

Of all the $C_{nm\alpha}$, the zonals are the best known at present; their determination involved most of the early work done in the field of mapping gravitation with artificial satellites. It was the analysis of the tracking of one of the first USA orbiting spacecraft, a VANGUARD, that revealed the existence of a strong third zonal indicating that the Earth is rather "pear-shaped", with the southern hemisphere slightly larger than the northern one (Eckels et al., 1959).

(b) $(n-2p+q) (\dot{M}+\dot{\omega}) - q\dot{\omega}+m\dot{\theta}' = 0$ (Resonance)

As already explained, this case is known as a perfect resonance: it occurs whenever the angular frequencies \dot{M} , $\dot{\omega}$ and $\dot{\theta}'$ are locked in step with each other, which is a rare case, but quite relevant to the study of the orbits of altimeter satellites. Then, the orbit crosses the gravitational perturbations associated with some of the $\Delta C_{nm\alpha}$ at

intervals equal to the period of \dot{M} , the natural frequency of the linearized system that, forced in this way, resonates. One example is the "frozen", repeat orbit, whose ground track repeats with a period of N_D "nodal days" which is an exact multiple of that of \dot{M} . An extreme case of this is the orbit of a geosynchronous satellite (often used to relay communications) whose ground track, ideally, is on a fixed point on the equator where it "repeats" for ever. Here the main resonant coefficients are C_{220} , and C_{221} , related to the "triaxiality", or lack of rotational symmetry, of the best fitting ellipsoid for the Earth.

As given here, the resonant condition requires an excitation of 0 frequency, instead of \dot{M} . This apparent contradiction with the physical explanation given just now is resolved by noticing that whenever $(n-2p+q) (\dot{M}+\dot{\omega}) - q\dot{\omega}+m\dot{\theta}'=0$ then $(n-2p+q\pm 1) (\dot{M}+\dot{\omega}) - (q\pm 1) \dot{\omega}+m\dot{\theta}' = \pm \dot{M}$, so any $\Delta C_{nm\alpha}$ that produces a zero frequency term must produce also forcing terms of frequencies \dot{M} and $-\dot{M}$ (either of which makes the linearized system resonate). Moreover, the amplitudes of the 0 and $\pm \dot{M}$ forcing terms are implicit functions of each other, as both depend explicitly only on the parameter q (in all of them, \bar{a} , \bar{I} , \bar{e} , n , m and p are the same).

As before, the linearized equations for Δa and Δe can be solved independently by direct integration with respect to time. Adding up all resonant terms and symbolizing their sums by $\Delta s_i^<(g)$,

$$\Delta s_i^{<(g)} = \left\{ \sum_{nmpq(\text{res})} \Delta C_{nma} s_{inmpq} \cos(\phi_{nmapqo} + \frac{\pi}{2}) \right\} (t-t_o^k)$$

$$= \langle s_i \rangle t + \Delta s_{io}^{<(g)k}, \quad (44)$$

where " $\sum_{nmpq(\text{res})}$ " indicates the sum over all the resonant combinations of n, m, p, q , while $\Delta s_{io}^{<(g)k} = - \langle s_i \rangle t_o^k$ (so inertia is not violated at the start of an arc), and $\langle s_i \rangle$ is the expression in curly brackets. The equation for ΔM , on the other hand, has a solution that depends on Δa because of the not negligible "interaction term" $-\frac{3\bar{n}}{2a} \Delta a$:

$$\Delta M^{<(g)} = \left\{ \sum_{nmpq(\text{res})} \Delta C_{nma} M_{nmpq} \cos(\phi_{nmapqo}) \right\} (t-t_o^k)$$

$$- \frac{3}{2} \frac{\bar{n}}{a} [\langle s_i \rangle (t-t_o^k)^2 + \Delta a_o^{<(g)k} (t-t_o^k)] . \quad (45)$$

In practice, the quadratic term in (45) is unlikely to become large enough to matter within any weekly arc. However, quadratic terms have to be included not only in ΔM , but in Δa and Δe as well, because true resonances are deep rather than perfect, with frequencies that are very small but never zero. The corresponding terms have, therefore, very long

periods, which over a much shorter interval, such as one week, can be approximated by quadrics:

$$\Delta s_i^{(g)} = \hat{s}_i^k t^2 + \langle s_i^k t + s_{i0}^k .$$

Including both periodical and deep resonant terms (if there are any), the complete solutions of the three linearized equations of motion (38) corresponding to gravitational model errors can be written as

$$\Delta a^{(g)} = \Delta \tilde{a}^{(g)} + \hat{a}^k t^2 + \langle a^k t + a_o^k \quad (46a)$$

$$\Delta e^{(g)} = \Delta \tilde{e}^{(g)} + \hat{e}^k t^2 + \langle e^k t + e_o^k \quad (46b)$$

$$\Delta M^{(g)} = \Delta \tilde{M}^{(g)} + \hat{M}^k t^2 + \langle M^k t + M_o^k \quad (46c)$$

where the constant terms a_o^k , e_o^k and M_o^k are such that, at the start of any weekly arc, $\Delta a^{(g)}(t_o^k) = \Delta e^{(g)}(t_o^k) = \Delta M^{(g)}(t_o^k) = 0$. The second degree terms in (46) are likely to be considerably smaller than the linear ones, so the non-periodic parts of the $\Delta s_i^{(g)}$ may depart only slightly from straight lines.

Errors in drag, etc., can also have very long period effects resembling weekly quadrics, as well as others looking rather like higher degree polynomials (expression (18)).

3.14 Orbit Error Due to Incorrect GM

At present, μ (often referred to as "GM", where "G" is the universal constant of gravitation and "M" is the mass of the Earth) is known to better than six significant places. According to (26), the effect of an error $\Delta\mu$ is equivalent to an error $\frac{\Delta\mu}{\mu} C_{nm\alpha}$ in each potential coefficient, or about $C_{nm\alpha} \times 10^{-6}$. This means that the only appreciable effect is that of $\frac{\Delta\mu}{\mu} C_{000}$, as the zero degree (or "central force") zonal (which has a unit value by definition) is almost three orders of magnitude larger than C_{200} , and five or more than all the rest. Therefore, to understand the influence of $\Delta\mu$ on the computed orbit, it is sufficient to consider the case where the field consists of the zero harmonic alone. In this field the orbit obeys Kepler's laws, so its frequency is $\dot{M} = (\mu/a^3)^{1/2}$. For a nearly circular orbit of mean radius \bar{r} , $\bar{a} \sim \bar{r}$, so $M \sim (\mu/\bar{r}^3)^{1/2}$. An error $\Delta\mu$ in μ requires a compensating bias Δr_μ in \bar{r} to keep the frequencies of the true and the computed orbits very close; accordingly, $\Delta r_\mu = \frac{1}{3} \frac{\Delta\mu \bar{r}}{\mu}$. Otherwise, the along track errors may become very large after several days. While $\Delta\mu$, through its influence on the adjusted initial state, causes more than a bias in Δr (see expression (23)), here Δr_μ is, nonetheless, its most distinctive and important effect. This bias is virtually the same for all the arcs, as long as \bar{r} does not change much. Such is the case throughout most of the mission of an altimeter satellite, where the effect of drag is relatively small because of the height, so $\Delta\mu$ will cause the altimetrically determined mean sea surface \bar{h}_{w_c} , for instance, to appear

higher or lower by the constant offset Δr_μ . Likewise, there may be an error in the size of the reference ellipsoid, approximately equal to ΔR (which may be partly related to $\Delta\mu$), so the estimate of the mean sea surface topography w_{oc} will be biased as well by $\Delta w_o \approx \bar{r}/3(\Delta\mu/\mu) - \Delta R$. However, for any meaningful oceanographic application, what matters is the slope between the sea surface and the best fitting equipotential; the non-zero global mean value (bias) of the computed topography can be ignored.

3.15 Expression of the Radial Error Excluding its Tidal Part

Going back to (16), one can see that Δa appears in Δr directly, while Δa , Δe and ΔM modulate together an oscillation of frequency \dot{M} . This causes the frequencies present in (42) to appear in Δr both unchanged and shifted by $\pm \dot{M}$. Because of the $-\dot{M}$ shift, terms whose original frequencies are very close to \dot{M} produce very long period oscillations in Δr , resembling, for a weekly arc, quadrics that can be lumped with that from the direct contribution of Δa . The $+\dot{M}$ shift, on the other hand, converts the sum of the deep resonant terms in Δa , Δe and ΔM into an oscillation of frequency \dot{M} modulated by a quadric.

Putting together the various parts that make up the radial error, one can get an approximate "weekly" expression for Δr . To this effect, replace (46) in (16) while taking into account (18), (23), (42), (43), (45) and the usual trigonometric identities for the sine and cosine of the sum and the product of two angles. The result is:

$$\begin{aligned}
\Delta r(t)^{(NT)} = & \sum_{nm\alpha pq(\text{nonres})} \Delta C_{nm\alpha} \{ r_{nmpq} \cos [((n-2p+q)(\dot{\omega} + \dot{M}) - q\dot{\omega} + m\dot{\theta}')t + \phi_{nm\alpha pq_0}] \\
& + r_{nmp(q+1)} \cos [((n-2p+q+1)(\dot{\omega} + \dot{M}) - (q+1)\dot{\omega} + m\dot{\theta}')t + \phi_{nm\alpha p(q+1)_0}] \\
& + r_{nmp(q-1)} \cos [((n-2p+q-1)(\dot{\omega} + \dot{M}) - (q-1)\dot{\omega} + m\dot{\theta}')t + \phi_{nm\alpha p(q-1)_0}] \} \\
& + A_k \cos \dot{M}t + B_k \sin \dot{M}t + C_k t \cos \dot{M}t + D_k t \sin \dot{M}t \\
& + E_k t^2 \cos \dot{M}t + F_k t^2 \sin \dot{M}t \\
& + \sum_{j=0}^J r_{kj} (t - t_o^k)^j, \tag{47}
\end{aligned}$$

where J is a small integer, t_o^k is such that $\bar{M}_0 = 0$ in (40c) (to eliminate a term $(q \pm \frac{0}{1}) M_0$ in the arguments of the cosines and simplify the formulae) and the $r_{nmp(q \pm \frac{0}{1})}$ depend on the $\Delta C_{nm\alpha}$. Notice that the subscripts "(g)" and "(ng)" have been replaced by "(NT)" (for "non-tidal"), as $\Delta r^{(NT)}$ has here both gravitational and non-gravitational causes, but excludes the effect of tides (to be discussed later). The coefficients r_{nmpq} are

$$r_{nmpq} = \tilde{a}_{nmpq}$$

$$r_{nmp(q+1)} = \frac{1}{2} (\tilde{M}_{nmpq} \bar{a} \bar{e} - \tilde{a}_{nmpq} \bar{e} - \tilde{e}_{nmpq} \bar{a})$$

$$r_{nmp(q-1)} = -\frac{1}{2} (\tilde{M}_{nmpq} \bar{a} \bar{e} + \tilde{a}_{nmpq} \bar{e} + \tilde{e}_{nmpq} \bar{a})$$

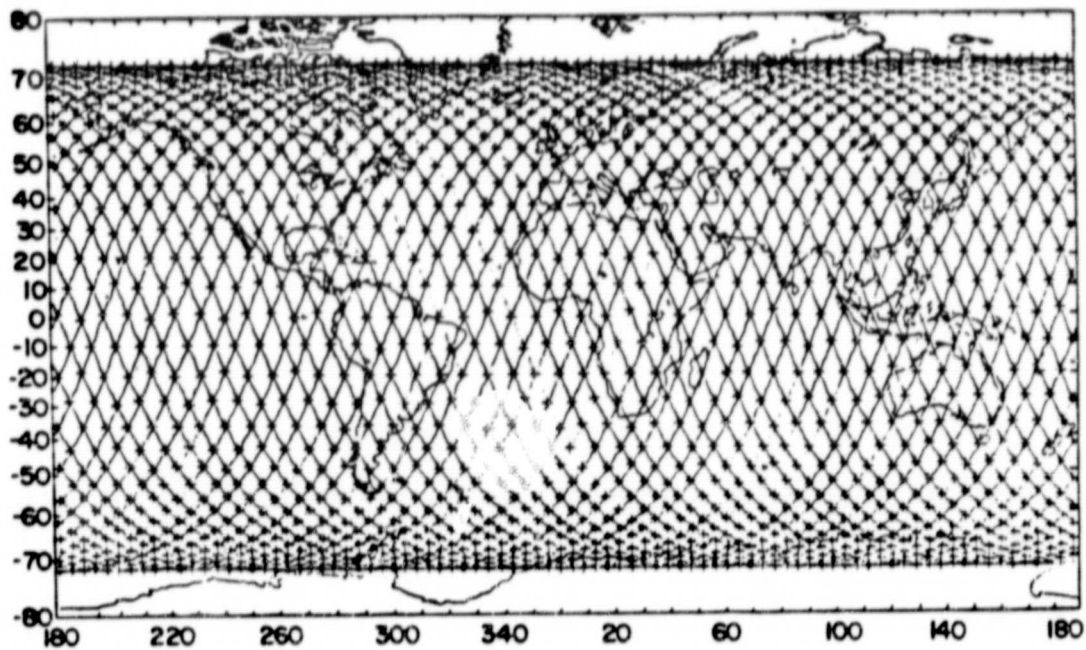
so they are functions of \bar{a} , \bar{e} and \bar{I} (through the $F_{nmp}(\bar{I})$, $G_{npq}(e)$, etc., in (38a-c)), but not of \bar{M} , $\bar{\omega}$ or $\bar{\Omega}$. For a satellite like GEOS-3, where the mean ellipse changes appreciably over the mission due to uncontrolled orbital decay caused mostly by air drag, the r_{nmpq} , $r_{nmp(q+1)}$ and ϕ_{nmpqo} , $\phi_{nmp(q+1)o}$ are also arc dependent, although the former are not likely to vary appreciably from week to week. This decay was prevented by orbital corrections in SEASAT and shall be prevented likewise in most future altimeter satellites, so expression (47) applies best to them. For arcs of up to one month (47) is still likely to be valid if the envelope of the increasing \dot{M} oscillation is approximated by a cubic or a quartic instead of a parabola.

The resonant part $C_{kt} \cos \dot{M}t + D_{kt} \sin \dot{M}t + E_{kt}^2 \cos \dot{M}t + F_{kt}^2 \sin \dot{M}t$ caused by gravitational field errors is only important in deeply resonant orbits like those discussed in the next chapter where, as shown by computer simulations, if the ΔC_{nma} were of the order of the published accuracies for the coefficients of GEM 9 (Lerch et al., 1977), these increasing oscillations could build up at a rate of several meters per week. As for the periodical terms, the power in the spectrum of that part of Δr caused by errors like those in GEM 9 would be distributed as follows, in the case of SEASAT: up to 1 cycle/revolution, 3m (r.m.s.); from 1 to 10 cy./rev., 2m; 10-20 cy./rev., 1m; 20-30 cy./rev., 0.1m; 30-40 cy./rev., 0.05m; above 40 cy./rev., less than 0.05m. More recent gravity field models, such as PGS-S4 (Lerch et al., 1982), are thought to reduce considerably all the components of Δr associated with them.

4.0 ORBITS WITH REPEATING GROUND TRACKS

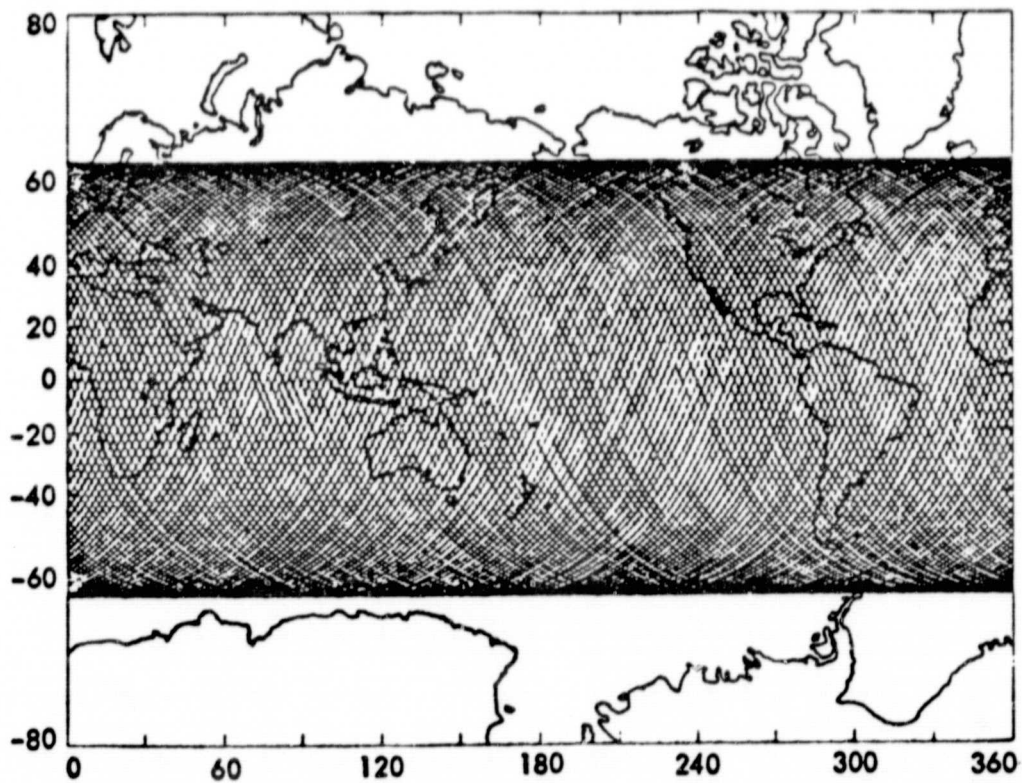
4.1 The "Frozen", Repeat Orbit

For many applications of altimetry it is desirable to choose the orbit so the satellite passes over the same places on Earth every few days, repeating its ground track periodically. This was done, experimentally, during the last month of operation of SEASAT (Cutting et al., *ib.*, 1978), and is planned for all civilian altimeter missions now being considered. Because of the disruption of the chosen orbit by drag, radiation pressure, and other disturbing forces, the ground track cannot be repeated exactly, but it is sufficient to keep it within a band a few kilometers wide (about ± 5 km for SEASAT (Bauer, *ib.* 1978), and probably about ± 1 km for the satellites that will follow over the next decade). This can be achieved by firing small rocket engines to correct the orbit every so often, for example less than once per month for ERS-1 (Dow and Klinkrad, *ib.*, 1982), so as to turn the drift back towards the ideal orbit. The maneuvers must be brief, as the thrust of the rockets cannot be modeled accurately enough for precise orbit determination, so measurements taken while they are operating are hard to interpret. For this reason, the precisely estimated ephemeris cannot run through one of these maneuvers; an arc must end just before and another one begin just after it. To get the desired repetition, it is sufficient that the maneuvers keep the mean ellipse of the estimated orbit so that, if this ellipse were the actual trajectory of the spacecraft, the ground track would repeat perfectly. For this, such mean trajectory should start and end at the same point (in Earth-fixed coordinates) in each repeat cycle.



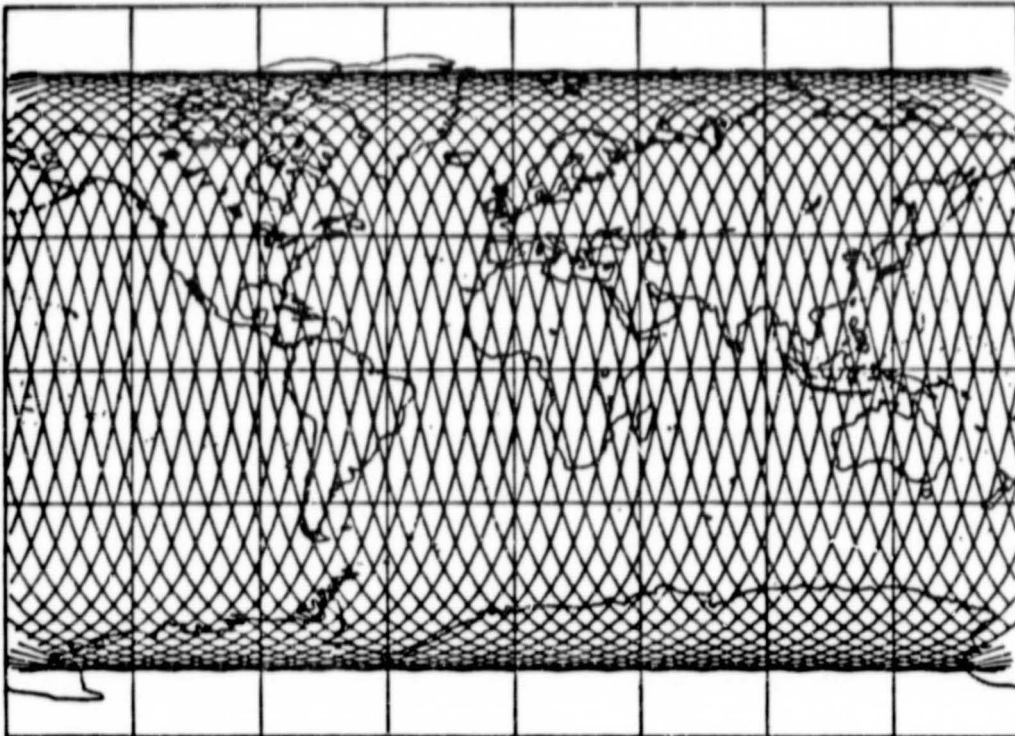
SEASAT: Actual 3-day repeat groundtrack

ORIGINAL PAGE IS
OF POOR QUALITY



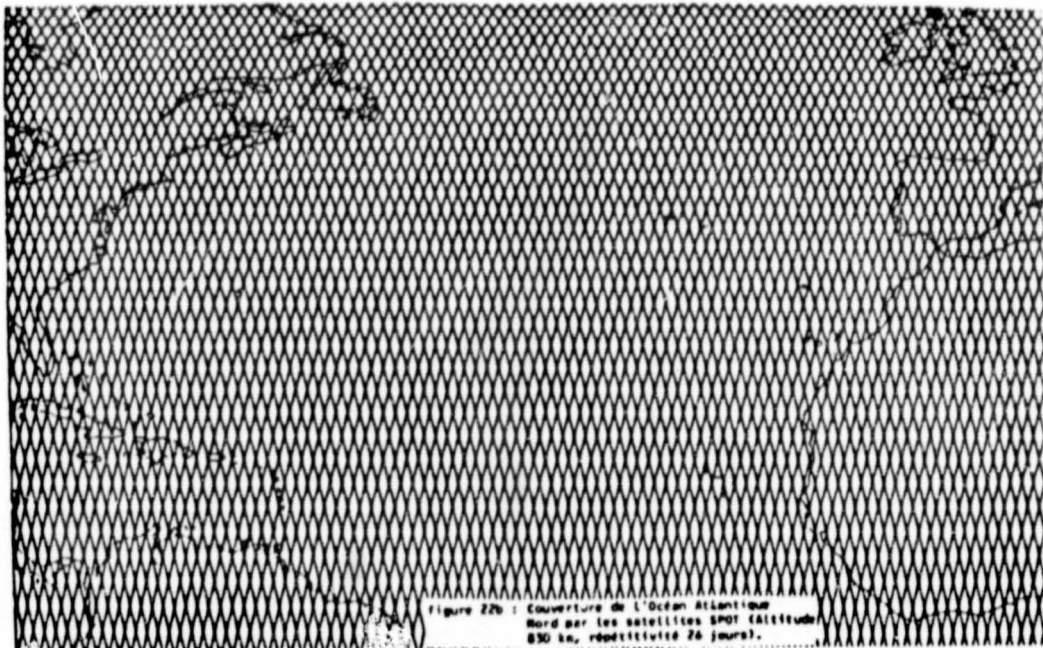
TOPEX: Projected 10-day repeat groundtrack

FIGURE 2(a). Repeating Groundtracks of SEASAT and TOPEX



ERS-1: Projected 3-day repeat groundtrack

ORIGINAL PAGE IS
OF POOR QUALITY



**POSEIDON: Projected 26-day repeat groundtrack
(shown only over the North Atlantic)**

FIGURE 2(b). Repeating Groundtracks of ERS-1 and POSEIDON

This is possible only if $\dot{\omega}$, \dot{M} and $\dot{\theta} = \dot{\Omega} - \dot{\theta}$ are all exact multiples of the fundamental angular frequency $\omega_{rc} = 2\pi/T_{rc}$, where T_{rc} is the repeat period. For altimeter missions T_{rc} has been chosen, up to now, of the order of a few days (three days for SEASAT, nine for TOPEX, three for ERS-1; Figure 2 shows the ground tracks of these satellites). The approximate expression (11) for $\dot{\omega}$ would require a very large mean eccentricity of the orbit (close to $\bar{e} = 1$) for the perigee to precess in a few days, making $\dot{\omega}T_{rc} = k2\pi$ ($k=0,1,2,\dots$), except when $\dot{\omega}$ is zero. Unfortunately, such an eccentric orbit would have its perigee deep underground. This leaves $\dot{\omega} = 0$ as the only practical choice. The question is: can one have both a small eccentricity and an $\dot{\omega}$ that is virtually 0? All zonals can produce secular perturbations in ω ; formula (11) gives only the effect of the largest of the zonals, C_{200} . However, when \bar{e} is very small, the position of the argument of perigee can be rotated through a large angle by very slight changes in the shape of the orbit, like those produced by the other zonals, particularly the second largest, C_{300} . As these perturbations are of different signs, their combined effect on the mean ellipse may cancel out that of C_{200} alone, thus making $\dot{\omega} = 0$ regardless of the inclination. Cook (1966) developed a theory for the mean ellipse to take into account the effect of an arbitrary number N of zonals. From Cook's theory one can get the values of \bar{e} and $\bar{\omega}$ that "freeze" the mean orbit assuming that \bar{a}, \bar{I} and the first N zonals are known:

$$\bar{\omega} = \frac{\pi}{2} \quad (48)$$

$$\bar{e} = \frac{1}{3} \sum_{n=3}^{N(\text{odd})} C_{n00} \left(\frac{R}{a}\right)^n \frac{(n-1)}{n(n+1)} P_{n1}(0) P_{n1}(\cos \bar{I}) [C_{200} \left(\frac{R}{a}\right)^2 (1 - \frac{5}{4} \sin^2 \bar{I})]^{-1}$$

$$\approx 1.182 \times 10^{-3} \left(\frac{R}{a}\right) \sin \bar{I} + 0 (C_{500}), \quad (49)$$

where the summation in (49) is over odd values of n . Notice that (48) fixes the mean perigee at the highest latitude reached by the ground track. This theory involves a number of approximations and breaks down for \bar{I} close to the critical inclinations ($\sim 63.4^\circ$ and $\sim 116.6^\circ$); in this special case, the theory of Hough (1981) shows the existence of "frozen" orbits with small \bar{e} and heights of about 1000km where $\bar{\omega} = \frac{\pi}{2}$ as in (98), although the equilibrium value of \bar{e} is not given by (49), but by another expression that also depends on the first N zonals. TOPEX's orbit is likely to have an inclination near the critical value of 63.4° .

Cook's formulas are used to this day (for example, see Dow and Klinkrad, ib. 1982). It is important to notice that expression (49) is a continuous function of \bar{a} and \bar{I} , so whenever a "frozen" orbit is possible at a given height and inclination, there are infinitely many others at heights and inclinations close to that one. SEASAT is a clear indication that this is the case at typical heights for altimeter satellites. How well can one "freeze" an orbit in a low degree zonal field? Recently I integrated numerically "frozen" orbits at various inclinations, using as the only driving force that of the field of the 9 first zonals of the GEM 9 model (Lerch et al., 1977). The initial conditions were adjusted iteratively, starting with the values given by (49), until, making allowances for the precession of the orbital plane, they "returned" to

their starting positions and velocities within 10^{-5} meters and 10^{-6} meters per second, respectively (Colombo, ib., 1984). Of course, a real orbit is subject to numerous perturbations that prevent it from being that "frozen" and, in any case, the accuracy with which a satellite can be put in a particular orbit (and kept there) is also limited. Fortunately, the kind of accuracy that can be achieved is enough for altimeter missions. Moreover, as any large perturbations are also likely to be slow in growing (i.e., have long periods), they can be kept in check by occasional orbit maneuvers.

4.2 Periodicity and Resonance

A complete first order perturbation theory for "frozen", repeat orbits is given in (Colombo, ib., 1984). What follows explains the part of this theory relevant to radial orbit errors.

When $\dot{\omega} = 0$ and the satellite completes a whole number N_R of revolutions in an exact number N_D of "nodal days",⁽¹⁾ the frequencies of the trigonometric functions in (38 a-b) and in (47) are all of the form

$$(n-2p+q) \dot{M} + m \dot{\theta}' = ((n-2p+q) N_R - m N_D) \omega_{rc} , \quad (50)$$

(1)A "nodal" day (length equal to $2\pi/|\dot{\theta}'|$) is very close to one sidereal day because $\dot{\Omega}$ in $\dot{\theta}' = \dot{\Omega} - \dot{\theta}$ is much smaller than $\dot{\theta}$.

where ω_{rc} is the angular repeat frequency of the orbit. The numbers N_R and N_D must be relative primes, i.e., have no integer factor in common other than 1. Otherwise, if the largest of such integers is N'_D , there will be a repeat every N'_D days as well as every N_D days, with $N'_D < N_D$. The minus sign of $-mN_D$ comes from $\dot{\theta}' = \dot{\Omega} - \dot{\theta} \sim -\dot{\theta}$, so $\dot{\theta}' < 0$, while here ω_{rc} is chosen positive, and \dot{M} is always positive, according to (9) and (9'). As before, terms in the analytical expressions of the gravitational errors can be separated into two classes: non-resonant and resonant.

The most important characteristic of the non-resonant part of the orbit error is that it is now a Fourier series whose terms are harmonics of the repeat frequency ω_{rc} . Therefore, this part, which is the most complex component of the error caused by the field model, is a periodical function of time, and its fundamental period is the same as the repeat period of the orbit.

This strong property reflects the rotational symmetries of the mean repeat orbit and its ground track, each coiled around the Earth in a spherical helix that closes on itself.

Resonances in a "frozen", repeat orbit occur when the frequency in (50) is zero. This happens for all $\Delta C_{nm\alpha}$ whose order satisfy

$$m = k N_R \quad (k = 0, 1, 2, \dots) . \quad (51)$$

The corresponding force errors are "encountered" by the computed satellite position at repeated intervals of exactly one revolution, which for a "frozen" orbit is also the period of \dot{M} , so the linearized equations of motion are driven by these errors at their natural frequency \dot{M} and have resonant solutions. For repeat periods of three days or longer (those of all satellites considered here), the lowest degree n of a $\Delta C_{nm\alpha}$ that causes resonance must be $n \geq m = k N_R \geq 43$ ($= 43$ for SEASAT, with a 3-day period). Expressions (32) and (33) show that, as n increases, the strength of the harmonics in the expansion of V must eventually fall off. At 1000 km, even resonant coefficient errors with $n \sim 43$ should have a very small effect on Δr . So the only case where resonance is likely to be important is when $k = 0$ and, thus, $m = 0$ (zonals).⁽¹⁾ Expression (38a) shows that Δa cannot have a secular part produced by zonal errors, because $\dot{\Delta a}$ is proportional to $(n-2p+q)$ and must be zero at resonance if $\dot{\omega}=0$. Therefore, field model errors may cause significant secular departures from the true values of all the elements but the semi-major axis, in contrast with surface model errors that can change this element as well.

(1) The main errors are due to the odd zonals, mostly because the term proportional to $e^{-1} \partial G_{npq}(e)/\partial e$ in (38c) is very large when e is small and $q=1$ ($\partial G_{npq}(e)/\partial e \sim 1$), and causes the effect of ΔM to prevail in Δr over those of Δa and Δe . If $q=1$, the resonant condition for $m=0$, i.e., $(n-2p+q)=0$, requires n to be odd.

4.3 The Stability of a "Frozen" Orbit

In a "frozen" orbit, zonal resonances will occur regardless of whether the ground track repeats itself or not, because the condition for resonance $(n-2p+q)=0$ does not involve \dot{M} or $\dot{\theta}$; zonal resonance is inherent in any "frozen" orbit. Zonal force errors are not affected by the rotation of the Earth, which shapes the ground track. Since the known values of \bar{a} , \bar{I} and the zonal coefficients used in formula (49) may be accurate but not perfect, and the effects of higher degree and order potential coefficients, as well as those of non-gravitational forces (drag in particular) are not considered in (48) and (49), the supposedly fixed \bar{e} and $\bar{\omega}$ will, in fact, change very gradually from their starting values.

At any time, the mean orbit defines a point in a six-dimensional Euclidean space with Cartesian coordinates \bar{a} , \bar{e} , \bar{I} , $\bar{\omega}$, $\bar{\Omega}$ and \dot{M} . As the orbit evolves, the point follows a slow trajectory in this space. Let Q be the point's projection on the plane of the axes \bar{e} and $\bar{\omega}$. If Q is initially identical with the "frozen point" P defined by (48) and (49), it will remain there indefinitely. Otherwise, as is shown in Figure 3, Cook's theory predicts that it will follow either a closed trajectory around P (libration) or else an open one where $\bar{\omega}$ eventually ranges from 0° to 360° (precession). Similar predictions are made by Hough's theory (ib, 1981) for near circular orbits close to the critical inclination. The trajectory will be closed if Q is initially near enough to P, open otherwise; in either case (taking $\bar{\omega}$ modulus 360°) Q returns to the same

starting position after the same length of time, which is the period corresponding to $\bar{\omega}$ as given by (11). Therefore, the closer Q is to P, the smaller its tangential velocity along its own trajectory, and the smaller, in general, the projection of this velocity on the $\vec{\omega}$ axis, or, approximately, the weekly average $\bar{\omega}$ (for SEASAT $\bar{\omega}$ was always very close to 1° per year).

Since the values of the zonals used to calculate the coordinates of P with (48) and (49) are only those of the N first C_{n00} and are subject to errors ΔC_{n00} , the true "frozen point" is P' and not P. As (48) does not depend on any parameter, both P and P' are on the same line, parallel to the \vec{e} axis, where $\bar{\omega} = \pi/2$. Even if Q is placed exactly at P, it cannot stay there, being forced by the zonal errors ΔC_{n00} to move instead along a trajectory that encircles P' , as shown in Figure 3. Initially, this trajectory will be very close to the local tangent, which is a straight line, so the variation in both \bar{e} and $\bar{\omega}$ will appear to be secular when observed over a sufficiently short time. As P and P' are likely to be quite close, the movement of Q can be very slow and one week can be regarded as a "short time". Because of drag, the semimajor axis will decrease gradually, so P will shift upwards along the line $\omega = \frac{\pi}{2}$ (see (49)), and Q will follow a slowly widening spiral instead of a closed curve.

In the event of the mean ellipse becoming too different from the chosen one, the rockets in the spacecraft can be used to correct the orbit, bringing it back to the right altitude and also shifting Q to Q' (Figure 3), on a path leading back (approximately) to P.

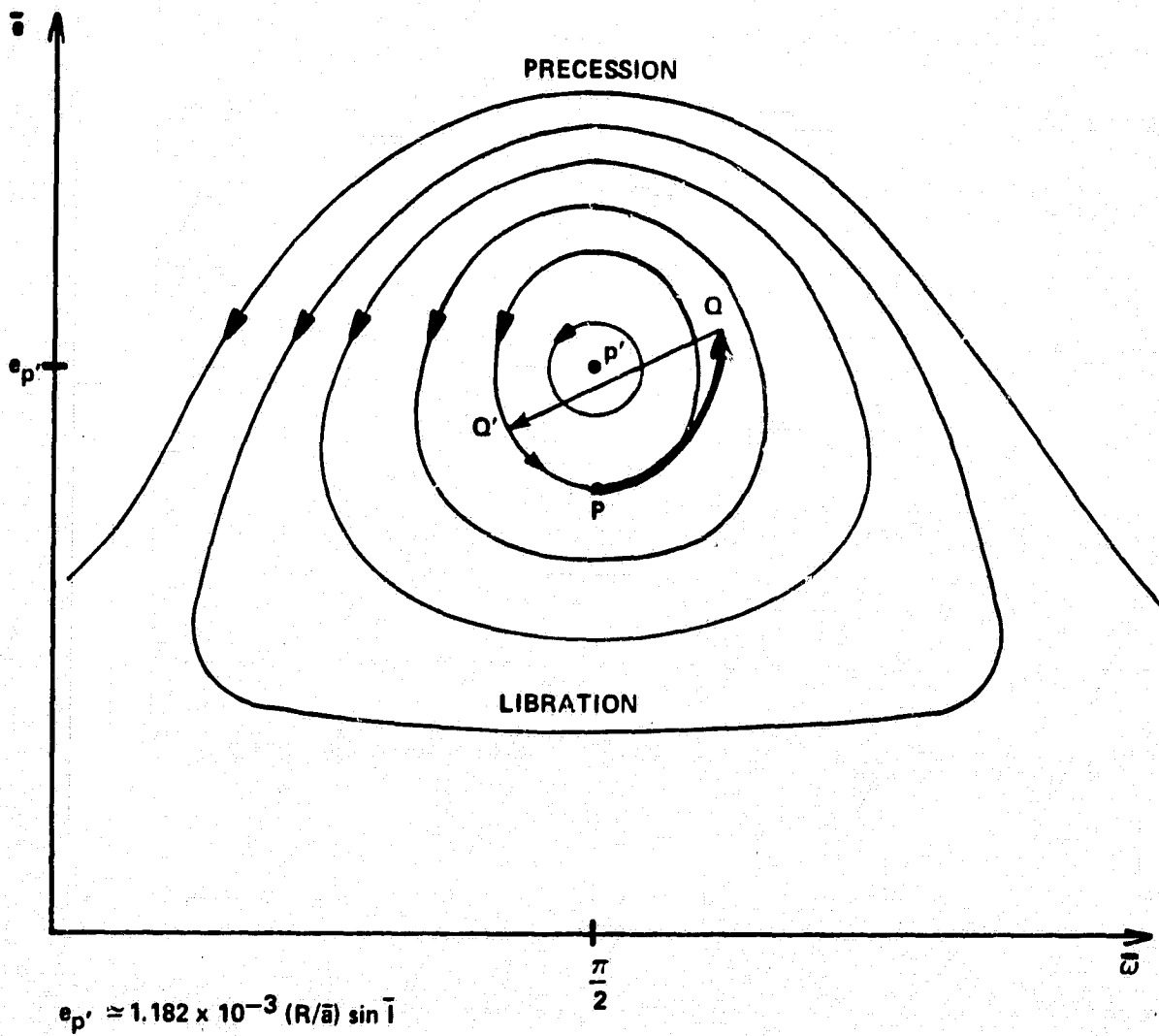


FIGURE 3. Long period evolution of the "frozen" orbit in the $\bar{e}, \bar{\omega}$ plane. P' is the true "frozen" point, P the computed "frozen" point; the line from Q to Q' indicates a corrective maneuver after Q has moved too far away from P .

4.4 The Repeating Ground Track

As clearly shown in Figures 2a-b, the ground track of a "frozen", repeat orbit is a curve of strong symmetries, including:

1. rotational symmetry about the \vec{z} axis;
2. periodicity (or self-closing, or time symmetry);
3. equatorial symmetry of its crossover points (approximate, the same as (5) below, because of the slight eccentricity of the orbit);
4. mirror symmetry about each of a set of $2N_R$ equally spaced meridians;
5. equatorial antisymmetry of the values of the Δt (the intervals between ascending and descending passes at the crossovers).

(a) Geometry

As a consequence of (1), (3) and (4), the crossovers are arranged along parallels; there are N_R equally spaced crossovers along each parallel; these parallels come in pairs equidistant from the equator (which is one of them only if N_R and N_D are both odd numbers). All

crossovers are aligned along the $2N_R$ meridians of symmetry and their connecting arcs form diamond-shaped partitions, each with the left and right vertices on two alternate meridians and the north and south vertices on the intermediate one.

Regarding the points of extreme north and south latitudes as "crossovers" where $\Delta t = 0$, there are at most $N_R + 2$ parallels with crossovers. Over the northernmost, perigee is reached, apogee over the southernmost; there ascending passes end and descending ones⁽¹⁾ begin, or vice versa. At each parallel, the intervals Δt (Modulus T_{rc}) have two different values of opposite signs: Δt_a and Δt_b , where $|\Delta t_a| + |\Delta t_b| = T_{rc}$; this is a consequence of (2). If N_R and N_D are both odd, the equatorial crossovers have $|\Delta t_a| = |\Delta t_b| = N_R T_o / 2 = N_D T_D / 2 = T_{rc} / 2$ (where T_o is the orbital period, and T_D the length of the nodal day). If either N_R or N_D is even (both cannot be even simultaneously, as they must be relative primes) the equator cuts through the middle of the lower half of one diamond, the top half of the next, and so on. If N_D is even and N_R is odd, there are at most $N_R + 1$ parallels with crossovers. The mirror symmetries about meridians with crossovers can be understood by imagining that, as the satellite reaches a crossover along an ascending pass, the North-South component of its velocity vector is suddenly reversed: In Earth-fixed coordinates the satellite (and its ground track) will follow a course symmetrical to the one that brought it to that crossover; this new course (when $\bar{\omega} = \frac{\pi}{2}$) is that of the descending pass

(1) $\bar{M} < 0$ and $\bar{M} > 0$, respectively.

over the crossover. The equal spacing in longitude between meridians with crossovers is a consequence of both this mirror symmetry and of the overall rotational symmetry. The equatorial antisymmetry of the intervals Δt follows from the approximate antisymmetry (respect to the geocenter) of the Earth and the slightly eccentric orbit when they are orientated according to their respective senses of rotation and revolution.

From the figures it is clear that the crossovers tend to crowd together towards the northern and southern edges of the band covered by the ground track. The overall pattern is that of a fishing net with its stitches aligned vertically and stretched in that direction towards the middle, without horizontal shrinking.

(b) Finding the Crossovers

For a crossover to take place, both the Earth and the satellite must come together twice: first during an ascending (or descending) pass, and again during a descending (or ascending) one. This means that, at the end of an interval equal to Δt , both the latitude and longitude of the subsatellite point must be the same as they were at the beginning. It also means that, since the argument of perigee is "frozen" at $\bar{\omega} = \frac{\pi}{2}$, the orbit must follow a path symmetrical to the meridian plane of the perigee in a system of coordinates where this plane is fixed. The beginning and end of this path occur at the same latitude ϕ both in this system and in the Earth-fixed one, and the time it takes the satellite to

complete it is Δt . Therefore Δt is a function of ϕ ; it also depends on T_0 and on the orbital inclination \bar{I} , so $\Delta t = f(\phi, \bar{I}, T_0)$. This relationship and the two ground track equations for ϕ and λ (Table 1c) provide a set of three equations in the unknowns Δt , ϕ and λ . Unfortunately, these are transcendental equations and have, as far as I know, no closed-form solution. Without this, to find the crossovers and their Δt it is necessary to search for approximate solutions, exploiting the symmetries of the ground track to save effort.

Starting at the highest latitude $\phi = \bar{I}$, choose a point in the ground track (ϕ_0, λ_0) directly under the perigee (i.e., $\phi_0 = \bar{I}$), so the corresponding true anomaly is $f=0$. Assume that the time of passage of the satellite over this point was $t_0=0$, and shift the origin of longitude so $\lambda_0=0$, which makes $\theta = \bar{\Omega} = -\frac{\pi}{2}$ (in this paragraph λ is defined, for convenience, in the interval $-\pi < \lambda < \pi$); select a small time-step $T \ll T_0$. The line $\lambda = \lambda_0$ is one of the $2N_R$ meridians with crossovers. To find the others, use the equation of the center to calculate f_T at $t=T$ (see Table 1c) knowing that $M_T = \bar{n}T$, where \bar{n} is the mean motion, and obtain ϕ_T and λ_T with the ground track equations. Repeat this process at $t=2T, 3T, \dots, kT$, continuing along the same descending pass until reaching a point $(\phi_{kT}, \lambda_{kT})$ just past the first meridian where $|\lambda| > \pi/N_R$. Estimate the location of this meridian and the time t_1 of passage through it by assuming that the satellite was moving with uniform velocity relative to the ground between points $k-1$ and k . If necessary, refine this estimate by starting from point $k-1$ with a time-step smaller than T . Once the location of the

intersection with the meridian is sufficiently well established, the coordinates (ϕ_1, λ_1) of this intersection correspond to a crossover point, and the other crossovers along the same parallel have coordinates $(\phi_1, \lambda_1 + j \pi/N_R)$, $j=1,2,\dots,N_R-1$. Find next the coordinates of the ground track points at times $t_1+T, t_1+2T, \dots, t_1+kT$, until $|\lambda| > 2\pi/N_R$, and repeat the search procedure just described, to locate the meridian where $|\lambda_2| = 2\pi/N_R$ and the corresponding t_2, ϕ_2, λ_2 of a second crossover. This determines, once more, the positions of all crossovers of latitude ϕ_2 . Continuing in this way, it is clear how the remaining crossovers (ϕ_i, λ_i) and their corresponding times t_i are to be found. When this is done, the positions of all the other crossovers in the ground track are also known. To obtain the crossover intervals between the ascending and the descending passes, for each value of i take $\Delta t'_i = 2t_i$ if the satellite motion is prograde (same sense as the Earth's rotation) and $\Delta t'_i = -2t_i$ if it is retrograde. Next, find N_{Ri} , the smallest positive integer for which

$$2|\lambda_i| = \{2\pi N_D (N_{Ri}/N_R)\} \text{ (Modulus } 2\pi).$$

The values of the two crossover intervals common to all crossovers at latitude ϕ_i are $|\Delta t_{ai}| = N_{Ri} T_0 + \Delta t'_i$ ($\Delta t_{ai} > 0$, if the motion is prograde, $\Delta t_{ai} < 0$, if retrograde), and $|\Delta t_{bi}| = T_{rc} - |\Delta t_{ai}|$, the sign of Δt_{bi} being opposite to that of Δt_{ai} . When great accuracy is not needed, one

may find the crossovers in the northern hemisphere, down to the equator, and then take advantage of the near equatorial symmetry of the ground track to locate the southern ones approximately, as the mirror images of their northern counterparts, using then the expression

$$t_{(N_R-i+1)} \approx T_0/2 - t_i$$

to finish the procedure in half the time.

Finally, to put the crossovers in the Greenwich longitude coordinate system, add the actual geographical longitude of the starting point, λ_0 , to each of the λ_i .

4.5 Orbit Error in a "Frozen", Repeat Orbit; its Geographical Characteristics

Neglecting, for the time being, the gravitational effect of the tides, the expression for Δr of gravitational and non-gravitational origin is the same as (47), except for the frequencies in the cosine terms:

$$\begin{aligned}
 \Delta r^{(N'I)}(t) = & \sum_{nmpq(\text{nonres})} \Delta C_{nma} \{ r_{nmpq} \cos[((n-2p+q)N_R - mN_D) \omega_{rc} t + \phi_{nmapq}] \\
 & + r_{nmp(q+1)} \cos[((n-2p+q+1)N_R - mN_D) \omega_{rc} t + \phi_{nmap(q+1)}] \\
 & + r_{nmp(q-1)} \cos[((n-2p+q-1)N_R - mN_D) \omega_{rc} t + \phi_{nmap(q-1)}] \\
 & + \frac{A}{K} \cos \dot{M}t + \frac{B}{k} \sin \dot{M}t + \frac{C}{k} t \cos \dot{M}t + \frac{D}{k} t \sin \dot{M}t + \frac{E}{k} t^2 \cos \dot{M}t + \frac{F}{k} t^2 \sin \dot{M}t \\
 & + \sum_{j=0}^J r_{jk} (t-t_o^k)^j.
 \end{aligned} \tag{52}$$

Here, in the $\phi_{nmap(q \pm \begin{smallmatrix} 0 \\ 1 \end{smallmatrix})}$, the term $\frac{1}{2} (1-(-1)^{n-m})$ of (39) can be replaced with $\frac{1}{2} (1-(-1)^m)$, because now $\bar{\omega}_o = \frac{\pi}{2}$ (Colombo, ib., 1984, Ch. 2, par. 2.2). The very small $\dot{\omega}$ due to the libration of the orbit about the "frozen point" has been ignored in the arguments

$((n-2p+(q\pm_1^0))N_R - mN_D)\omega_{rc} t$, because its effect on the true value of these arguments must remain negligible over weeks and even months, as explained later.

Since the mean orbit is "frozen", and kept so by corrective maneuvers wherever necessary, the $r_{nmp(q\{\pm_1^0\})_o}$, which depend only on \bar{a} , \bar{e} and \bar{I} among the elements, are virtually constant. So it is now both possible and convenient, as shall be seen when discussing altimetry in connection with ocean tides, to choose a time origin for the phase angles $\phi_{nmap(q + \{\pm_1^0\})_o}$ (expression (39)) that is different from that of the start of the arc t_o^k (which still appears in the arc-dependent part at the end of (52), either implicitly or explicitly). Instead, in the periodic terms of a "frozen", repeat orbit, " t_o " is the first time when $\bar{M} = 0$ at the beginning of the repeat part of the mission.

The periodical part of the orbit errors, according to (52), must look "frozen" to an observer who occupies the same geographical position every time the satellite passes by, as both the errors and the sightings occur with the same fundamental repeat period. The linearized equations of motion (including those for I , ω and Ω not given in (38)) show that periodical parts are present in all Δs_i , and therefore in all combinations of them besides Δr , like the along and the across track errors. So the differences (or residuals) between tracking data and the corresponding computed values of the ranges or range-rates (computed according to the positions and velocities of the estimated orbits) may

exhibit also periodical parts as they are, to first order, linear combinations of the orbit errors.

After subtracting altimetric heights determined at about the same locations along overlapping passes, temporal variations in the sea surface must be observable unless they are synchronous with the repeat period of the orbit, but the periodical part of Δr must vanish. This is, of course, very convenient when one wishes to study such changes in height as tides, etc., because a substantial part of the orbit error can be "filtered-out" in a simple way.

Because of the existence of a large periodical component that depends only on position along the ground track, Δr must show a strong spatial correlation. This correlation was found, empirically, by Anderle and Hoskin (1977) when they analyzed computer-simulated values of Δr . Inspection of (52) also shows that, if $\tilde{\Delta r}_a$ and $\tilde{\Delta r}_d$ are the values of the periodical component along ascending and descending passes, respectively, then $\tilde{\Delta r}_a$ and $\tilde{\Delta r}_d$ depend on ϕ and λ alone. Moreover, $\tilde{\Delta r}_a$ and $\tilde{\Delta r}_d$ are different functions of position, so their differences at the crossing points of ascending and descending passes are not zero (except for some components of zonal origin, as explained later). In the more general case (expression (47)) of satellites like GEOS-3, a smaller part of Δr (corresponding to terms where $q=m=0$, for example) has these periodical characteristics exactly, but still a considerable degree of geographical correlation can be expected for errors within passes separated in time by less than $1/4$ of the apsidal period $2\pi/\dot{\omega}$ (i.e., less than a month apart).

How "frozen" an orbit must be for the effective cancellation of the periodical part of Δr in the differences between overlapping passes to take place? All significant components of the orbit error due to the field model, at a height of about 1000 km, are produced by $\Delta C_{nm\alpha}$ with $n, m < 40$, so they must have wavelengths ν longer than $\nu_{\text{MIN}} \sim 360^\circ/40 = 9^\circ$. The time T between orbit corrections should be short enough to prevent an excessive departure from exact periodicity when $\dot{\omega} \neq 0$. The unwanted phase-shift due to $\dot{\omega}$, according to (47), is $q\dot{\omega}T$, where $|q| \leq 2$ for any terms big enough to matter. Therefore, $q\dot{\omega}T$ must be less than $\frac{1}{4} \nu_{\text{MIN}}$ (because a sinewave may reach its full amplitude in a quarter-cycle), so

$$T < \frac{9^\circ}{4} \frac{1}{2\dot{\omega}} \quad (53)$$

In the case of SEASAT, $\dot{\omega} \sim 1^\circ$ per month, so $T < 1.13$ months. Orbit decay, mostly produced by air drag, changes \bar{a} and, consequently, \dot{M} , and $\dot{\theta}$ through $\dot{\Omega}$ (see expressions (9'), (10) and (40a)). This causes a growing misclosure of the ground track that can reach several kilometers within T months. This is much less than ν_{MIN} , and the effects of variations in the other mean elements are smaller still, so the motion of the perigee is the main factor affecting the repetition of Δr . While T is not going to be the same for all satellites, it is likely that a maneuver a month, at most, will be enough to keep the orbit satisfactorily "frozen" in all cases.

4.6 Observability of Zonal, Initial State and Other Errors in Differences of Altimetric Heights

As the time origin has been chosen when the "frozen" mean orbit reaches perigee, so $M_0 = 0$ and $\bar{M} = \dot{M}t$, then $\phi_{nm\alpha pq_0} = 0$ in (39) for any periodical terms in (38) which are associated with a zonal coefficient error ($m = \alpha = 0$). Accordingly, expressions (47) and (50) show that, for the zonals, the periodical radial errors in the "frozen" orbit are sums of cosines of $j \dot{M}t = j\bar{M}$ ($j = 1, 2, 3, \dots$), so they are even functions of \bar{M} . With the perigee fixed at $\bar{\omega} = \frac{\pi}{2}$, \bar{M} is uniquely related to the latitude of the subsatellite point; therefore, the periodical components of Δr due to the zonals depend on latitude alone. This conclusion is not affected by the choice of time origin, as it might appear at first, because the periodical terms under consideration belong to the "steady state" response of the linearized equations, which does not depend on either the time origin or on the initial conditions. It is easy to show that this latitude-dependence is true of all periodical errors associated with $\Delta C_{nm\alpha}$ that are even functions of \bar{M} and whose order satisfy the resonant condition (51), although those coming from the zonals are by far the largest, as already explained.

A similar conclusion applies to the $\cos \dot{M}t$ term (in 47), so this component of the "once per revolution" part of Δr , due to the initial state errors (expression (23)), must be also a function of latitude only, at least within the same arc. Therefore, in height differences along overlapping passes and in crossover differences, observability is nil for

periodical errors of zonal origin, and very restricted for any other errors whose periodical components have frequencies that are harmonics of \dot{M} (Wagner, ib. 1984).

The observability problems considered so far affect only those components of Δr in (52) of frequency $k\dot{M}$ ($k=0,1,2,\dots$) and where $\{\alpha+[1-(-1)^{n-m}]\pi/2=0$ (i.e., sine terms are observable, cosine ones are not). For total lack of observability in crossover differences, the necessary and sufficient condition is that the intervals Δt between ascending and descending passes at all crossovers must be exact multiples of some "basic" interval $\Delta t_B < \Delta t_{\min}$ (where Δt_{\min} is the shortest of the Δt); if $\Delta t_B = \Delta t_{\min}$, then all Δt are exact multiples of Δt_{\min} . The unobservable components of Δr , if the general condition were satisfied, would be $\omega_u = 2\pi/\Delta t_B$ and its harmonics $k\omega_u$ (where $k=0,1,2,\dots$). Assuming that there is at least one repeat ground track where the condition is met, and that for it N_R and N_D are both odd numbers, this grid must have crossovers at the equator with $\Delta t_E = N_D T_D / 2$, as explained in a previous paragraph, where T_D is the length of the nodal day. This Δt_E must be a multiple of Δt_B , the same as Δt_{\min} . If the inclination of the orbit is increased, and the semimajor axis adjusted slightly to maintain a repeating ground track with the same N_R and N_D , then Δt_E must remain constant, in nodal days, but Δt_{\min} must increase. Otherwise, as can be shown quite easily from purely geometrical considerations, Δt_{\min} would not be long enough for the satellite to pass over the same point of the Earth's surface twice within one orbital period. So the new value of Δt_{\min} , measured in nodal days, must be longer than before, while

Δt_E stays the same: the congruence needed to have totally unobservable frequencies no longer holds. In consequence, total unobservability is not an invariant property of the repeating ground track. This does not preclude the existence of tracks where the Δt are close to meeting the necessary and sufficient condition. In fact, as reported by Douglas et al. (1984), that of SEASAT came close to having Δt that were all multiples of Δt_{\min} . Because N_R and N_D are both odd in this case and the satellite is retrograde (it moves contrary to the rotation of the Earth) one can show, on the basis of the geometrical properties of its ground track, that if all Δt , including Δt_E , were exact multiples of Δt_{\min} , then $\Delta t_{\min} = N_R/(N_R+1) T_O$, where T_O is the orbital period. As $N_R=43$ for SEASAT, $\Delta t_{\min} = 43/44 T_O \approx 0.977 T_O$, so $\omega_u = 2\pi/\Delta t_{\min} \approx 1.023 \dot{M}$, which is the value of ω_u given by Douglas et al. (ib). In reality, each Δt missed being an exact multiple of Δt_{\min} by a small margin, according to the diagrams in their paper. In any case, all periodical components of Δr associated with the $\Delta C_{nm\alpha}$ have frequencies (in the case of SEASAT) rather different from ω_u or its harmonics, as can be verified by making $N_R=43$ and $N_D=3$ in (52). The non-periodical part of Δr (same expression) has most of its spectral power concentrated within two narrow bands, one containing $\omega=0$, which is always unobservable, and the other centered at the partly unobservable \dot{M} and, thus, also near $\omega_u = 1.023 \dot{M}$. Nevertheless, as simulation studies indicate very clearly, there is no problem in observing part of this component as a gradual, cumulative change in the size of the crossover differences over a succession of repeats of the ground track. On the other hand, if one were to treat the

lines within these bands as independent from each other and to estimate their amplitudes and phases from those same differences by least squares, it is highly likely that the solution may turn out to be unstable. The way around this difficulty is to acknowledge that the lines are not independent, but strongly related to each other through the few arc parameters A_k , B_k , etc. in (52), on which they all depend. In other words, this part of the error should be modelled, not as a sum of a large number of steady oscillations, but as the sum of the few aperiodic terms of (52), instead. The bias r_{0k} and the oscillation $A_k \cos \dot{M}t$, both discontinuous from arc to arc, are not fully observable in crossover differences. Their changes in amplitude can be detected, if ascending and descending passes belong to different arcs, but not their individual values.

There may be further limitations to the observability of Δr in crossover differences because work with these is restricted, in essence, to oceanic crossovers. Over land, the roughness of the terrain makes the interpolation of heights between consecutive measurements unreliable, and crossover differences are always made out of interpolated heights, as it is most unlikely that two measurements would be taken exactly on the same spot.

4.7 Numerical Simulations of the Error in a "Frozen", Repeat Orbit

Table 2 presents the results of a computer sensitivity study of the effects of zonal resonances on the envelope of the "once per revolution" oscillation in Δr . Shown are the values of: the " $\Delta C_{nm\alpha}$ ", which are

really the differences between zonal potential coefficients of two gravitational field models (PGS-S3 and PGS-S4, Lerch et al., ib. (1982)) from $n=2$ to $n=9$; the published standard deviation for the errors of the same zonals in a well known model (GEM 10, Lerch et al., ib. 1977); the contribution of each zonal to the increase of the "once per revolution" oscillation expressed as an average weekly rate; the sum of these rates, or total rate. The results correspond to the "frozen", repeat orbit of SEASAT over an interval equal to its repeat period, or 3 days. They were obtained by first integrating numerically the orbit with one of the two field models, and then solving (also numerically) the exact (i.e, coupled and time varying) variational equations (21b) to get the individual radial effects of the ΔC_{n00} as accurately as possible. As expected, the contributions of the odd zonals to the errors were the largest (see footnote after equation (51)). Since the size of the actual $\Delta C_{nm\alpha}$ should be much the same up to degree 29 (if one believes the published standard deviations for the coefficients of GEM 10 to be both true and representative of the "state of the art"), the overall effect of zonal errors may be several times larger than the total given in the table. As the pelagic tides are supposed to be only a few decimeters in amplitude, this error cannot be ignored when studying such oceanographic phenomena. Regarding the secular changes in a , e and M (not shown in the table) the calculations indicated that ΔM was, by far, the one that influenced Δr the most.

TABLE 2

Increasing radial oscillations caused by gravitational zonal errors
 ΔC_{n00} .

Degree n	σ_{n00} (GEM9) x 10 ⁻⁹	ΔC_{n00} (PGS-S3/PGS-S4) x 10 ⁻⁹	Rate in meters/week
2	1.	-0.51	-0.02
3	1.	-1.65	-1.40
4	1.	1.00	-0.02
5	2.	0.50	-0.17
6	2.	-2.68	0.05
7	2.	1.16	-1.84
8	2.	-3.80	-0.06
9	2.	-2.65	5.41
		<u>Total Rate:</u>	1.95

These results correspond to a sensitivity study of SEASAT's repeat orbit where the zonal errors have been taken as equal to the differences between the zonal coefficients of field models PGS-S3 and PGS-S4. The published standard deviations of GEM 9 for the same coefficients are given for comparison. The coefficients are fully normalized and dimensionless.

A fully normalized coefficient is: $\bar{C}_{nm\alpha} = \left[\frac{(n+m)!}{(2-\delta_{m0})(2n+1)(n-m)!} \right]^{1/2} C_{nm\alpha}$.

The theory has been tested also by full simulations of Δr , done by F.J. Lerch and his assistant, N. Weiss, at Goddard Space Flight Center, whose help is greatly appreciated. "True" orbits, based on the ephemeris of SEASAT, were integrated numerically using the program GEODYN (Martin et al., 1b., 1976) with a given field model (the "true field") and used to create "range data" between "terrestrial stations" (whose coordinates were specified) and the "spacecraft". With a field model (the "incorrect model") different from the "true" one used before, "computed" orbits were fitted to the "data" by adjusting their initial states. The "radial errors" were the differences between the "computed" and the "true" radial positions. These simulated errors, over a period of six days, exhibited the characteristics that one would expect from expression (52): the presence of resonant terms with linear and quadratic parts, the former exceeding the latter by an order of magnitude, and shorter period perturbations repeating themselves with the same frequency as the ground track, every three days. For these perturbations, the departure from perfect repetition did not exceed 1 cm in any of the cases studied. Carl A. Wagner at NOAA has obtained similar results (personal communication). The repetition of the shorter period components was checked by studying the differences between errors at passes of the "spacecraft" over the same points along the ground track at 3 day intervals. The results suggest that expression (52) represents quite faithfully the main qualitative characteristics of Δr due to the imperfections of the field model alone. Figure 4a shows what a typical plot of the resonant part looks like over six days, or two consecutive repeat cycles of SEASAT. The error caused by the field model has a component at frequency \dot{M} that is cancelled

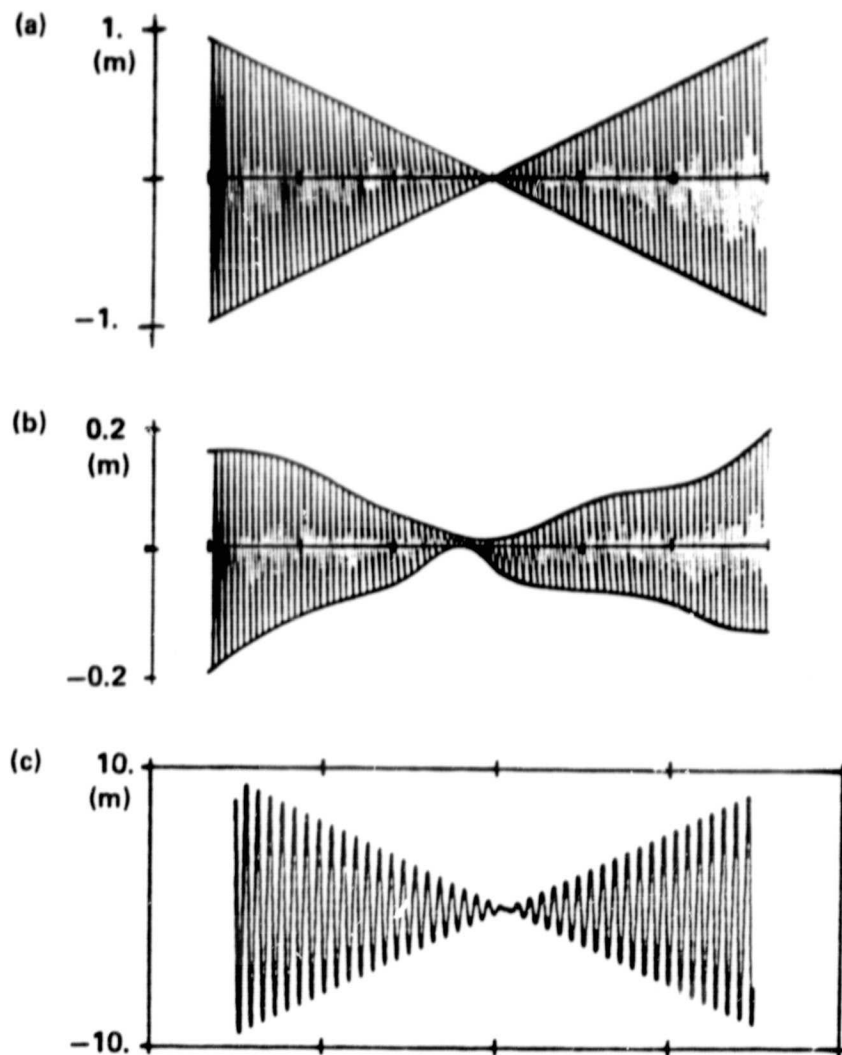


FIGURE 4. Simulated radial differences between "true" and "computed" orbits (with adjusted initial state).

- (a) Typical "bow-tie" pattern produced by GEM 9-like zonal errors. SEASAT, 6-day arc (two 3-day repeats).
- (b) Error caused by the drag model (Jacchia 1965-Jacchia 1971).
- (c) Error caused by wrong reflectivity coefficient (set equal to zero) in the presence of radiation pressure. ERS-1, one full 3-day repeat, heliosynchronous arc (from Wakker et al. (1983)).

by an oscillation of the same frequency and opposite sign produced by the error in the adjusted initial state which, in this way (see expression (23)), "absorbs" part of the gravitational error. This gives the envelope of the resonance its "bow-tie" shape, a name suggested to me by Richard Eanes.

The distribution of air density at satellite altitudes has two main large scale components: a zonal one (atmospheric oblateness) and a bulge that follows the Sun and thus turns once per year around the Earth's axis in inertial space. The atmospheric models used to calculate drag represent mainly these characteristics. Since they do so imperfectly, their errors have also a zonal part and a residual bulge that turns with a very slow angular velocity. The levels of the heating and ionizing solar radiation and of the magnetic flux do influence the air density; therefore, the density models are in error to the extent that they do not account properly for these and other variables. If these factors remained constant, both the large scale density and the model errors would be invariant in inertial space, except for the slow rotation of the bulge, so the "frozen" orbit would cross them with a frequency very close to \dot{M} and the density errors would set off resonances. In reality, both solar and magnetic activities fluctuate, modulating the density. However, if one followed the practice of adjusting the drag coefficient once every day when estimating the orbit, the effect of all these fluctuations could be greatly reduced, as suggested by one of the simulations of Δr done with a "true" atmospheric density and an "incorrect model" (the models in Jacchia (1965) and Jacchia (1971), respectively), both used with the actual

recorded changes in solar and magnetic activities that took place in the second week of September of 1978. The gravitational field was assumed to be perfectly known, and the true drag coefficient of the satellite to be constant, like that of a "cannonball". Figure 4b shows the sort of radial error that was observed. In it there is also an oscillation of frequency \dot{M} with an envelope somewhat resembling a "bow-tie", superimposed to which there is a fluctuation of much longer period, that can be represented by a low degree polynomial. While the envelope of the oscillation is more complex than in Figure 2a, the "secular" trend still dominates. Without a daily adjustment of the drag coefficient, the "polynomial" part was much more pronounced. Therefore, expression (52) describes quite well the radial errors observed in all the simulations (as long as the drag coefficient was adjusted once a day when non-gravitational forces were present).

Like the distribution of atmospheric density in the case of drag, the main sources of radiation pressure (direct sunlight, albedo reflection and re-radiation in the infrared from the Earth) are "static" in inertial space, following the slow, apparent annual motion of the Sun. Therefore, one would expect part of the error in a model of this force to "set off resonances" in Δr , much as the errors in atmospheric drag do. For a heliosynchronous satellite in a repeat orbit, the resonances must be most pronounced, because the angle between the orbit plane and the direction to the Sun is "frozen". This effect seems to be present in Figure 4c, taken from Wakker et al. (1983), which shows the differences over a 3-day repeat of ERS-1 between two simulated orbits, one with radiation pressure applied and the other without it.

5.0 TIDES

5.1 The Tidal Forces

The attraction at a point \underline{x} on the Earth's surface by a "disturbing body" (Sun, Moon, etc.) whose center of mass is at another point \underline{r}^* can be discussed in terms of the gravitational potential of this body at \underline{x}

$$V^*(\underline{x}) = \frac{\mu^*}{|\underline{r}^* - \underline{x}|}$$
$$= \frac{\mu^*}{R} \sum_{n=0}^{\infty} \left(\frac{R}{r^*}\right)^{n+1} P_{n0}(\cos \psi_x^*) \quad , \quad (54)$$

where ψ_x^* is the geocentric zenith distance of the disturbing body at \underline{x} , r^* is the distance between the body and the geocenter, μ^* is the mass of the body times the universal constant of gravitation G , and R is the mean radius of the Earth. Here our planet is considered to be a sphere and the disturbing body, because of its great distance, a point-like object with all its matter concentrated at the center of mass. These approximations are sufficient for the present discussion. The ellipticity of the Moon may also have to be taken into account when estimating the orbits of artificial satellites over very long arcs (several months).

As the system of coordinates is geocentric, it falls along with the Earth towards the attracting body with an acceleration

$$\underline{E}_a^* = \text{Total attraction of body on the Earth} / \text{Mass of the Earth } (M_e)$$

$$\approx G M^* (\underline{r}^*)^{-3} \underline{r}^*$$

(55)

which is also an approximation, as the Earth is a sizable body of nearly ellipsoidal shape and not a particle, so its center of mass is not quite the same as its center of gravity in the field of the disturbing body (Wahr, 1979, Ch. 2). For an Earth-fixed observer, \underline{E}_a^* cancels out the attraction of the disturbing body at the geocenter. Away from this point, the observer notices an increasing force. In an inertial coordinates system, the explanation for this is that the observer only perceives the difference between ∇V^* and the acceleration of his own quasi-inertial system \underline{E}_a^* . To use Newton's equations of motion in the observer's system in a simple way, $-\underline{E}_a^*$ is treated as the gradient of a fictitious gravitational potential

$$V_a^*(\underline{x}) = \oint_{\text{geocenter}}^{\underline{x}} (-\underline{E}_a^*) \cdot d\underline{r} = -\frac{\mu^*}{R} \left\{ \frac{R}{r^*} + \left(\frac{R}{r^*} \right)^2 \cos \psi_x^* \right\}$$

$$= -\frac{\mu^*}{R} \sum_{n=0}^1 \left(\frac{R}{r^*} \right)^{n+1} P_{n0}(\cos \psi_x^*), \quad (56)$$

where " $\oint_A^B \underline{y} \cdot d\underline{r}$ " indicates the line-integral between points A and B of the scalar product of \underline{y} and the oriented line element $d\underline{r}$. By doing this with the force exerted by each individual body and then adding the respective V_a^* 's in the right hand side of the equations of motion (19), these become formally like the equations of an inertial system and can be integrated accordingly. This is often done when computing orbits in "inertial space" (as the saying goes, though this is not to be taken literally). Expression (56) is the line integral of $-\frac{E^*}{a}$ along a path from the geocenter to \underline{x} with μ^*/r^* as the constant of integration (a constant in space, not in time). Adding (54) and (56) gives the expression of V_T^* , the tidal potential as observed in the geocentric system,

$$\begin{aligned}
 V_T^*(\underline{x}) &= V^*(\underline{x}) + V_a^*(\underline{x}) \\
 &= \frac{\mu^*}{R} \sum_{n=2}^{\infty} \left(\frac{R}{r^*}\right)^{n+1} P_{n0}(\cos \psi_x^*) \quad . \quad (57)
 \end{aligned}$$

According to the addition theorem for spherical harmonics

$$\begin{aligned}
 P_{n0}(\cos \psi_x^*) &= 2 \sum_{m=0}^n (1 + \delta_{m0})^{-1} \frac{(n-m)!}{(n+m)!} P_{nm}(\sin \phi) P_{nm}(\sin \phi^*) \cos m(\lambda^* - \lambda) \\
 &= 2 \sum_{m=0}^n (1 + \delta_{m0})^{-1} \frac{(n-m)!}{(n+m)!} P_{nm}(\sin \phi) Y_{nm0}(\phi^*, \lambda^* - \lambda) \quad , \quad (58)
 \end{aligned}$$

where (ϕ, λ) are the geographical latitude and longitude of \underline{x} , while (ϕ^*, λ^*) are those of the point on Earth from where the disturbing body can be seen at the zenith (so ϕ^* is the declination and λ^* the right ascension minus θ , of the body). Replacing $(\frac{R}{r})^{n+1} P_{no}(\cos \psi_x^*)$ with its expression according to (31) in terms of the osculating Keplerian elements $a^*, e^*, I^*, \omega^*, M^*$ of the disturbing body in the quasi inertial equatorial system, while truncating the expansion at⁽¹⁾ $n = 2$ and $|q| = 2$ because r^* is very large compared to R and e^* is small for both the Sun and the Moon (other bodies do not matter here), (57) becomes (see Kaula, 1964)

$$V_T^*(\underline{x}) = \frac{\mu}{a^*} \sum_{m=0}^2 \left(\frac{R}{a^*}\right)^3 \frac{2}{(1+\delta_{m0})} \frac{(2-m)!}{(2+m)!} P_{nm}(\sin \phi) \sum_{p=0}^2 F_{2mp}^{(I^*)} \sum_{q=-2}^2 G_{2pq}(e^*)$$

$$\cos [(2-2p+q)(\omega^*+M^*)-q\omega^*+m(\Omega^*-\theta-\lambda) - \frac{\pi}{4} (1-(-1)^{2-m})].$$

(59)

Traditionally, tidal theory has been formulated in ecliptical rather than equatorial coordinates, because in this system the inclinations of the disturbing bodies are very stable, which simplifies the mathematical treatment of their motions. The transformation of (59) to the ecliptical system is explained in (Marsh et al., 1983). If $s_i(\text{Sun})$ and $s_i(\text{Moon})$ stand for the various ecliptical Keplerian elements of the Sun and the Moon, respectively, then $\bar{I}_{(\text{Sun})}$ and $\bar{\Omega}_{(\text{Sun})}$ are both zero, by definition,

(1) To study some very minor tides, degrees 3 and 4 are included.

and the origin of Ω is the direction of the vernal equinox, as in the equatorial system. Instead of Keplerian elements, it is common practice, in tidal work, to use the following linear combinations of them:

$L = \theta + \lambda - s - \pi/2$, the mean local lunar time (expressed as an angle);

$s = (\bar{\omega} + \bar{M} + \bar{\Omega})_{(\text{Moon})}$, the lunar mean longitude;

$h = (\bar{\omega} + \bar{M})_{(\text{Sun})}$, the solar mean longitude;

$N = -\bar{\Omega}_{(\text{Moon})}$, the mean longitude of the lunar ascending node with a minus sign;

$p = \bar{\omega}_{(\text{Moon})}$, the mean longitude of the lunar perigee;

$p' = \bar{\omega}_{(\text{Sun})}$, the mean longitude of the solar perigee.

Here the word "longitude" refers to the "dog-legged" astronomical longitudes ($\Omega + \omega + M$), etc., which are very close to the ordinary longitudes in the ecliptical system because of the small inclinations of the orbits. Like the mean arguments $\bar{\omega}$, \bar{M} and $\bar{\Omega}$ of artificial satellites, the mean variables s , h , N , p_0 and p_1 change almost linearly over long intervals, in this case of the order of a century (thus the expression, "secular variations") so they are represented quite accurately by cubics,

like $s = s_0 + s_1t + s_2t^2 + s_3t^3$, etc. (see The "Explanations" to the American Ephemeris and Nautical Almanac) where the "rate" s_1 is orders of magnitude larger than s_2 and s_3 . The departures from linear change represented by s_2 and s_3 are mostly due to the gravitational forces exerted on the Earth and the Moon by the other planets. All the variables defined above, including the Earth's Greenwich angle θ , have mean speeds or frequencies that remain virtually constant over decades.

The Keplerian elements a^* , e^* and I^* are nearly constant in the ecliptical system, the Sun-Earth-Moon system being a very stable one, while ω^* , M^* and Ω^* change at approximately constant rates, as in the orbit of a satellite. This is particularly true of the Sun; in the case of the Moon, whose mass is much smaller, the pull of solar gravitation alters the orbit to the extent that, in the same way as the temporal variations (in inertial space) of the non-zonal part of the Earth's spinning field requires the introduction of the angular velocity $\dot{\theta}$ (through $-m\dot{\theta}$) in the theory of the motion of a spacecraft, the mean angular velocities of the "orbit" of the "moving" Sun must be included in the formulation of the motion of the Moon (Brown, 1905, Brouwer and Clemence, ib. 1966, Ch. 12). So the expansion of $V_T^{(\text{Moon})}$ must contain both lunar and solar frequencies, at least when the perturbations of the lunar elements are formulated using a first order analytical theory; only solar frequencies appear in $V_T^{(\text{Sun})}$. For this reason some tides are known as "lunisolar", others as "lunar", and yet others as "solar", on account of the origins of their frequencies. Instead of analytical

approximations, one could use direct estimates of the osculating Keplerian elements; these elements are available (in ecliptical coordinates) from precise astronomical ephemerides based on long series of observations (see Seidelmann, 1982). This last approach is adopted sometimes for the very accurate calculation of satellite orbits (Williamson and Christodoulidis, private communications).

Regardless of the body of origin, r^* , ϕ^* and λ^* in (58) can be expanded in trigonometric functions of the ecliptical variables L, s, h, p, N, p' (Brown, ib. 1905). Considering only the second harmonic of V^* , as in (59), and replacing V^* , ϕ^* and λ^* with their expansions, the result has the general form at the Earth's surface ($|\underline{x}|=R$):

$$V_T^*(\underline{x}) = \sum_{m=0}^2 P_{nm}(\sin\phi) \sum_{\beta_1=m}^{\beta_1} \beta_2 \beta_3 \beta_4 \beta_5 \beta_6 V_{\beta_1 \beta_2 \beta_3 \beta_4 \beta_5 \beta_6}$$

$$\cos [\beta_1' L + \beta_2' s + \beta_3' h + \beta_4' p + \beta_5' N + \beta_6' p' + (m-n) \frac{\pi}{2}],$$

(60)

where the integers β_i' are related to the β_i as follows:

$$\beta_1 = \beta_1'$$

$$\beta_i = \beta_i' + 5 \quad (i=2,3,4,5,6)$$

The β_i are always positive or zero, except in some unimportant cases where the amplitude $V_{\beta_1 \dots \beta_6}$ is very small; moreover, $\beta_1 = m$. The number D whose digits are the β_i :

$$D = \beta_1 \beta_2 \beta_3 \beta_4 \beta_5 \beta_6$$

is the Doodson number, which identifies uniquely each line in the tidal spectrum, or tidal constituent, besides providing complete information (once the various mean rates are known) on the value of its frequency ω_τ and on the phase angle χ_τ :

$$\omega_{\beta_1 \dots \beta_6} = \beta_1 \dot{L} + \beta_2 \dot{s} + \beta_3 \dot{h} + \beta_4 \dot{p} + \beta_5 \dot{N} + \beta_6 \dot{p}' \quad (61a)$$

$$= \omega_\tau$$

$$\chi_{\beta_1 \dots \beta_6} = \beta_1 L_0 + \beta_2 s_0 + \beta_3 h_0 + \beta_4 p_0 + \beta_5 N_0 + \beta_6 p'_0 \quad (61b)$$

$$= \chi_\tau$$

Because of the choice of L as a variable, the speed of the Moon orbit seems to appear in all tidal frequencies, but it cancels out with $\beta_2 \dot{s}$ for the "solar tides". The number $\beta_1 \beta_2 \beta_3 \beta_4 \beta_5 \beta_6$ and the amplitude $V_{\beta_1 \dots \beta_6}$ were computed and tabulated by Doodson (1921) for virtually all the important tidal constituents. The first digit β_1 , which is also "m" in (58), ranges between 0 and 2 according to (59). Because it multiplies

$\dot{\theta}$, which is part of \dot{L} , and $\dot{\theta}$ is much larger than the other rates involved, β_1 represents the separation of the tidal spectrum into three wide-apart main bands or species: long period ($\beta_1 = m = 0$), diurnal ($\beta_1 = 1$) and semi-diurnal ($\beta_1 = 2$). In turn, each species is divided into finer bands or groups, separated by intervals of $(\beta_2^{\dot{s}} + \beta_3^{\dot{h}})$ or, approximately, by multiples of one cycle per lunar month. Within each band, the individual lines are separated by multiples of one cycle every 8.85 years ($\beta_4^{\dot{p}}$), 18.61 years ($\beta_5^{\dot{N}}$), and 25800 years ($\beta_6^{\dot{p}'}$), (1) respectively. Usually, it is sufficient to add together all lines separated by less than one cycle per year from each other, and to consider these sums as the actual tidal constituents; if great precision over very long periods is needed, the hyperfine structure of the spectrum must be considered in full detail. The dominant constituents are far larger than the rest, and correspond to the principal tides M2, S2, K1, O1, etc., in the classical notation introduced by Darwin in the 1880's. Some of them, together with their Doodson numbers, are shown in Table 3. The equilibrium amplitude $g^{-1} v_{\beta_1 \dots \beta_6} P_{n\beta_1}(\sin\phi)$ (where $g \approx \mu/R^2$) is the size of the oscillation in the equilibrium figure of a perfectly fluid Earth that the tidal constituent would produce on its own (sometimes this is known as the "geoid tide"), and varies with latitude. Because of the continental boundaries, the submarine topography and the rotation of the Earth, ocean tides with periods of less than several years are not "in equilibrium", and have rather complex spatial structures.

(1) \dot{p}' is, in fact, the rate of precession of the Earth's axis, treated here as a movement of the Sun's "perigee" because of the way in which the ecliptical coordinates are defined ($\dot{\Omega}(\text{Sun})=0$).

TABLE 3

Principal Constituents of the Tidal Potential^(a)Caused by Both the Sun and the Moon

<u>Darwin's Name</u>	<u>Doodson Number</u>	<u>Period (hours)</u>	<u>Peak Amplitude of the Equilibrium Tide (meters)</u>
M ₂	255.555	12.42	0.2423
S ₂	273.555	12.00	0.1128
N ₂	245.655	12.66	0.0464
K ₂	275.555	11.97	0.0307
K ₁	165.555	23.93	0.1416
O ₁	145.555	25.82	0.1005
P ₁	163.555	24.07	0.0468
Q ₁	135.655	24.86	0.0193
M _o	055.555*	∞	0.1356
S _o	055.555*	∞	0.0629
M _m	065.455	661.31	0.0222

(a) The periods are those of the main constituents of the semi-diurnal, diurnal and long period bands. "Equilibrium tides" of semi-diurnal period peak at the equator, diurnal ones, at mean latitudes, and long period ones, at the poles.

(*) "Frozen" lunar and solar tides (respectively).

In what follows, expression (60) will be written in the following simplified way:

$$V_T^*(\underline{x}) = \sum_{\tau} V_{\tau} P_{2m}(\sin\phi) \cos(\omega_{\tau}t + \chi_{\tau} + m\lambda + (n-n) \frac{\pi}{2}), \quad (62a)$$

where " \sum_{τ} " indicates the sum of all significant tidal constituents, and "*" has been dropped from the right hand side, as the solar or lunar origin of a particular constituent is of no further interest here. Now, according to (61a) and to the definition of L , $m = \beta_1$ is a function of ω_{τ} :
 $m = \text{Int} \left[\frac{\dot{\theta}}{|\dot{\omega}_{\tau}|} + 1/4 \right]$, "Int [.]" meaning "the integer part of". In the new expression of $V_T^*(\underline{x})$,

$$V_{\tau} = V_{\beta_1 \beta_2 \beta_3 \beta_4 \beta_5 \beta_6} \quad (62b)$$

$$(\beta_1 = m)$$

is the amplitude,

$$\omega_{\tau} = \beta_1(\dot{\theta} - \dot{s}) + \beta_2 \dot{s} + \beta_3 \dot{h} + \beta_4 \dot{p} + \beta_5 \dot{N} + \beta_6 \dot{p}' \quad (62c)$$

is the (angular) frequency and

$$\chi_{\tau} = \beta_1(\theta_0 - s_0 - \pi/2) + \beta_2' s_0 + \beta_3' h_0 + \beta_4' p_0 + \beta_5' N_0 + \beta_6' p_0' \quad (62d)$$

is the astronomical phase. It is a useful and universal convention that χ_{τ} is the phase at $t_0' = 0.00$ hours, Greenwich mean time, of the day in which the instant "t" falls (so "t", in fact, is $t - t_0'$). But in the discussion that follows, in order to make the treatment of tides consistent with that of the radial orbit error, χ_{τ} is defined as

$$\chi_{\tau} = \chi_{\tau}(t_0) - \omega_{\tau} t_0, \quad (62d')$$

(as in (62d))

where " t_0 " is t_0^k for the general case corresponding to (47), but (as explained in the comments that follow (52)) for "frozen", repeat orbits t_0 is such that $\bar{M}(t_0) = 0$ at the start of the "repeat" part of the mission. This choice is preferable for writing formulas: for actual calculations, the conventional one is more accurate and freer of numerical round-off problems.

The change in the geographical coordinates of the point where the spin axis intersects the Earth's surface, or polar motion, reflects mostly the free wobble of the Earth (Chandler Wobble). Polar motion produces a fluctuation in the centrifugal force experienced by objects fixed to the planet, so it changes the acceleration of gravity acting on them, and causes deformations and movements in the body, oceans and atmosphere similar to those due to the tidal potential (but much smaller). This response is known as the pole tide. Since its period is completely unrelated to the lunar and solar frequencies (about 1.18 years), it can be detected in sensitive gravimetric tidal records as a separate and very weak oscillation, particularly at high latitudes. Precession and nutation also affect gravity, but they are themselves parts of the overall tidal response to the pull of the Sun and the Moon, and their effects on the solid Earth, oceans and atmosphere are incorporated into the diurnal tides (see Wahr, 1982).

The tidal potential V^* , according to (57), is rotationally symmetrical about the line from the Earth to the disturbing body. Its equipotential surfaces have an interesting geometry: the surface $V^* = 0$ is a double cone with its vertex at the geocenter (opening both towards and away from the body). This cone, which gets broader as the body gets closer, is the asymptotic surface of a family of revolution hyperboloids of two sheets, which are the other equipotentials. The tidal acceleration ∇V^* has the same rotational symmetry and is also equal in magnitude and opposite in sign at points equidistant from the geocenter about the

Earth-body line. This description holds provided that terms in (57) of degree $n > 2$ can be neglected and one does not get so close to the disturbing body that it no longer can be treated as point-like. In the case of a satellite free-falling around the Earth, the field of "residual gravity" measured in a system fixed to the spacecraft has also this configuration (with the Earth as the disturbing body). Detailed and charming discussions of this geometry can be found in two papers (1977 and 1982) by the late A. Marussi. At the Earth's surface, the combination of the geopotential V with V^* creates, in the nearly spherical equipotential surfaces of V , a slight deformation shaped as a symmetrical ellipsoidal bulge pointing towards the disturbing body: this bulge is the total "equilibrium tide". Since the Sun and the Moon lie at or near the ecliptic, this bulge is tilted with respect to the Earth's spin axis, so the rotation of the latter carries the points of its own surface through the bulge. At mid- and low-latitudes the points cut through both "lobes" of the bulge, experiencing a twice-daily variation in V^* . Closer to the poles, only one lobe is cut (most of the time) so the diurnal species prevails far from the equator, and the twice-diurnal closer to it. As the mean value of V^* is not zero along parallels, there is a component that changes only as the body moves slowly along its orbit: this is the long period species. The ellipticity and precession of the orbit modulates both the bulge and the species, splitting these into bands and those, in turn, into lines.

It is interesting to notice that, according to (57), the tidal potential increases as r^* decreases. Imagine that the system of coordinates is chosen at the center of mass of a body which, like the Moon, orbits a more massive one, like the Earth, and that the two bodies get closer, until the attraction of the main one exceeds the self-gravitational force that pulls the other together, and breaks it up. The distance at which this catastrophe occurs is known as the "Roche limit". Maybe this is the process that once created the rings of Jupiter, Saturn and Uranus out of the disintegration of icy moons, and now keeps those rings from coalescing again into larger bodies. In the case of Io, the innermost of the large moons of Jupiter, the tidal forces are sufficiently vigorous to heat the interior by continuous friction, probably keeping it partially molten and causing the spectacular vulcanism for which this world is now famous. Terrestrial tides, though much less energetic, play a significant role in the deceleration of the Earth-Moon system.

5.2 The Tidal Response

The attractions of the Sun and the Moon torque the slightly elliptical spinning Earth, causing the precession of its figure axis, one cycle of which takes about 25800 years. The relative positions of the Earth and the disturbing bodies vary as they move, so the torque is modulated at the orbital frequencies both in intensity and in direction. The result is a "nodding" motion of the Earth's axis, or nutation (see Leick, 1978). Precession and nutation are movements of the Earth as a

whole. Because the planet is not perfectly rigid, the changes in the attractions of the disturbing bodies also produce small movements, or tides, which vary from place to place, as well as slight variations in the spin rate $\dot{\theta}$ (not considered here any further). These tides are the subject of the rest of this section; the reader can find a very clear and up-to-date discussion of the (somewhat arbitrarily separated) components of the tidal response of the Earth: precession, nutation and tides, in (Wahr, *ib.* 1982).

5.3 Linearity and Time-Invariance

The joint attractions of the Sun and the Moon cause displacements of the matter in the interior, oceans and atmosphere of the Earth that are very small compared to the size of the planet; that joint pull itself is quite small when compared to the gravitational force the whole planet exerts on each of its parts. It is, therefore, not surprising that those displacements, their interactions, and the resulting fluctuations in the gravitational field can all be described accurately by first order, or linear, approximations to the response of a nonlinear system (the Earth) to the disturbing forces. Over an interval of a few centuries, the large scale mechanical characteristics of the Earth are likely to stay virtually constant, so it seems reasonable to expect those linear approximations to be also time-invariant, perhaps after making some minor simplifying assumptions. If such is the case, the spectra of the various components

of the tidal response (ocean tides, body tides, etc.) should have their lines situated at precisely the same frequencies as their driving forces, which are those given by expression (62c). This is in very close agreement with observation (except for some small anomalies in shallow seas that suggest some nonlinear frequency mixing), which means also that both the disturbing forces and the frequencies of the resulting tides can be calculated very accurately from purely astronomical data.

The formulation of a realistic nonlinear model for the Earth, and its linearization with respect to some reasonable and convenient undisturbed state to obtain a good time-invariant approximation, are quite complex matters, as is the solution of the resulting linear partial differential equations. Nevertheless, because of their time-invariance, and of the nearly spherical symmetry of the Earth, the linearized equations have solutions with strikingly simple and helpful properties, summed up in the ideas of "admittance function" and "Love numbers".

5.4 The Admittance Function

A long record of observations of ζ_0 , the "surface-bottom" ocean tide, at a station of latitude and longitude (ϕ, λ) , can be approximated quite accurately by a trigonometric series:

$$\zeta_o(\phi, \lambda, t) = \sum_{\tau} \sum_{\beta=0}^1 a_{\beta\tau}(\phi, \lambda) \cos(\omega_{\tau}t + \chi_{\tau} - \beta \frac{\pi}{2})$$

$$= \sum_{\tau} \zeta_{o\tau}(\phi, \lambda, t), \quad (63)$$

where ω_{τ} is the tidal frequency and χ_{τ} the astronomical argument, as per (62 c-d), of the ocean tidal component $\zeta_{o\tau}$. Now, according to (62a)

$$V_{T\tau}(\phi, \lambda, t) = V_{\tau} P_{2m}(\sin \phi) \cos [\omega_{\tau}t + \chi_{\tau} + m\lambda + (m-n) \frac{\pi}{2}]$$

$$(64)$$

(with $m = \text{Int} [\hat{\theta}/|\omega_{\tau}| + \frac{1}{4}]$)

is the constituent of frequency ω_{τ} of the tidal potential at (ϕ, λ) . Over the Earth's surface $V_{T\tau}$ consists only of second degree spherical harmonics, under the approximations made in its derivation. The admittance function relating $\zeta_{o\tau}$ to $V_{T\tau}$ is the complex quantity

$$Y(\phi, \lambda, \omega_{\tau}) = \frac{|\zeta_{o\tau}(\phi, \lambda)|}{|V_{T\tau}(\phi, \lambda)|} e^{i\varepsilon_{\tau}(\phi, \lambda)}, \quad (65a)$$

where

$$\zeta_{o\tau}(\phi, \lambda) = \left[\sum_{\beta=0}^1 a_{\beta\tau}^2(\phi, \lambda) \right]^{1/2} \text{sign} [V_{\tau}] \quad (65b)$$

and

$$\epsilon_{\tau}(\phi, \lambda) = -tg^{-1} [a_{1\tau}(\phi, \lambda)/a_{0\tau}(\phi, \lambda)] - m\lambda - (n-m) \frac{\pi}{2} \quad (65c)$$

are the amplitude of the constituent of ζ_0 of frequency ω_{τ} , and its phase shift relative to the corresponding constituent of V^* . The accumulated evidence (Hendershott and Munk, *ib.*, 1970) suggests that $Y(\phi, \lambda, \omega_{\tau})$ is a smooth function of ω_{τ} , so it varies very little in modulus and phase across each of the narrow bands that make up the tidal spectrum. For this reason, if $\omega_{\tau(\text{central})}$ is the frequency of a line within one of these bands situated near the center, it is valid to assume that

$$\epsilon_{\tau}(\phi, \lambda) = \epsilon_{\tau(\text{central})}(\phi, \lambda) \quad (66a)$$

and

$$\frac{\zeta(\phi, \lambda)}{o\tau} = \frac{\zeta(\phi, \lambda)}{o\tau(\text{central})}, \quad (66b)$$

$$\frac{V(\phi, \lambda)}{T\tau} = \frac{V(\phi, \lambda)}{T\tau(\text{central})}$$

so

$$\frac{a(\phi, \lambda)}{o\tau} = \frac{a(\phi, \lambda)}{o\tau(\text{central})} \quad (67)$$

$$\frac{a(\phi, \lambda)}{l\tau} = \frac{a(\phi, \lambda)}{l\tau(\text{central})}$$

for $0 < \beta < 1$ and all ω_{τ} in that band. From the last relationship and (63) follows that

$$\zeta_{o(\text{band})}(\phi, \lambda, t) = \sum_{\beta=0}^1 a(\phi, \lambda) \sum_{\tau(\text{band})} (V_{\tau}/V_{\tau(\text{central})}) \cos(\omega_{\tau} t + \chi_{\tau} - \beta \frac{\pi}{2}), \quad (68)$$

where " $\sum_{\tau(\text{band})}$ " indicates that the sum is over the constituents in the band only. To speed up calculations at the price of a slight loss of accuracy, one can make use of the relationships

$$\cos(\omega_{\tau} t + \chi_{\tau} - \beta \frac{\pi}{2}) = \cos \chi_{\tau} \cos(\omega_{\tau} t - \beta \frac{\pi}{2}) - \sin \chi_{\tau} \sin(\omega_{\tau} t - \beta \frac{\pi}{2})$$

and, to first order in $(\omega_{\tau(\text{central})} - \omega_{\tau})t$,

$$\begin{Bmatrix} \cos \\ \sin \end{Bmatrix}(\omega_{\tau} t - \beta \frac{\pi}{2}) \approx \begin{Bmatrix} \cos \\ \sin \end{Bmatrix}(\omega_{\tau(\text{central})} t - \beta \frac{\pi}{2}) + (\omega_{\tau(\text{central})} - \omega_{\tau})t \begin{Bmatrix} \sin \\ -\cos \end{Bmatrix}(\omega_{\tau(\text{central})} t - \beta \frac{\pi}{2}).$$

So, instead of (68),

$$\zeta_{o(\text{band})}(\phi, \lambda, t) \approx \sum_{\beta=0}^1 a(\phi, \lambda) \sum_{\tau(\text{band})} \left\{ A_{\tau(\text{band})}(t) \cos(\omega_{\tau(\text{central})} t - \beta \frac{\pi}{2}) + B_{\tau(\text{band})}(t) \sin(\omega_{\tau(\text{central})} t - \beta \frac{\pi}{2}) \right\}, \quad (69)$$

where

$$A_{\tau(\text{band})}(t) = \sum_{\tau(\text{band})} (V_{\tau}/V_{\tau(\text{central})}) [(\omega_{\tau(\text{central})} - \omega_{\tau})t \sin \chi_{\tau} + \cos \chi_{\tau}] \quad (70a)$$

and

$$B_{\tau(\text{band})}(t) = \sum_{\tau(\text{band})} (V_{\tau}/V_{\tau(\text{central})}) [(\omega_{\tau(\text{central})} - \omega_{\tau})t \cos \chi_{\tau} - \sin \chi_{\tau}] \quad (70b)$$

provided that $|(\omega_{\tau(\text{central})} - \omega_{\tau})t| \ll |(\omega_{\tau(\text{central})} t + \chi_{\tau})|$. In actual calculations this condition can be met by updating the phases χ_{τ} in the above expressions sufficiently often (for a given band), and using these new values with "t" counting from the time of the last resetting, until the next update. This saves the effort of having to compute one sine and one cosine value at every instant where (68) has to be evaluated, for every frequency in the band. For solar tides, the V_{τ} must be corrected to account for the "radiational tide potential" (Cartwright and Tayler (1971)). Radiational tides are caused mostly by the periodical heating of the atmosphere by the Sun, which modifies the air pressure at the sea surface, forcing the ocean at the same frequencies as the solar tides. This thermally driven variation of the atmosphere accounts for most of the atmospheric "tides", with the gravitation of the Sun and the Moon playing a lesser role.

5.5 Love Numbers

ζ_0 can be regarded as a function defined for all ϕ and λ but which is identically zero over land. Such a function must have an infinite spherical harmonic expansion because, although very smooth over the oceans, it is discontinuous across the coastal boundaries. Furthermore, ζ_0 is at each point a sum of trigonometric functions of time, as in (63), so its complete expansion in space and time is

$$\begin{aligned} \zeta_0(\phi, \lambda, t) &= \sum_{\tau} \sum_{n=0}^{\infty} \left\{ \sum_{m=0}^n \sum_{\alpha=0}^1 \sum_{\beta=0}^1 \zeta_{nm\alpha\beta\tau} Y_{nm\alpha}(\phi, \lambda) \cos(\omega_{\tau} t + \chi_{\tau} - \beta \frac{\pi}{2}) \right\} \\ &= \sum_{\tau} \sum_{n=0}^{\infty} \zeta_{0n\tau}(\phi, \lambda, t), \end{aligned} \quad (71)$$

where the $\zeta_{nm\alpha\beta\tau}$ are the spherical harmonic coefficients of a $\beta_{\tau}(\phi, \lambda)$ ($\beta=0,1$) in (63).⁽¹⁾ Putting (70) and (71) together:

$$\begin{aligned} \zeta_{0(\text{band})}(\phi, \lambda, t) &\approx \sum_{n=0}^{\infty} \sum_{m=0}^n \sum_{\alpha=0}^1 \sum_{\beta=0}^1 \zeta_{nm\alpha\beta\tau(\text{central})} Y_{nm\alpha}(\phi, \lambda) \\ &\quad \left\{ A_{\tau(\text{band})}(t) \cos(\omega_{\tau(\text{central})} t - \beta \frac{\pi}{2}) + B_{\tau(\text{band})}(t) \sin(\omega_{\tau(\text{central})} t - \beta \frac{\pi}{2}) \right\}. \end{aligned} \quad (72)$$

(1) Tide-lands notwithstanding, in a global scale it is reasonable to regard the coasts, as well as the ocean floor, as impermeable and well defined boundaries. Under this assumption, the conservation of mass requires that $\zeta_{n0}=0$ in (71) et seq., so $\zeta_{000\beta\tau}=0$ for all β and all τ (if $\omega_{\tau} \neq 0$). However, the same notation shall be used later for the spherical harmonic expansions of tidal models and their errors; some of them do not satisfy the conservation constraint, so the zero harmonic has been kept in (71) et seq.

The altimeter measures the total tide, not individual components, and the concept of admittance makes it easier to take into account the "sidebands" when estimating the "main tides" from altimetry (such as M2, S2, K1, etc.). In what follows, $\zeta_{on\tau}(\phi, \lambda, t)$ (the expression between curly brackets in (71)) shall be called, for short, the "n spherical harmonic" of ζ_0 (at frequency ω_τ).

The tidal displacement of water changes the forces acting on the body of the Earth, which yields because this body is not rigid. These related movements of water and solid matter modify the gravitational potential. Since the responses are nearly linear and the Earth is close to having spherical symmetry, the spherical harmonic expansion of ζ_0 is related to those of the vertical displacement δ' of the bottom and of the tidal-induced change in potential $V^{(\zeta_0)}$ as follows:

$$\delta'(\phi, \lambda, t) = \sum_{\tau} \sum_{n=0}^{\infty} \alpha_n h_{n\tau} \zeta_{on\tau}(\phi, \lambda, t) \quad (73)$$

and

$$V^{(\zeta_0)}(\phi, \lambda, t) = g \sum_{\tau} \sum_{n=0}^{\infty} \alpha_n (1 + k_{n\tau}') \zeta_{on\tau}(\phi, \lambda, t) \left(\frac{R}{r}\right)^{n+1}. \quad (74)$$

Here

$$\alpha_n = \frac{3\rho_w}{\rho_e(2n+1)},$$

$g = \mu/R^2$ is the mean acceleration of gravity on the Earth's surface, ρ_w the mean density of water and ρ_e the mean density of the Earth. $h'_{n\tau}$ and $k'_{n\tau}$ are known as load Love numbers (Munk and McDonald, 1960; Farrell, 1972) because δ' and $V^{(\zeta_0)}$ are the result of the loading of the body of the planet by the ocean tide on its surface. Their dependence on ω'_τ as well as on n is stressed here to bring the formulation in line with that of Wahr (ib., 1979) for ordinary Love numbers, which probably is the most realistic one at present; the extension to load Love numbers can be found in (Sasao and Wahr, 1981). In the past this dependence has been largely ignored, because the theory was restricted mostly to the spherical, non-rotating case, where the main free oscillatory modes have a frequency considerably higher than any tidal component. Wahr has included the effect of both rotation and oblateness in his computations. The latter requires the use of functions slightly different from the $Y_{nm}^{(\phi, \lambda)}$; however, the difference in the results is less than 1% and can be ignored here.

The tidal potential has an expansion on the Earth's surface given by (62a). V^* causes a deformation of the body of the Earth, or body tide, resulting in a vertical displacement δ and a change in potential $V^{(\delta)}$ which are, approximately,

$$\delta(\phi, \lambda, t) = \sum_{\tau} k_{2\tau} V_{T\tau 2}(\phi, \lambda, t) \quad (75)$$

(here $V_{T\tau 2}(\phi, \lambda, t)$ is the same as $V_{T\tau}(\phi, \lambda, t)$ in (64)),

and

$$V(\phi, \lambda, t) = \sum_{\tau} h_{2\tau} V_{T\tau 2}(\phi, \lambda, t) \left(\frac{R}{r}\right)^3. \quad (76)$$

The contribution of ζ_0 to the geocentric tide ζ_G of expression (1) is

$$\begin{aligned} \zeta_G - \delta &= \zeta_0 + \delta' \\ &= \sum_{\tau} \sum_{n=0}^{\infty} (1 + \alpha_n h'_{n\tau}) \zeta_{0n\tau}(\phi, \lambda, t). \end{aligned} \quad (77)$$

The $h_{2\tau}$ and $k_{2\tau}$ are known simply as Love numbers, after the man who first wrote about them (Love, 1909). In the interval $2 < n < 25$, which includes most spatial frequencies of interest, the approximate sizes of these various numbers change monotonically from

$$h_{2\tau} \approx 0.612, \quad k_{2\tau} \approx 0.302, \quad h'_{2\tau} \approx -1.007, \quad k'_{2\tau} \approx -0.310, \quad \alpha_2 \approx 0.11,$$

to

$$h_{25\tau} \approx 0.047, \quad k_{25\tau} \approx 0.002, \quad h'_{25\tau} \approx -2.194, \quad k'_{25\tau} \approx -0.046, \quad \alpha_{25} \approx 0.011$$

(from Table 1 in Hendershott, 1972). The largest departures from these values occur within the diurnal band.

The values of $h_{2\tau}^\tau$, $k_{2\tau}^\tau$, $h_{2\tau}^{\tau 2}$ and $k_{2\tau}^{\tau (1)}$ can be calculated by using a simplified linear model for the departures of the particles that made up the body of the Earth from their undisturbed state, selecting a plausible set of physical parameters for the matter of the planetary interior, and integrating numerically a set of ordinary differential equations related to the linear model. The integration variable is depth, in the interval from the geocenter to the surface, and the Love numbers are the integrated values at the surface. Usual approximations include a spherical or elliptical body where density, elastic parameters, etc. vary only with depth and viscosity is zero, so there is no energy dissipated by the tidal motions. The mechanical parameters are discontinuous at the boundaries separating the core (divided in solid inner core and liquid outer core), the mantle and the crust, sometimes with an additional change between upper and lower mantle. In consequence, the published values of the Love numbers vary according to the linear Earth models used for their computation. Wahr (ib., 1979) has assumed an elliptical, vertically stratified, dissipationless Earth with no oceans. A slightly more accurate formulation, including dissipation, would require the introduction of small additional phase shifts $\epsilon_{n\tau}$ on top of the χ_τ in

(1) There is a component V_F of the total tidal potential, in the long period species ($m=0$), which is actually constant in time (and virtually a second zonal in space, see expression (62)). It produces an equally constant change in the Earth's equatorial bulge and, thus, in the value of C_{200} compared to what it would be if our planet were alone in space. The Love numbers for the resulting stationary body tide are probably those of a "liquid Earth", as our planet is supposed to have been "flowing" towards its actual figure of hydrostatic equilibrium over the eons that this "frozen tide" has been acting on it. There is also a slight discrepancy between the "bulge" of the mean ocean surface and that of the geoid, equal to the "frozen" component of the ocean tide V_F/g (S_0 and M_0 in Table 3).

the arguments of the tidal functions. This appears unnecessary here. The main variation of the Love numbers with ω_T occurs when the frequency is close to one cycle per day (diurnal tides) and is caused by a resonance in the fluid core (Wahr, ib., 1979 and Wahr and Sasao, 1981). For semi-diurnal tides the Love numbers are virtually independent of ω_T . Horizontal changes in density, etc., further complicate the picture, but they do not have to be considered here; they would only matter in highly accurate or local studies of tides.

5.6 Representing The Ocean Tides

The mathematical model for the ocean tides is derived from the nonlinear Navier-Stokes equations of hydrodynamics, linearized by ignoring small quadratic terms in the unknowns and using first order formulations for the forces related to turbulence, bottom friction, crustal bending (δ') and self gravitation ($v(\zeta_0)$). In Cartwright (ib., 1977), Hendershott (1972), Schwiderski (ib. (1980b)) and Parke and Hendershott (1980) one can find information on the historical development of the linear theory and of the methods for integrating the tidal equations. Alternatively, the use of nonlinear terms to represent bottom friction yields a system of equations that is overall nonlinear and can only be solved by numerical integration in space and in time (Estes, 1980). On the other hand, a purely linear system requires numerical integration in space alone, the time variable being eliminated by working with the Fourier transform of ζ_0 (as in Pekeris and Accad, 1969). The

simplest linear equations are those of Laplace. Usual assumptions made in obtaining tidal equations are that the Earth is spherical, the depth z of the ocean is nowhere significant compared to the planetary radius and to the horizontal size of the tidal waves, that the small meridional component of the Coriolis force can be ignored, and that the velocity of the horizontal tidal current is independent of depth. In fact, the velocity does change from the surface down, but because the density of ocean water is well stratified there are two main types of waves: those described by the tidal equations, which move the surface up and down to produce ζ_0 , creating horizontal currents that are virtually independent of depth, and those that do not move the surface appreciably (also known as internal waves) but cause currents that vary with depth. Clearly, only waves of the first type can be mapped with an altimeter or with conventional tidal gauges.

Figures 5 and 6 show the charts of the M2 constituent obtained by Schwiderski (1979). The lines in Figures 5 and 6 present the amplitude $\zeta_{0T}(\phi, \lambda)$ in cm and the phase in degrees. The lines of equal phase (or cotidal lines) in Figure 6 show, successively, where the tidal waves crest at about half an hour intervals. Looking at these lines in their proper sequence makes an "animated picture" of the waves as they turn about their fixed nodal points or amphidromes (where the amplitude is always zero). Notice how smooth the waves are.

Goad (1980) has computed the power spectrum of Schwiderski's M2 tide up to degree $n=180$, showing a fast rise up to degree $n=8$ and then a fall of more than an order of magnitude at $n=20$; from there on the spectrum trails off to zero slowly, reflecting the discontinuities of ζ_0 along the coasts. For the other semi-diurnal components the general shape of the maps, including the approximate location of the amphidromes, is quite similar as for M2. The same is true for the diurnal components, although their patterns are quite different concerning the locations of the amphidromes, etc., from those of the semi-diurnals.

While the waves of individual constituents are virtually periodical, the total tide is not, because the orbital frequencies of the Moon are not harmonics of those of the Sun. Therefore ζ_0 never repeats itself exactly.

A fluid motion can be described in terms of a velocity potential ϕ and a stream function ψ (see Lamb (1932)), and both ζ_0 and $\Delta\zeta_0$ can be expanded into what can be a fast converging series of velocity potential base functions ϕ_i (Froudman, 1916; Rao and Schwab, 1976):

$$\left\{ \begin{matrix} \zeta_0 \\ \Delta\zeta_0 \end{matrix} \right\}(\phi, \lambda, t) = \sum_{\tau} \sum_{i=0}^{\infty} \sum_{\beta=0}^1 \left\{ \begin{matrix} \zeta_{i\beta\tau} \\ \Delta\zeta_{i\beta\tau} \end{matrix} \right\} \phi_i(\phi, \lambda) \cos(\omega_{\tau} + \chi_{\tau} - \beta \frac{\pi}{2}), \quad (78)$$

where the $\zeta_{i\beta\tau}$ and $\Delta\zeta_{i\beta\tau}$ are real numbers.

The ϕ_i are specific to a given ocean basin, as they depend on the bathymetry and the coastal outline, and form a complete set of orthogonal functions over that basin, in the sense that

$$\iint_{(\text{basin})} \phi_i \phi_j d\sigma = D_i \delta_{ij}, \quad (79)$$

where the positive constants D_i are zero if $i \neq j$,

and

$$\iint_{(\text{basin})} \phi_i \zeta_0 d\sigma \neq 0 \quad (80)$$

for at least one value of i , unless ζ_0 is identically zero. Integration here is confined to the oceanic regions, and $d\sigma$ is the spherical element of area

$$d\sigma = R^2 \cos\phi d\phi d\lambda. \quad (81)$$

Notice that the ϕ_i are independent of ω_T ; in fact, they can be used to describe a wide variety of vertical motions of the sea surface within a given ocean, besides tides. These functions do not have analytical closed expressions except when the shape of the ocean is unrealistically simple. To compute $\phi_i(\phi, \lambda)$ one must solve numerically an eigenvalue-eigenfunction problem involving a differential operator related to the unforced linearized tidal equations, with the boundary condition that, along the coast,

$$z \frac{\partial \phi_i}{\partial n} = 0 \quad . \quad (82)$$

Here, "z" is the depth of the ocean, and " $\partial/\partial n$ " represents partial differentiation in the direction normal to the coast. The calculations can be done only with a digital computer, but, once the ϕ_i have been obtained, this disadvantage can be offset by the speed with which the expansion (78) of ζ_0 converges and by several benefits associated with orthogonality. Rao and Schwab (ib., 1976) and Sanchez et al. (1984) have studied the use of these interesting functions for parameterizing tides and other oscillatory motions of large bodies of open water without having to make assumptions on the amount of internal dissipation and bottom friction, usually poorly known. The ϕ_i can represent any long-wave vertical displacements of water, even when the energy dissipation is unknown, in much the same way as spherical harmonics can be used to represent any gravitational potential, even when there is no knowledge of the mass distribution that generates the field.

If the bottom of the ocean is replaced with a horizontal surface lying at a depth of "no motion", the ϕ_i calculated with this new boundary can be used to parameterize the stationary sea surface topography w_0 corresponding to the global circulation.

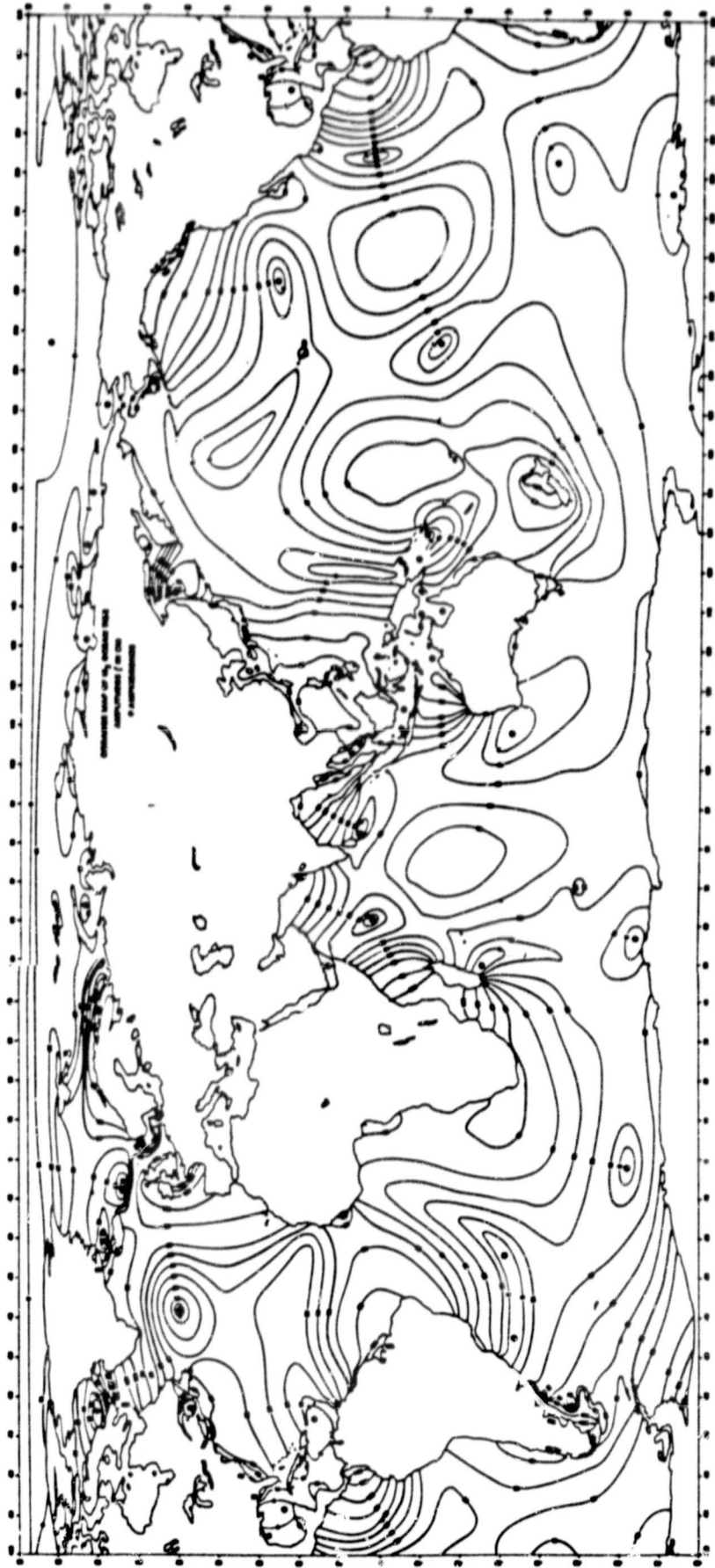


FIGURE 5. M2 equal amplitude (orange) lines. Absolute values shown at intervals of 10 cm; amplitudes are zero only at amphidromes (dark dots inside closed contours, for their locations see also Figure 6). Original chart taken from Schwiderski (1979).

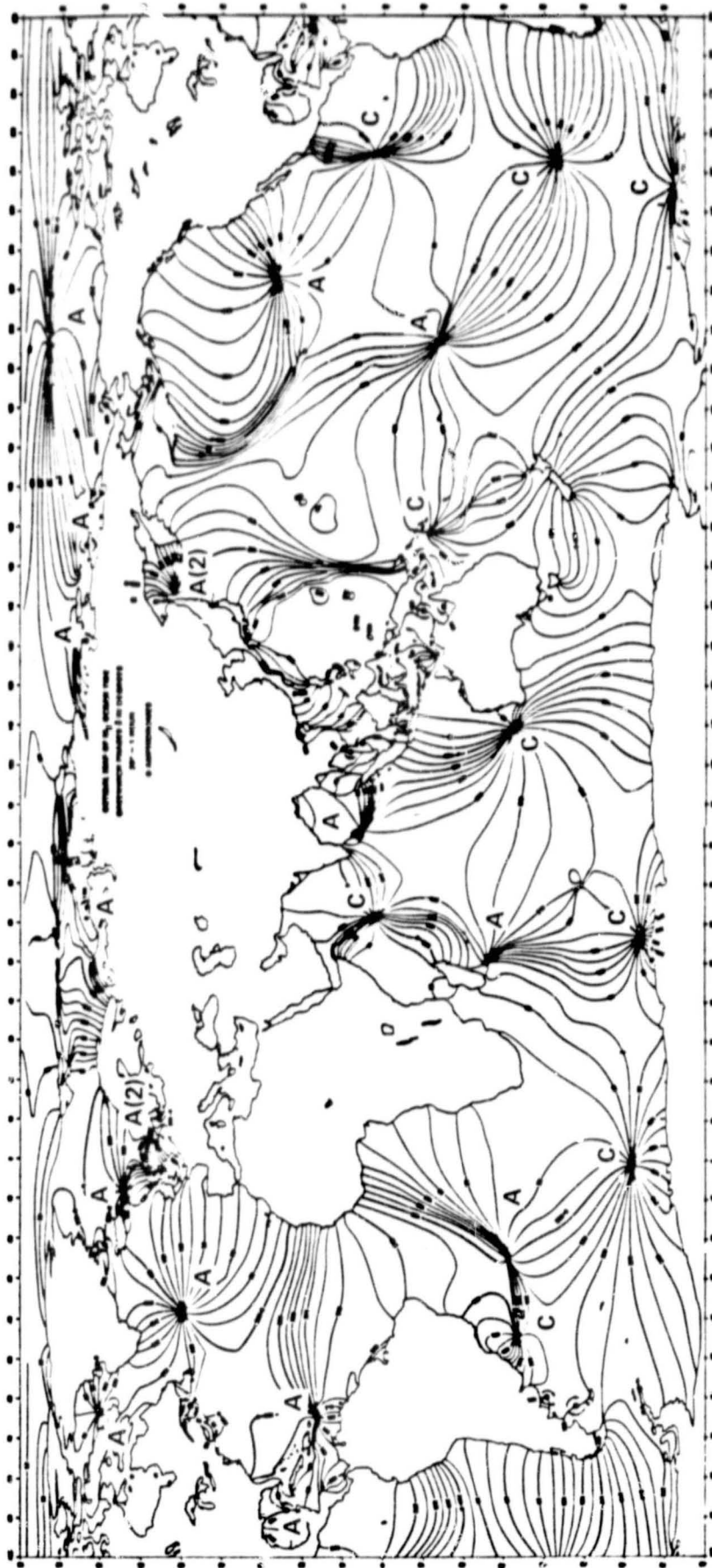


FIGURE 6. M2 equal phase (cotidal) lines at intervals of 15° (1/2 hour). The senses in which waves turn are indicated by the letters C (clockwise) and A (anticlockwise) placed near the amphidromic points; when two such points are very close this is indicated by A(2).

5.7 The Tidal Part of the Orbit Error

The attractions of the Sun and the Moon, together with the tidal changes they induce in the gravitational field of the Earth (expressions (74) and (76)), affect the orbit of a satellite and must be considered when computing its position and velocity. The direct influence of the celestial bodies can be calculated with such accuracy that the results can be regarded as exact. The solid Earth and ocean tides are less well known, so there may be significant errors in the calculated values of $V(\zeta_0)$ and $V^{(\delta)}$. The body tide δ has a limited frequency range, mostly below two cycles per revolution, because only the second harmonic V_T^* has an important effect (expression (76)). As the existing models of δ are quite accurate, only the long period effects of their small errors $\Delta\delta$ are likely to matter, adding to the polynomial terms and to the "quadratic" oscillations in Δr (expressions (47) and (52)). Therefore, shorter period errors related to tides are probably due mostly to $\Delta\zeta_0$, the uncertainty in the ocean tidal charts. The perturbations of spacecraft orbits have been used to learn about the broader features of tides, and to try to estimate directly Love numbers and other important geophysical parameters (Lambeck et al. (1974), Felsentreger et al. (1979), Marsh et al. ib. (1983)).

The error $\Delta\zeta_0$ can be represented by an expansion like (71) for ζ_0 , with the coefficients $\zeta_{nm\alpha\beta\tau}$ substituted by the errors $\Delta\zeta_{nm\alpha\beta\tau}$ in these coefficients. Replacing $Y_{nm\alpha}^{(\phi, \lambda)}$ with its equivalent in Keplerian

elements (expressions (29-30)) and using the relationships for the products of sines and cosines,

$$\Delta \zeta_0(t) \approx \frac{1}{2} \sum_{\tau} \sum_{n=0}^{\infty} \sum_{m=0}^n \sum_{\alpha=0}^1 \sum_{\beta=0}^1 \Delta \zeta_{nm\alpha\beta\tau} \sum_{p=-n}^n F_{nmp}(\bar{I}) \cos [((n-2p)(\dot{\omega} + \dot{M}) + m\dot{\theta} \pm \omega_{\tau})t + \phi_{nm\alpha p 0_0} \pm (\chi_{\tau} - \beta \frac{\pi}{2})] , \quad (83)$$

where $\phi_{nm\alpha p 0_0} = (n-2p)(\bar{\omega}(t_0^k) + \bar{M}(t_0^k)) + m\dot{\theta}(t_0^k)$; the osculating ω , M and $\dot{\theta}$ have been approximated by $\dot{\omega}t + \bar{\omega}(t_0^k)$, etc.; and χ_{τ} is as in (62d'). Because of the nearly linear relationships between tidal phenomena, rewriting expression (74) with the harmonics of $\Delta \zeta_0$ instead of those of ζ_0 gives the effect $\Delta V^{(\Delta \zeta_0)}$ of $\Delta \zeta_0$ along the orbit. So, replacing $(\frac{R}{r})^{n+1} Y_{nm\alpha}(\phi, \lambda)$ in (74) with its equivalent in Keplerian elements according to (31), gives (Lambeck et al., ib., 1974):

$$\Delta V(t)_0^{(\Delta \zeta_0)} = \frac{\mu}{2R^2} \sum_{nm\alpha\beta\tau} \alpha_n (1 + k'_{n\tau}) \left(\frac{R}{a}\right)^{n+1} \Delta \zeta_{nm\alpha\beta\tau} \sum_{p=-n}^n F_{nmp}(\bar{I}) \sum_{q=-\infty}^{\infty} G_{npq}(\bar{e}) \cos [((n-2p+q)(\dot{\omega} + \dot{M}) - q\dot{\omega} + m\dot{\theta} \pm \omega_{\tau})t + \phi_{nm\alpha p q 0} \pm (\chi_{\tau} - \beta \frac{\pi}{2})] . \quad (84)$$

Neglecting the contribution of the error in δ , the sum of the shorter period perturbations that form the "periodical" part $\Delta\tilde{r}^{(T)}$ of the tidal radial error is given by

$$\Delta\tilde{r}^{(T)}(t) = \frac{1}{2R} \sum_{nmpq\alpha\beta\tau} \alpha_n (1+k'_{n\tau}) \Delta\zeta_{nm\alpha\beta\tau} \{r_{nmp(q+\{\pm 1\})\tau} \cos[(n-2p+q)(\dot{\omega}+\dot{M}) - q\dot{\omega} + m\dot{\theta}' \pm \omega)t + \phi_{nm\alpha\beta(q+\{\pm 1\})\tau} \pm (\chi_{\tau}-\beta \frac{\pi}{2})]\} ,$$

(85)

where " $(q+\{\pm 1\})$ " stands for " q ", " $(q+1)$ " and " $(q-1)$ ", respectively, and "(T)" for "tidal". The frequencies present in $\Delta\tilde{r}^{(T)}$ differ from those in $\Delta r^{(NT)}$ (expressions (47) or (52)) by $\pm \omega_{\tau}$, so the actual values of the coefficients $r_{nmp(q+\{\pm 1\})\tau}$ are also different (see (16), (38) and (43)), thus the subscripts "nmpq τ ". Terms where the ω_{τ} are subtracted are prograde; the others are retrograde (the change in the argument has the same or opposite sense to that caused by the rotation of the Earth).

As in expression (47) for $\Delta r^{(NT)}$, the mean elements and their rates generally change, very slowly, as the orbit decays, though they may be considered as constants during each weekly arc; the $r_{nmp(q+\{\pm 1\})}$ change accordingly in (85).

5.8 The Case of the "Frozen", Repeat Orbit

When $\dot{\omega} = 0$ and exactly N_R revolutions take place in precisely N_D nodal days, the ground track repeats itself with a frequency $\omega_{rc} = 2\pi/T_{rc}$, where $T_{rc} = N_D \times$ (length of the nodal day). Then the frequencies in the arguments of the cosines in (85) are, with the possible exception of ω_τ , multiples of ω_{rc} , so $\Delta r^{(T)}$ becomes

$$\Delta r^{(T)}(t) = \frac{1}{2R} \sum_{nmpq\alpha\beta\tau(\text{nonres})} \alpha_n (1+k'_{n\tau}) \Delta \zeta_{nm\alpha\beta\tau} r_{nmp}(q+\{\pm 1\})_0 \tau$$

$$\cos[(((n-2p+(q+\{\pm 1\})_0)N_R - m N_D)\omega_{rc} \pm \omega_\tau)t + \phi_{nm\alpha\beta}(q+\{\pm 1\})_0 \pm \chi_\tau - \beta \frac{\pi}{2}].$$

(86)

When dealing with this type of orbit, the time origin t_0 for the $\phi_{nm\alpha\beta}(q+\{\pm 1\})_0$ and χ_τ is as in expression (52) and in (62'c), so $\bar{M}(t_0) = 0$ early in the repeat part of the mission.

The error $\Delta \zeta_G$ in the geocentric tide is present in the residual altimetric sea surface heights according to (7). Assuming that the error in the body tide is small enough compared to $\Delta \zeta_0$ to be neglected, expressions (29), (30) and (77) imply that

$$\Delta z_G(t) \approx \frac{1}{2} \sum_{nm\alpha\beta\tau} (1 + \alpha_n h_{n\tau}^{\prime}) \Delta z_{nm\alpha\beta\tau} \sum_{p=-n}^n F_{nmp} (\bar{I})$$

$$\cos [((n-2p)(\dot{\omega} + \dot{M}) + m\dot{\theta} \pm \omega_\tau)t + \phi_{nm\alpha\beta 0_0} \pm (\chi_\tau - \beta \frac{\pi}{2})].$$

(87)

In the case of the "frozen", repeat orbit this formula becomes

$$\Delta z_G(t) \approx \frac{1}{2} \sum_{nm\alpha\beta\tau} (1 + \alpha_n h_{n\tau}^{\prime}) \Delta z_{nm\alpha\beta\tau} \sum_{p=-n}^n F_{nmp} (\bar{I})$$

$$\cos [(((n-2p)N_R - mN_D) \omega_{rc} \pm \omega_\tau) t + \phi_{nm\alpha\beta 0_0} \pm (\chi_\tau - \beta \frac{\pi}{2})].$$

(88)

Comparing (86) and (88) one sees that the periodical terms in both $\Delta \tilde{r}^{(T)}$ and Δz_G have the same frequencies when these errors are treated as time series. Consequently, $\Delta \tilde{r}^{(T)}$ and Δz_G are "lumped together" in the residual sea heights and can be separated only by using the Love numbers $k_{n\tau}^{\prime}$, so these must be known reasonably well. The same comment can be made regarding the $h_{n\tau}^{\prime}$ needed, in turn, to obtain Δz_0 from Δz_G .

5.9 The Lasing of Ocean Tides With the Mean Sea Surface and With Each Other

When observed with an altimeter from a "frozen", repeat orbit, a tidal constituent of frequency ω_τ would appear, at the same points along the repeating ground track, to rise and fall between consecutive overflights at the slower frequency

$$\omega_{\tau(\text{strobed})} = \omega_\tau - \omega_{rc} \text{Int} [\omega_\tau / \omega_{rc} + 1/2]. \quad (89)$$

(Int [x] = integer part of x). This phenomenon is analogous to the apparent slowing down of a rotating wheel, or the plate of a record player, when illuminated at regular intervals by short flashes of light. The "strobed" frequency $\omega_{\tau(\text{strobed})}$ would be zero if ω_τ were an exact multiple of the repeat frequency ω_{rc} . The corresponding tidal constituent would appear "frozen" in time and inseparable from static features of the sea surface such as the geoid undulations or the stationary sea surface topography. This may happen with some tides depending on the inclination, eccentricity and height of the orbit ($\omega_{rc} = (\dot{\theta} - \dot{\Omega}) / N_D$, and $\dot{\Omega}$ depends on \bar{a} , \bar{e} and \bar{I} according to (10)). Moreover, two different tides of frequencies ω_{τ_1} and ω_{τ_2} may appear "lumped" together if their "strobed" frequencies are the same. For small \bar{e} and altitudes of about 1000 km this is possible when the inclination is somewhere between 70° and 110° , which is one reason why the

projected orbit of TOPEX has been chosen with an $\bar{I} \sim 64^\circ$. In the case of SEASAT, where $\bar{I} \sim 108^\circ$, some tides (like O1 and N2) were aliased with each other and some (like P1) with the mean sea surface, as mentioned by Mazzega (1984). Details of this problem are discussed at some length in two reports: one by NASA's TOPEX Science Working Group (1981, Appendix B.2), and the other by a similar group organized by CNES in France to discuss POSEIDON (ib., 1983).

5.10 The Complete Expression of the Radial Orbit Error

The total error Δr is the sum of the tidal and non-tidal components $\Delta r^{(T)}$ and $\Delta r^{(NT)}$ (expressions (47) and (85)):

$$\begin{aligned}
 \Delta r(t) &= \Delta r^{(T)}(t) + \Delta r^{(NT)}(t) \\
 &= \sum_{nm\alpha p q(\text{nonres})} \Delta C_{nm\alpha} r_{nmp}(q + \{\pm 1\}^{\circ}) \\
 &\quad \cos [((n-2p + (q + \{\pm 1\}^{\circ}))(\dot{\omega} + \dot{M}) - (q + \{\pm 1\}^{\circ}) \dot{\omega} + m\dot{\theta})t + \phi_{nm\alpha p}(q + \{\pm 1\}^{\circ})_0] \\
 &\quad + \frac{1}{2R} \sum_{nm\alpha\beta q\tau(\text{nonres})} \alpha_n^{(1+k'_{n\tau})} \Delta \zeta_{nm\alpha\beta\tau} r_{nmp}(q + \{\pm 1\}^{\circ})_{\tau} \\
 &\quad \cos [((n-2p + (q + \{\pm 1\}^{\circ}))(\dot{\omega} + \dot{M}) - (q + \{\pm 1\}^{\circ}) \dot{\omega} + m\dot{\theta} + \dot{\tau})t \pm \omega_{\tau}t \\
 &\quad + \phi_{nm\alpha p}(q + \{\pm 1\}^{\circ})_0 \pm (\chi_{\tau} - \beta \frac{\pi}{2})] + A_k \cos \dot{M}t \\
 &\quad + B_k \sin \dot{M}t + C_k t \cos \dot{M}t + D_k t \sin \dot{M}t \\
 &\quad + E_k t^2 \cos \dot{M}t + F_k t^2 \sin \dot{M}t + \sum_{j=0}^J r_{jk} (t - t_0^k)^j,
 \end{aligned} \tag{90}$$

where the terms that modulate the $\sin \dot{M}t$ and the $\cos \dot{M}t$, and those in the polynomial at the end, are the aggregate of all the very long period and resonant contributions from errors in the models of both gravitational and non-gravitational forces, as well as uncertainties in the initial state. Expression (90) describes all significant elements of Δr over a weekly arc.

The non-tidal part of the error in (90) has the same structure as a sum of additional tidal components of frequencies $0, \dot{\omega}, 2\dot{\omega}, \dots$, (corresponding to $q=0, 1, 2, \dots$, with their amplitudes becoming negligible above $2\dot{\omega}$), one of which is "static" ($q=0$).

The corresponding expression for the especial case of the "frozen", repeat orbit is, from (52) and (86),

$$\begin{aligned}
 \Delta r(t) = & \sum_{nm\alpha p q(\text{nonres})} \Delta C_{nm\alpha} r_{nmp}(q+\{\pm 1\}^0) \\
 & \cos[\(((n-2p+(q+\{\pm 1\}^0))N_R+mN_D)\omega_{rc}t+\phi_{nm\alpha p}(q+\{\pm 1\}^0))] \\
 & + \frac{1}{2R} \sum_{nm\alpha\beta q\tau(\text{nonres})} \alpha_n(1+k'_{n\tau}) \Delta \zeta_{nm\alpha\beta\tau} r_{nmp}(q+\{\pm 1\}^0)\tau \\
 & \cos[\(((n-2p+(q+\{\pm 1\}^0))N_R+mN_D)\omega_{rc} \pm \omega_\tau)t \\
 & + \phi_{nm\alpha p}(q+\{\pm 1\}^0)_0 \pm (\chi_\tau - \beta \frac{\pi}{2})] \\
 & + A_k \cos \dot{M}t + B_k \sin \dot{M}t + C_k t \cos \dot{M}t \\
 & + D_k t \sin \dot{M}t + E_k t^2 \cos \dot{M}t + F_k t^2 \sin \dot{M}t \\
 & + \sum_{j=0}^J f_k (t-t_o^k)^j.
 \end{aligned} \tag{91}$$

Here, because the orbit is stabilized by occasional maneuvers, the $r_{nmp}(q+\{\pm 1\}^0)$ and $\dot{\omega}, \dot{M}, \dot{\theta}$ can be regarded as constants over the whole mission.

6.0 IMPLICATIONS FOR THE ANALYSIS OF ALTIMETRY

6.1 General

Expression (7) shows that the residual sea height Δh_w contains, besides the orbit error (Δr), information on the unknown parts of the geoid (ΔN) and the tides ($\Delta \zeta_G$), the non-tidal variations (w_t) and the mean sea surface topography (w_o) of the general circulation.

The fine details of the geoid can be determined very clearly by mapping the mean sea surface with altimetry, because the orbit error Δr and the topography w_o introduce distortions at much longer wavelengths. Those details often outline quite well the submerged trenches, ridges and mountains that produce them because of incomplete isostatic compensation. This was recognized soon after the first use of an altimeter in SKYLAB (Leitao and McGoogan, 1975; McGoogan et al., 1975). Today, high resolution maps of the sea surface, like those produced by Marsh and Martin (1982), reveal aspects of the ocean crust of great interest to geologists and geophysicists (Watts, 1979).

In addition to being useful over the sea for studying the gravitational field and oceanographic phenomena, altimetry is valuable to some extent over land (Brooks, 1981) and particularly over ice (Brooks et al., 1978). The main problem on land is the roughness of the surface observed; a normal sampling rate of one measurement per second (about

every eight kilometers along track) would be insufficient for mapping mountain areas, for example. Other applications, such as the study of wave height, surface winds, etc. (Mognard et al., 1984), based on the shape and intensity of the returning radar pulses, rather than on their timing, are not affected by the orbit error.

6.2 Crossover Points and Overlapping Arcs

The difference between two heights measured on the same spot at times t_1 and t_2 is, according to (7),

$$\begin{aligned} \delta h_w(t_1, t_2) &= \Delta h_w(t_1) - \Delta h_w(t_2) \\ &= \Delta r(t_1) - \Delta r(t_2) + \Delta \tau_G(t_2) - \Delta \tau_G(t_1) + w_t(t_1) - w_t(t_2) \\ &\quad + \Delta \Lambda(t_2) - \Delta \Lambda(t_1). \end{aligned} \tag{92}$$

The permanent part $\Delta N + w_0$ is totally absent, and only Δr , the tides and other time-varying features are observable to some extent. Of course, measurements very rarely happen to be taken so close to each other that the cancellation of $\Delta N + w_0$ is complete. Normally it is necessary to interpolate $\Delta h_w(t_1)$ and $\Delta h_w(t_2)$ from measurements just preceding and just following passage over the point in question. There are two types of point: a crossover point is the intersection of an ascending and

a descending arc of the ground track (each named after the nearest equatorial crossing), while an overlap point lies where two or more parallel arcs (or colinear arcs) run on top of each other; the height difference in (92) shall be called a crossover difference, or an overlap difference, accordingly. In a "frozen", repeat orbit, all points are overlap points, but only some are also crossover points.

Over arcs of a few thousand kilometers Δr can be represented closely by a constant and a linear terms, or "bias+tilt". For many years now the "bias+tilt" model has been used for estimating Δr from crossover differences, by least squares adjustment, in order to correct the data (Rummel and Rapp, 1977, Mather et al., 1977). Extensions of this idea, involving either polynomials or Fourier series, are explained in Goad et al. (1980). Similar procedures for correcting overlap differences were also developed in the early days (Mather et al., 1978). A system of observation equations for estimating biases and tilts out of differences of either type is rank-deficient, and to solve it is necessary to "fix" first some carefully selected "master arcs", or to minimize the discrepancies along each arc between h_{w_c} and N_c using some model of the geoid (see Rowlands, 1981).

As explained earlier, in a "frozen", repeat orbit the radial error contains a significant component that is a function of latitude alone, and unobservable in crossover differences. Therefore, application of the "bias+tilt" method may leave zonal "wrinkles" in the estimated mean sea

surface. Fortunately, most of the data available today were obtained with GEOS-3 and SEASAT in non-repeat, or "general" orbits. This situation is likely to be reversed by future missions, where most satellites will be in repeating orbits. However, after the fuel of the stabilizing engines is exhausted, the satellites will gradually drift towards more "general" orbits under various disturbing influences (or may be maneuvered towards them while there is still some fuel left) yielding more suitable "master arcs" to rectify the mean sea surface, as long as their altimeters continue to operate for a substantial part of one apsidal period ($2\pi/\dot{\omega}$). In such orbits, most of the radial error of gravitational origin is observable in the crossover differences over that interval.

According to (47) and (52), $\Delta r(t_1) - \Delta r(t_2)$ in (92) is a function of the $\Delta C_{nm\alpha}$, so these may be estimated from crossover differences (Shum, 1982). The shorter period effects of the zonal errors are unobservable when the ground track repeats, and one would expect that also those produced by low order $\Delta C_{nm\alpha}$ might be hard to observe (Wagner, ib., 1984). The situation is somewhat better in non-repeating orbits, where all $\Delta C_{nm\alpha}$ are estimable, in principle. In any case, the use of crossover differences can be an interesting way of employing altimetry to improve or calibrate existing gravity field models, in combination with ordinary satellite tracking data, terrestrial gravity measurements, etc.

6.3 Direct Mapping of Ocean Tides

Because of the convenient structure of the orbit error, "frozen", repeat orbits provide the best data for studying tides, particularly in the form of overlap differences. According to expressions (85), (86), (87) and (88), the tide-related signal is the sum of $\Delta\zeta_G$ and $\Delta r^{(T)}$, both of which, in the case of a repeating ground track, have exactly the same temporal frequencies. The overlap differences can be modelled using the observation equation

$$\begin{aligned} \delta h_w(t_1, t_2) = & \sum_{\gamma=1}^2 \sum_{i \in \tau(\text{central})} \Delta \zeta_{i\beta T} B_i(\phi, \lambda) \left\{ -A_{\tau(\text{band})}(t_\gamma) \cos(\omega_{\tau(\text{central})} t_\gamma - \beta \frac{\pi}{2}) \right. \\ & - B_{\tau(\text{band})}(t_\gamma) \sin(\omega_{\tau(\text{central})} t_\gamma - \beta \frac{\pi}{2}) + A_{k_\gamma} \cos \dot{M} t_\gamma + B_{k_\gamma} \sin \dot{M} t_\gamma \\ & + C_{k_\gamma} t_\gamma \cos \dot{M} t_\gamma + D_{k_\gamma} t_\gamma \sin \dot{M} t_\gamma + E_{k_\gamma} t_\gamma^2 \cos \dot{M} t_\gamma \\ & \left. + F_{k_\gamma} t_\gamma^2 \sin \dot{M} t_\gamma + \sum_{j=0}^J r_{i_\gamma} (t_\gamma - t_{k_\gamma}^o)^j \right\} (-1)^{(\gamma-1)}, \end{aligned} \quad (93)$$

where $\gamma=1$ corresponds to t_1 and $\gamma=2$ to t_2 . The terms of the sum " \sum " represent the "lumped tide" $\Delta\zeta_G + \Delta r^{(T)}$, with $A_{\tau(\text{band})}$ and $B_{\tau(\text{band})}$ given by (70). In what follows, regardless of t_2 , the instant t_1 always belongs to the first repeat of the ground track, thus $A_{k_1} = A_1$, $B_{k_1} = B_1$, etc. So all the overlap differences are with respect to the first arc, which should not be shorter than one repeat period T_{rc} . The base functions B_i for

parameterizing the "lumped tide" in space can be anything convenient, including spherical harmonics if the estimate is world-wide. The velocity potential functions ϕ_i (see expression (78) et seq.) are orthogonal and complete over the ocean basins, so they can represent the "lumped tide".

Solving a redundant system of observation equations based on (93) by the least squares method, one can separate the non-periodical part of Δr from the "lumped tide". Then, this "lumped tide" may be corrected iteratively (for example) to obtain $\Delta \zeta_0$. To start with, one can guess that $\Delta r^{(T)} + \Delta \zeta_0$ is identical to $\Delta \zeta_0$, making in this way a first estimate of the yielding of the solid Earth δ' and the perturbation of the potential $V^{(\Delta \zeta_0)}$. This requires a numerical spherical harmonic analysis⁽¹⁾ of that guess of $\Delta \zeta_0$ and then use of the resulting $\Delta \zeta_{nm\alpha\beta\tau}$ according to (73) and (86) to get the corresponding values of δ' and $\Delta r^{(T)}$. Correcting the "lumped tide" by subtracting these values will result in a new estimate of $\Delta \zeta_0$, which can be corrected likewise in turn, etc. Because $\Delta r^{(T)}$ and δ' are probably small compared to $\Delta \zeta_0$, the

(1) It is possible to do this numerical analysis, to very high degree and order, using fast algorithms like those described (including program listings) in (Colombo, 1981). Recently Tscherning et al. (1983) have compared the efficiency of these and other algorithms, all of which approximate integration over the sphere with numerical quadratures on grided data. For sufficiently fine grids, computing the coefficients in this way, reconstituting the data from the computed coefficients, finding the differences between the reconstituted and the original data, and iterating this procedure, can be shown to be equivalent, in the limit, to a full least squares adjustment of the coefficients. The first iteration corresponds to the well-known practice of "pre-whitening" in ordinary Fourier analysis, and may increase the number of significant figures recovered considerably. To avoid numerical problems, the coefficients calculated in these large analyses are always fully normalized.

iterations are likely to converge. As $\alpha_n h'_n < 0.1$, δ' is one order of magnitude less than ζ_0 , and so is the radial effect of $\Delta V^{(\Delta\zeta_0)}$ on the adjusted orbit, or ephemeris (5 cm at most for STARLETTE (1000 m altitude) according to Marsh et al. ib. (1983)). The terms in $\Delta r^{(T)}$ can be separated in two groups: those with periods of the order of months, which are filtered out together with the non-tidal orbit error, and those with periods of less than T_{rc} , that remain in the "lumped tide". Of the latter, only terms whose frequencies are less than one cycle per day may have to be corrected for, as their amplitudes decrease quickly with the period. The process described here assumes that the Love numbers are adequately known, the same as the solid Earth tide δ . Moreover, the contribution to δ' and $\Delta r^{(T)}$ of the tides in the polar regions not spanned by the ground track would have to be estimated relying on pre-existing tidal charts. The use of the ϕ_i for parameterizing the successive approximations to $\Delta\zeta_0$, starting with $\Delta\zeta_G$, may be advantageous because of their "tide-like" nature, and their orthogonality over the oceans.

Once Δr and δ' have been separated from ζ_G in a global way, a method like that of Cartwright and Alcock (1981) can be used for the regional refinement of the tidal map. Estes (ib., 1980) has simulated a global estimation of tides from altimetry (with a somewhat simplistic error model) and his work suggests that a faithful picture may be obtained from a few months' worth of data. A satellite with a coverage as dense as the

one projected for POSEIDON (Figure 2) should help greatly to obtain very detailed charts.

If the geocentric tide ζ_G can be mapped reliably with altimetry, it may be possible to use the measurements of ζ_0 taken with deep-sea pressure gauges (Zetler, 1980), to estimate $\delta' + \delta$ directly at the locations of those gauges. This may be helpful in studying ocean loading effects, the body tide, and the rheology of the Earth's interior.

A quite conservative sufficient condition for separating the non-tidal orbital error $\Delta r^{(NT)}$ from the tidal signal $\Delta \zeta_G + \Delta r^{(T)}$ is that their respective spectra should have no frequency in common. In a "frozen", repeat orbit the portion of $\Delta r^{(NT)}$ present in the overlap differences consists of the "quadratic once per revolution" oscillation and the polynomial terms in (52). Its spectrum is confined to two bands: the first extends, approximately, from 0 to $2\dot{\omega}$ and the second from $\dot{M}-2\dot{\omega}$ to $\dot{M}+2\dot{\omega}$ ($\dot{\omega} \sim$ one cycle every 30 years for SEASAT). The tidal signal, as seen from the satellite according to (86), (88) and (89) has all its components at frequencies that differ from the harmonics of ω_{rc} by $\pm \omega_{\tau(\text{strobed})}$. As 0 and \dot{M} are harmonics of ω_{rc} , the sufficient condition requires that

$$2|\dot{\omega}| < |\omega_{\tau(\text{strobed})}|, \quad (94)$$

so all the spectral lines of $\Delta r^{(T)}$ fall outside the two main bands of $\Delta r^{(NT)}$. However, this guarantees good separability only if the duration T_{dr} of the data stream analyzed satisfies

$$T_{dr} > |2\pi / (|\omega_{T(strobed)}| - 2|\dot{\omega}|)|. \quad (95)$$

For all past altimeter missions, and for any contemplated future ones, $T_{dr} < 4$ years, so the tidal components that can be resolved from the measurements of a single satellite must have "strobed" periods not much longer than 4 years, assuming that the data were free from errors. As the period of $2\dot{\omega}$ must be of the order of one decade, all those "resolvable" components should satisfy (95) and be, therefore, separable from the resonant terms in (93).

In the case of ordinary non-repeating orbits where the perigee precesses once or more per year, expression (90) shows that the orbit error must resemble a periodical up and down motion with its main components at frequencies 0, $\dot{\omega}$ and $2\dot{\omega}$, and with spatial wavelengths as small as 1000 km. These components can be seen as additional "tides", which would have to be included in the model, greatly increasing the number of parameters to be adjusted; otherwise, they may bias the estimates of the real tides.

All attempts at mapping ζ_0 with GEOS-3 data, originally thought to be a reasonably straightforward operation (Zetler and Maul, 1971), have turned out rather disappointing results. The poor distribution in time

and in space of these measurements (collected over disjoint intervals of no more than 20 minutes, because of the lack of an onboard data storage device), the somewhat low accuracy of the instrument and the non-repeating nature of the orbit, all have conspired to frustrate those efforts (Maul and Yanaway (1978), Bretreger (1979), Won and Miller (1979), Masters et al. (1979) and Coleman (ib., 1981)). The first estimates of the M2 tide showing clear agreement with the amplitudes and phases observed at maritime stations or plotted in existing tidal maps have been those of Cartwright and Alcock (ib., 1981) for the northeastern Atlantic, of Mazzega (1983) for the Indian Ocean, and of Mazzega (1984, ib) for the whole world, all based on measurements from the last month of SEASAT. Although these workers have taken no advantage of the structure of the orbit error (treated by them like white noise), their results are better probably because of the special nature of Δr along the repeating ground track, while the accuracy and the spatial coverage of the data must have helped also, even when the total observing period was short.

7.0 CONCLUSIONS

The nature of the orbit determines that of the radial orbit error. There is a geographical component in this error, due to the gravitational field model, that is largest in the case of "frozen", repeat orbits. Because of the precise repetition of the ground track every few days, this is the kind of orbit likely to be used in most future missions, and has been used already for SEASAT.

In the differences in altimetric heights along the colinear passes of a repeating ground track, the radial error left consists of a slowly increasing oscillation plus a low degree polynomial (if the arc is about a week long). This error, produced mostly by resonances of zonal origin, is easy to model and to separate from oceanic variations because it has a much longer wavelength. Its main contribution to the power spectrum of the total error should be confined to very low frequencies and to a narrow peak at about one cycle per revolution; this seems to agree well with experience (Marsh and Williamson, *ib.*, 1980). It is important to have accurate and dense tracking and also good models of the non-gravitational forces. The use of incorrect models of these forces may increase significantly the resonant part of the radial error. It is easy to deal with the long period effects of the errors in non-gravitational models, because they belong mostly to the "resonant" part of Δr . The shorter period effects of these errors, on the other hand, cannot be treated adequately with the type of analytical theory used here. Therefore, the

present conclusions (insofar as they are based on that theory) are reliable only if the models are good enough to make such effects quite small.

To separate the main tidal components from each other and from the mean sea surface, heliosynchronous and high inclination orbits should be avoided. However, for studying other time-varying features, using repeat heliosynchronous orbits could make the effects of non-gravitational force model errors more tractable, particularly those caused by the complex and often changing shapes of the spacecraft. If the attitudes of the various parts of the satellite (particularly the solar panels on which most of those forces act) are stabilized with respect to the Sun by making their orientations in inertial space functions only of the spacecraft's position relative to the plane of the ecliptic, then the pressures of solar radiation and of Earth's re-radiation, and the errors in their models, will be functions of that position as well (except for small variations in the Earth's albedo, the slow annual changes in solar declination and in apparent luminosity of the Sun with distance as the Earth moves in its elliptical orbit, etc.) Under the assumptions, over long periods of time, the errors in the computed values of these forces will repeat themselves almost exactly once per revolution. Their contributions to the radial error will consist of a resonant part (an extreme example of which seems to be present in one of the graphs in Figure 4), and of a part that repeats along the ground track and thus largely disappears from overlap differences. As the atmospheric helium bulge follows the Sun, similar

considerations would apply to drag model errors. Departures from this well-behaved pattern due to changes in solar radiation intensity and magnetic flux could be reduced by such a simple procedure as the daily adjustment of the drag and reflectivity coefficients (reality, of course, can be wonderfully messy, so these ideas are to be taken with a grain of salt).

In a "frozen", repeat orbit, part of the radial error is "lumped together", in the altimeter measurements, with the error in the geocentric tide, but they can be separated using Love numbers.

"Frozen", repeat orbits are best for studying temporal variations (like tides) by analyzing colinear pass differences, because the radial error left in them is easy to filter out; however, since a significant part of Δr is also unobservable in crossover differences, these orbits are worst for modelling the mean sea surface by the "bias + tilt" method.

In the crossover differences of ordinary, non-repeating orbits, where the mean perigee is not "frozen", the radial error can be observed and corrected better than in the repeating case, by the "bias + tilt" method, provided the times of the ascending and descending passes at the crossovers are distributed over a substantial part of one apsidal cycle. In this sense, non-repeat orbits are best for mapping the mean sea surface. The same applies to the use of crossover differences for calibrating or correcting existing gravity field models.

Improving the force models, the gravitational one in particular, is essential to the determination of the stationary sea surface topography w_0 , which requires both precise knowledge of the orbit and of the geoid.

The difference between the geocentric tide (observed with satellite-borne altimeters) and the "surface-bottom" tide (sensed with deep-sea pressure gauges) is the sum of the body tide δ and the crustal bending δ' . Once long series of accurate measurements from altimeters and pressure gauges are available, it may become possible to map these vertical movements directly, across the oceans.

REFERENCES

- Anderle, R.J., and Hoskin, R.L., 1977, Correlated errors in satellite altimeter orbits. *Geophysical Research Letters*, Vol. 4, pp. 421-423.
- Bauer, T.A., 1978, SEASAT Mission summary. Jet propulsion Laboratory, Inter-office Memorandum 312/78.8-123.
- Bender, P.L., and Larden, D.R., 1982, TOPEX orbit determination using GPS signals plus a sidetone ranging system. Presented at the Third International Geodetic Symposium on Satellite Doppler Positioning, Las Cruces, Vol. II, pp. 1253-1258.
- Bretreger, K., 1979, Ocean tide models from GEOS-3 altimetry in the Sargasso sea. *Australian Journal of Geodesy, Photogrammetry and Surveying*, Vol. 30, pp. 1-14.
- Brooks, R.L., 1981, Terrain profiling from SEASAT altimetry. NASA Report CR-156878.
- Brooks, R.L., Campbell, W., Ramseier, R.O., Stanley, H.R., and Zwally, H.J., 1978, Ice sheet topography by satellite altimetry. *Nature*, Vol. 274, pp. 539-543.

Brower, D., and Clemence, G.M., 1961, Methods of celestial mechanics. Academic Press.

Brown, E.W., 1905, Monthly Notices of the Royal Astron. Soc., Vol. 65, p. 285.

Cartwright, D.E., 1977, Oceanic tides. Reports on Progress in Physics, Vol. 40, pp. 665-708.

Cartwright, D.E., and Tayler, R.J., 1971, New computations of the tide-generating potential. Geophysical Journal of the Royal Astronomical Society, Vol. 23, pp. 45-74.

Cartwright, D.E., and Alcock, G.W., 1981, On the precision of sea surface elevations and slopes from SEASAT altimetry of the northeast Atlantic Ocean. Oceanography from Space, Plenum Press, J.F.R. Gower, editor, pp. 885-895.

Cheney, R.E., Marsh, J.G., and Beckley, B.D., 1983, Global mesoscale variability from collinear tracks of SEASAT altimeter data. Journal of Geophysical Research, Vol. 88, C7, pp. 4343-4354.

Coleman, R., 1981, A geodetic basis for recovering ocean dynamic information from satellite altimetry. UNISURV S-19, Reports from the School of Surveying, the University of New South Wales (doctoral dissertation).

Colombo, O.L., 1981, Numerical methods for harmonic analysis on the sphere. Dept. of Geodetic Science and Surveying, The Ohio State University, Report 310.

Colombo, O.L., 1984, The global mapping of gravity with two satellites. Netherlands Geodetic Commission, Publications on Geodesy (New Series), Vol. 7, No. 3.

Colquitt, E.S., Malyevac, C.W., and Anderle, R.J., 1980, Doppler computed SEASAT orbits. The Journal of the Astronautical Sciences, Vol. 28, pp. 391-404.

Cook, G.E., 1966, Perturbations of near-circular orbits by the Earth's gravitational potential. Planetary and Space Sciences, Vol. 14, pp. 433-444.

Cutting, E., Born, G.H., and Frautnick, J.C., 1978, Orbit analysis for SEASAT. The Journal of the Astronautical Sciences, Vol. 26, pp. 315-348.

Doodson, A.T., 1921, The harmonic development of the tidal potential. Proceedings of the Royal Society of London, Sec. A., Vol. 100, pp. 305-329.

Douglas, B.C., Agreen, R.W., and Sandwell, D.T., 1984. Observing global ocean circulation with SEASAT. *Marine Geodesy*, Vol. 8, pp. 67-83.

Dow, J.M., and Klinkrad, H., 1982, Orbit determination and control for the ERS-1 altimetry mission. Presented at the 3rd International Symposium on the Use of Artificial Satellites for Geodesy and Geodynamics, Ermioni, 1982.

Eckels, A., O'Keffe, J.A., Squires, R.K., 1959, VANGUARD measurements give pear-shaped component of Earth's figure. *Science*, Vol. 129.

Estes, R.H., 1980, A simulation of global ocean tide recovery using altimeter data with systematic orbit error. *Marine Geodesy*, Vol. 3, pp. 75-139.

Farrel, W.E., 1972, Deformation of the Earth by surface loads. *Reviews of Geophysics and Space Physics*, Vol. 10, p. 761.

Felsentreger, T.L., Marsh, J.G., and Williamson, R.G., 1979, M2 ocean tide parameters and the deceleration of the Moon's mean longitude from satellite orbit data. *Journal of Geophysical Research*, Vol. 83, pp. 1837-1842.

Gaposchkin, E.M., 1978, Recent advances in analytical satellite theory. "Applications of Geodesy to Geodynamics", Proceedings of the 9th International GEOP Research Conference, Dept. of Geodetic Science and Surveying, The Ohio State University, Report No. 280, pp. 197-206.

Giacaglia, G.E.O., 1977, The equations of motion of an artificial satellite in nonsingular variables. Celestial Mechanics, Vol. 15, pp. 191-215.

Goad, C.C., 1980, The computation of tidal loading effects with integrated Green's functions. Proceedings of the Second International Symposium on Problems Related to the Redefinition of North American Vertical Geodetic Networks, Ottawa, pp. 587-602.

Goad, C.C., Douglas, B.C., and Agreen, R.W., 1980, On the use of satellite altimeter data for radial ephemeris improvement. The Journal of the Astronautical Sciences, Vol. 28, pp. 419-428.

Hancock, D.W., Forsythe, R.G., and Lorell, J., 1980, SEASAT altimeter sensor file algorithms. IEEE Journal of Oceanic Engineering, Vol. 5, pp. 93-99.

Heiskanen, W.A., and Moritz, H., 1967, Physical Geodesy. Freeman, San Francisco.

Hendershott, M.C., and Munk, W., 1970, Tides. Ann. Rev. Fluid Mechanics, Vol. 2, pp. 205-224.

Hendershott, M.C., 1972, The effects of solid Earth deformation on global ocean tides. Geophysical Journal of the Royal Astronomical Society, Vol. 29, pp. 389-402.

Hobson, E.W., 1931, The theory of spherical and ellipsoidal harmonics. Cambridge University Press, reprinted by Chelsea Publishing Co., 1965.

Hotine, M., 1969, Mathematical geodesy. ESSA Monograph 2, U.S. Dep. of Commerce.

Hough, M.E., 1981, Orbits near critical inclination, including lunisolar perturbations. Celestial Mechanics, Vol. 25, pp. 111-136.

Jacchia, L.G., 1965, Static diffusion models of the upper atmosphere with empirical temperature profiles. Smithsonian Institution Astrophysical Observatory (SAO) Special Report 170.

Jacchia, L.G., 1971, Revised static models of the thermosphere and exosphere with empirical temperature profiles. SAO Special Report 332.

Kaplan, M.H., 1976, Modern spacecraft dynamics and control. John Wiley and Sons.

Kaula, W.M., 1961, Analysis of gravitational and geometric aspects of geodetic utilization of satellites. *Geophysical Journal*, Vol. 5, pp. 104-133.

Kaula, W.M., 1964, Tidal dissipation by solid friction and the resulting orbital evolution. *Reviews of Geophysics*, Vol. 2, pp. 661-685.

Kaula, W.M., 1966, *Theory of satellite geodesy*. Blaisdell Publishing Co.

Kaula, W.M., 1967, Theory of statistical analysis of data distributed over a sphere. *Reviews of Geophysics*, Vol. 5, pp. 83-107.

Kaula, W.M., 1967b, Geophysical implications of satellite determinations of the Earth's gravitational field. *Space Science Reviews*, Vol. 7, pp. 769-794.

King-Hele, D.G., 1964, *Theory of satellite orbits in an atmosphere*. Butterworths and Company, London.

Kolenkiewicz, R., and Martin, C., 1982, SEASAT altimeter height calibration, *Journal of Geophysical Research*, Vol. 87, pp. 3189-3198.

Lamb, H., 1932, *Hydrodynamics*. Cambridge University Press (reprinted by Dover).

Lambeck, K., Cazenave, A., Balmino, G., 1974, Solid Earth and ocean tides estimated from satellite orbit analyses. *Reviews of Geophysics and Space Physics*, Vol. 12, pp. 421-434.

Lambeck, K., and Coleman, R., 1983, The Earth's shape and gravity field: a report of progress from 1958 to 1982. *Geophysical Journal of the Royal Astronomical Society*, Vol. 74, pp. 25-54.

Leitao, C.D., and McGoogan, J.T., 1975, SKYLAB radar altimeter: Short wavelength perturbations detected in ocean surface profiles. *Science*, Vol., 186, pp. 1208-1209.

Lerch, F.J., Klosko, S.M., Laubscher, R.E., Wagner, W.A., 1977, Gravity model improvement using GEOS-3 (GEM 9 & 10). NASA Goddard Space Flight Center, Document X-921-77-246.

Lerch, F.J., Wagner, C.A., Klosko, S.M., and Putney, B.H., 1981, Goddard Earth models for oceanographic applications (GEM 10B and 10C). *Marine Geodesy*, Vol. 5, pp. 2-43.

Lerch, F.J., Marsh, J.G., Klosko, S.M., and Williamson, R.G., 1982, Gravity model improvement for SEASAT. *Journal of Geophysical Research*, Vol. 87, pp. 3281-3296.

Lerch, F.J., Klosko, S.M., Wagner, C.A., and Patel, G.B., 1984, On the accuracy of recent Goddard gravity models. Submitted to the Geophysical Journal of the Royal Astronomical Society.

Leick, A., 1978, The observability of the celestial pole and its nutations. Dept. of Geodetic Science and Surveying, The Ohio State University, Report No. 262.

Levitus, S., and Dort, A.H., 1977, Global analysis of oceanographic data. Bulletin of the American Meteorological Society, Vol. 58, pp. 1270-1284.

Lisitzin, E., 1974, Sea level changes. Elsevier, Amsterdam.

Love, A.E.H., 1909, The yielding of the Earth to disturbing forces. Proc. of the Royal Soc. London, Vol. 82., pp. 73-88.

MacArthur, J.L., 1980, Altimeter designs: SEASAT-1 and future missions. Marine Geodesy, Vol. 3, pp. 39-61.

Marsh, J.G., and Williamson, R.G., 1980, Precise orbit analyses in support of the SEASAT altimeter experiment. The Journal of the Astronautical Sciences, Vol. 28, pp. 345-370.

Marsh, J.G., and Martin, T.V., 1982, The SEASAT altimeter mean sea surface model. *Journal of Geophysical Research*, Vol. 87, pp. 3269-3280.

Marsh, J.G., and Williamson, R.G., 1982, SEASAT altimeter timing bias estimation. *Journal of Geophysical Research*, Vol. 87, pp. 3232-3238.

Marsh, J.G., 1983, Satellite Altimetry, *Reviews of Geophysics and Space Physics*, Vol. 21, pp. 574-580 (included in the U.S. National Report for 1979-1982 to the 18th General Assembly of the IUGG).

Marsh, J.G., Lerch, F.J., and Williamson, R.G., 1983, Geodynamic and geodetic parameter estimation from STARLETTE laser tracking data. Submitted to the *Journal of Geophysical Research*.

Martin, T.V., Oh, I.H., Eddy, M.F., and Kogut, J.A., 1976, GEODYN system description, Vol. 1. Report, NASA Goddard Space Flight Center.

Marussi, A., 1977, The tidal field of the Earth. *Proceedings of the 1st International Symposium on Inertial Technology for Surveying and Geodesy*, Ottawa, pp. 409-416.

Marussi, A., 1982, On the structure of the tidal field. Lectures, Third International Summer School in the Mountains on Geodesy and Global Geodynamics, Mont, published by the Technical University at Graz, H. Moritz and H. Sünkel, editors.

Masters, E.G., Coleman, R., and Bretreger, K., 1979, On orbital errors and the recovery of regional ocean tide models using satellite altimetry. Australian Journal of Geodesy, Photogrammetry and Surveying, Vol. 31, pp. 127-152.

Mather, R.S., Coleman, R., Rizos, C., and Hirsh, B., 1977, A preliminary analysis of GEOS-3 altimeter data in the Tasman and Coral seas. Unisuro G26, School of Surveying, University of New South Wales, pp. 27-46 (the completed study was published in the GEOS-3 special issue of J.G.R., Vol. 84, pp. 3853-3860, after the death of the first author).

Mather, R.S., Coleman, R., and Hirsh, B., 1978, The analysis of temporal variations in regional models of the Sargasso sea from GEOS-3 altimetry. NASA Goddard Space Flight Center, Document TM-79549.

Maul, G.A., and Yanaway, A., 1978, Deep sea tides determination from GEOS-3, NASA Wallops Flight Center, Document CR-141435.

Mazzega, P., 1983, The M2 oceanic tide recovered from SEASAT altimetry in the Indian ocean. Nature, Vol. 302, pp. 514-516.

Mazzega, P., 1984, M2 model of the global ocean tide derived from SEASAT altimetry. Submitted to Marine Geodesy.

McGoogan, J.T., Leitao, C.D., and Wells, W.T., 1975, Summary of SKYLAB S-193 altimeter altitude results. NASA Document X-6935.

Mognard, N.M., Campbell, W.J., and Brassier, C., 1984, World ocean mean monthly waves, swell, and surface winds for July through October 1978 from SEASAT radar altimeter data. Marine Geodesy, Vol. 8, pp. 159-181.

Moritz, H., 1980, Advanced physical geodesy. Abacus Press, England.

Munk, W.H., and MacDonald, G.J.F., 1960, The rotation of the Earth. Cambridge University Press.

Ondrasik, V.J., and Wu, S.C., 1982, A simple and economical tracking system with subdecimeter Earth satellite and ground receiver position determination capabilities. Presented at the Third International Symposium on the Use of Artificial Satellites for Geodesy and Geodynamics, Ermioni.

Parke, M.E., and Hendershott, 1980, M.C., M2, S2, K1 models of the global ocean tide on an elastic Earth. Marine Geodesy, Vol. 3, pp. 379-408.

Pekeris, C.L., and Accad, Y., 1969, Solution of Laplace's equation for the M2 tide in the world oceans. Philosophical Transactions of the Royal Soc. London, Ser. A, Vol. 265, p. 413.

POSEIDON: Objectifs Scientifiques. 1983, Centre National d'Etudes Spatiales (CNES). Report of a study group.

Proudman, J., 1916, On the dynamical theory of tides. Part II. Flat seas. Proceedings of the London Mathematical Society, Ser. 2., Vol. 18, pp. 21-50.

Putney, B.H., 1976, General theory for dynamical satellite geodesy. National Geodetic Satellite Program, NASA SP-365.

Rao, D.B., and Schwab, D.J., 1976, Two dimensional normal modes in arbitrary enclosed basins on a rotating Earth: application to lakes Ontario and Superior. Phil. Trans. Royal Soc. London, A. 281, pp. 63-69.

Rao, C.R., 1965, Linear statistical inference and its applications. John Wiley & Sons.

Rapp, R.H., 1979, Potential coefficient and anomaly degree variance revisited. Dept. of Geodetic Science and Surveying, The Ohio State University, Report 293.

Rapp, R.H., 1982, The Earth's gravity field to degree and order 180, using SEASAT altimeter data, terrestrial data, and other data. Dept. of Geodetic Science and Surveying, the Ohio State University, Report 322.

Reigber, C., 1981, Representation of orbital element variations and force function with respect to various reference systems. Bulletin Géodésique, Vol. 55, pp. 111-131.

Reigber, C., 1983, Current status of general gravity models. Presented at the 18th General Assembly of the IUGG, Hamburg.

Rizos, C., 1980, The role of the gravity field in sea surface topography studies. Unisurv S 17, School of Surveying, Univ. of New South Wales (doctoral dissertation).

Rowlands, D., 1981, The adjustment of SEASAT altimeter data on a global basis for geoid and sea surface height determinations. Dept. of Geodetic Science and Surv., The Ohio State University, Report 325.

Rubincam, D.P., 1982, On the secular decrease of the semimajor axis of LAGEOS' orbit. Celestial Mechanics, Vol. 26, pp. 361-382.

Rummel, R., and Rapp, R.H., 1977, Undulation and anomaly estimation using GEOS-3 altimeter data without precise satellite orbits. Bulletin Géodésique, Vol. 51., pp. 73-88.

Sanchez, B.V., Rao, D.B., and Wolfson, P.G., 1984, An objective technique for extrapolating tidal fields in a closed basin. Submitted to Marine Geodesy.

Sasao, T., and Wahr, J., 1981, An excitation mechanism for the free "core nutation". Geophysical Journal of the Royal Astron. Soc., Vol. 64, pp. 729-746.

Schutz, B.E., Tapley, B.D., Eanes, R.J., Marsh, J.G., Williamson, R.G., and Martin, T.V., 1980, Precision orbit determination software validation experiment. The Journal of the Astronautical Sciences, Vol. 28., pp. 327-344.

Schwiderski, E.W., 1979, Global ocean tides, part II: The semidiurnal principal lunar tide (M2), atlas of tidal charts and maps. Report of the Naval Surface Weapons Center NSWC TR 79-414.

Schwiderski, E.W., 1980, On charting global ocean tides. Reviews of Geophysics and Space Physics, Vol. 18, pp. 243-268.

Schwiderski, E.W., 1980(b), Ocean Tides, Part I: Global ocean equation. Part II: A hydrodynamical interpolation model. Marine Geodesy, Vol. 3, pp. 161-255.

Seidelmann, P.K., 1982, Orbital motion of the planets, theoretical and observational. Celestial Mechanics, Vol. 26, pp. 149-160.

Shum, C.K., 1982, Altimeter methods in satellite geodesy. Doctoral dissertation, Department of Aerospace Engineering and Engineering Mechanics, The University of Texas at Austin.

Smart, W.M., 1931, Textbook on Spherical Astronomy. Cambridge University Press (sixth edition, 1977, revised by R.M. Green).

Stanley, H.R., 1979, Satellite altimetry. Reviews of Geophysics and Space Physics, Vol. 17, pp. 1418-1421 (included in the US National Report for 1975-78 to the 17th General Assembly of the IUGG).

Tapley, B.D., Born, G.H., and Parke, M.E., 1982, The SEASAT altimeter data and its accuracy assessment. Journal of Geophysical Research, Vol. 87, pp. 3179-3188.

TOPEX Science Working Group Report, 1981, Satellite altimetric measurements of the ocean. NASA/Jet Propulsion Laboratory.

Tscherning, C.C., Rapp, R.H., and Goad, C.C., 1983. A comparison of methods for computing gravimetric quantities from high degree spherical harmonic expansions. Manuscripta Geodaetica, Vol. 8, pp. 249-272.

von Arx, W.S., 1966, Geophysical applications based on an orbiting microwave altimeter and gradiometer. Space Research: Directions for the Future, National Academy of Sciences National Research Council, Publication 1403.

Wagner, C.A., and Colombo, O.L., 1979, Gravitational spectra from direct measurements. Journal of Geophysical Research, Vol. 84, pp. 4699-4712.

Wagner, C.A., 1983, The accuracy of the low-degree geopotential: Implications for ocean dynamics. *Journal of Geophysical Research*, Vol. 88, pp. 5083-5090.

Wagner, C.A., 1984, Radial variations of a near circular satellite orbit due to gravitational errors: Implications for satellite altimetry. Presented at the Spring Meeting of the AGU, Cincinnati.

Wahr, J.M., 1979, The tidal motions of a rotating, elliptical, elastic and oceanless Earth. Doctoral dissertation, Department of Physics, The University of Colorado.

Wahr, J.M., and Sasao, T., 1981, A diurnal resonance in the ocean tide and in the Earth's load response due to the resonant free "core nutation". *Geophysical Journal of the Royal Astronomical Society*, Vol. 64, pp. 747-765.

Wahr, J., 1982, Computing tides, nutations and tidally-induced variations in the Earth's rotation rate for a rotating, elliptical Earth. Lectures, Third International Summer School in the Mountains on Geodesy and Global Geodynamics, Admont, H. Moritz and H. Sunkel, editors.

Wakker, K.F., Ambrosius, B.A.C., and Aardoom, L., 1983, Precise orbit determination for ERS-1. European Space Agency Contract Report, Delft University of Technology, Department of Aerospace Engineering.

Watts, A.B., 1979, On geoid heights derived from GEOS-3 altimeter data along the Hawaiian-Emperor seamount chain. *Journal of Geophysical Research*, Vol. 84, pp. 3817-3826.

Won, I.J., and Miller, L.S., 1979, Oceanic geoid and tides from GEOS-3 satellite data in the Northwestern Atlantic ocean. *Journal of Geophysical Research*, Vol. 84, pp. 3833-3842.

Wunsch, C., 1980, Low frequency variability of the sea, in "Evolution of Physical Oceanography, Scientific Surveys in Honor of Henry Stommel," B.A. Warren and C. Wunsch, editors, MIT Press, pp. 342-374.

Wunsch, C., and Gaposchkin, E.M., 1980, On using satellite altimetry to determine the general circulation of the oceans with application to geoid improvements. *Reviews of Geophysics and Space Physics*, Vol. 18, pp. 725-745.

Zetler, B.D., and Maul, G.E., 1971, Precision requirements for a spacecraft tide program. *Journal of Geophysical Research*, Vol. 76, pp. 6601-6605.

Zetler, B.D., 1980, IAPSO compilation of pelagic tides. *Marine Geodesy*, Vol. 3, pp. 273-287.